

**FORCE EFFECTS ON LAMINATED RUBBER-METAL SPRING USING
TRANSMISSIBILITY TEST NUMERICAL APPROACH**

MUHAMMAD IHSAN BIN MADZUKI



**This report submitted
in fulfillment of the requirements for the degree of
Bachelor of Mechanical Engineering (Plant & Maintenance)**

Faculty of Mechanical Engineering

UNIVERSITI TEKNIKAL MALAYSIA MELAKA

2017

DECLARATION

I declare that this project entitled “Force Effect on Laminated Rubber Metal Spring Using Transmissibility Test Numerical Approach” is the result of my own work excepts as cited in the references.



APPROVAL

I hereby declare that I have read this project report and in my opinion this report is sufficient in terms of scope and quality for the award of the degree of Bachelor of Mechanical Engineering (Plant & Maintenance).



DEDICATION

To my beloved mother, father, wife, siblings and all my friends.



ABSTRACT

The purpose of this project is to study and analyses the laminated rubber-metal spring model by using the finite element analysis software. The model is drawn part by part and assembly by using the CATIA solid modelling software. By using the ANSYS FEA finite element analysis software, the natural rubber rod is analyses with 5 different type of natural rubber rod. This 5-different type of the natural rubber rod that been drawn and be analyses. The 5 different types of the natural rubber rod are the nature rubber rod without embedded plate, the nature rubber rod with 1 embedded aluminium alloy plate, the nature rubber rod with 2 embedded aluminium alloy plate, the nature rubber rod with 3 embedded aluminium alloy plate and the last one is the nature rubber rod with 4 embedded aluminium alloy plate. Every type of the natural rubber rod was analysed by using the 5-different force which is 200N, 400N, 600N, 800N, and 1000N. The result and data of the analysis then is show and represent based on the graph and table. By referring the result, the comparison of the value of the modal analysis, stress frequency response and the deformation frequency response of each type of the natural rubber rod is done, As the summary of the project, the number of embedded plate on the natural rubber rod will affect the result of the modal analysis, stress frequency response and the deformation frequency response.

ABSTRAK

Tujuan project ini adalah untuk mengkaji dan menganalisis model model spring getah berlapis dengan logam dengan menggunakan perisian analisis. Model tersebut telah dilukis bahagian demi bahagian dan digabung dengan menggunakan perisian permodelan pepejal CATIA. 5 jenis rod getah asli telah dianalisis dengan menggunakan perisian ANSYS FEA. 5 jenis rod getah asli tersebut yang telah sediakan telah dianalisis. 5 jenis rod getah asli tersebut ialah rod getah asli tanpa plat aluminium aloi yg tertanam di dalamnya, rod getah asli dengan 1 plate aluminium aloi tertanam di dalamnya, rod getah asli dengan 2 plate aluminium aloi tertanam di dalamnya, rod getah asli dengan 3 plate aluminium aloi tertanam di dalamnya, dan rod getah asli dengan 4 plate aluminium aloi tertanam di dalamnya. Setiap jenis rod getah asli telah dianalisis dengan menggunakan daya 5 yang berbeza iaitu 200N, 400N, 600N, 800N, dan 1000N. Keputusan dan data dari analisis telah di paparkan dalam bentuk graf dan jadual. Merujuk kepada keputusan dan data yang diperolih, perbandingan diantara setiap analisis telah dilakukan. Sebagai penutup untuk project ini, ternyata bilangan plate aluminium aloi yang tertanam di dalam rod getah asli akan memberi kesan kepada analisis.

ACKNOWLEDGEMENT

Bismillahirrahmanirrahim,

Alhamdulillah. Thanks to Allah SWT, who with His willing give me the opportunity to complete this Final Year Report (FYP) This project report was prepared for Faculty of Mechanical Engineering (FKM), Universiti Teknikal Malaysia Melaka (UTeM), basically for student in 4th year to complete the requirement for student undergraduate program that leads to the degree of Bachelor of Engineering in Mechanical. This report is based on the methods given by the university.

First of all, I would like to express my deepest appreciation to my parents, Mr. Madzuki Bin Ismail and Madam. Rokiah Binti Ahmad for their supports and encouragement throughout this endeavour. Special thanks to my supervisor, Dr. Mohd Azli Bin Salim for his invaluable guidance, mentorship, wisdom and professionalism for my academic pursuit. Dr. Mohd Azli Bin Salim has been an excellent mentor and has provided unfailing support throughout my final year project conduction. Last but not least, to all my lecturers and dearest friends who involved in this project work, I would like to extend million thanks to them for their patience and kind advice to make this project work possible. Thank you.

CONTENTS

CHAPTER	CONTENT	PAGE
	DECLARATION	ii
	APPROVAL	iii
	DEDICATION	iv
	ABSTRACT	v
	ABSTRAK	vi
	ACKNOWLEDGEMENT	vii
	TABLE OF CONTENTS	viii
	LIST OF FIGURES	xii
	LIST OF TABLES	xix
	LIST OF ABBREVIATIONS	xxiv
	LIST OF SYMBOLS	xxv
CHAPTER 1	INTRODUCTION	1
	1.1 Background	1
	1.2 Problem Statement	2
	1.3 Objective	3
	1.4 Scope of Project	3
	1.5 Report Outline	3
CHAPTER 2	LITERATURE REVIEW	5
	2.1 Introduction	5
	2.2 Transmissibility of a Laminated Rubber-Metal	5
	2.2.1 Lumped Parameter Model	6
	2.2.2 Result for Different Number of Layer Embedded	9

2.3	Dynamic Analysis of Laminated Rubber-Metal Spring Using Finite Element Method	11
2.3.1	Isolator Model	12
2.3.2	Material Properties for Isolator Model	13
2.3.3	Finite Element Analysis Method	13
2.3.4	Comparison for Finite Element Analysis Result	14
2.4	Parameter Assessment on Laminated Rubber-Metal Spring	14
2.4.1	Parameter Selection	15
2.4.2	Analysis Result Laminated Rubber Metal Spring	16
2.5	Finite Element Analysis for Leaf Spring	16
2.5.1	Harmonic Response Analysis	17
2.6	Modal Analysis Study	17
2.6.1	Vibration Mode Shape Frequency and Natural Frequency	17
CHAPTER 3	RESEARCH AND METHODOLOGY	19
3.1	Introduction	19
3.2	Overall Flowchart	20
3.3	Data Collection	21
3.4	Computer Aided Design	22
3.4.1	Step in 3-D Modelling by CATIA	23
3.4.2	Step for Design a Part by CATIA	26
3.4.3	Laminated Rubber – Metal Spring Component	29
3.5	Finite-Element Analysis	33
3.5.1	Modal Analysis on ANSYS Software	34
3.5.2	Harmonic Response Analysis on ANSYS Software	42

CHAPTER 4	RESULT AND DISCUSSION	45
4.1	Analysis of Nature Rubber Rod by ANSYS Finite Element Analysis	45
4.2	Modal Analysis	46
4.2.1	Modal Analysis of the Type 1 Nature Rubber Rod	46
4.2.2	Modal Analysis of the Type 2 Nature Rubber Rod	49
4.2.3	Modal Analysis of the Type 3 Nature Rubber Rod	51
4.2.4	Modal Analysis of the Type 4 Nature Rubber Rod	53
4.2.5	Modal Analysis of the Type 5 Nature Rubber Rod	55
4.3	Frequency Response of the Nature Rubber Rod	57
4.3.1	Stress Frequency Response of the Nature Rubber Rod with 1 Embedded Aluminium Alloy	57
4.3.2	Deformation Frequency Response of Nature Rubber Rod with 1 Embedded Aluminium Alloy	64
4.3.3	Stress Frequency Response of the Nature Rubber Rod with 2 Embedded Aluminium Alloy	70
4.3.4	Deformation Frequency Response of Nature Rubber Rod with 2 Embedded Aluminium Alloy	76
4.3.5	Stress Frequency Response of the Nature Rubber Rod with 3 Embedded Aluminium Alloy	82

4.3.6	Deformation Frequency Response of Nature Rubber Rod with 3 Embedded Aluminium Alloy	88
4.3.7	Stress Frequency Response of the Nature Rubber Rod with 4 Embedded Aluminium Alloy	94
4.3.8	Deformation Frequency Response of Nature Rubber Rod with 4 Embedded Aluminium Alloy	100
4.4	Summary	106
CHAPTER 5	CONCLUSION AND RECOMMENDATION	112
1.1	Conclusion	112
1.2	Recommendation	113
	REFERENCES	114
	APPENDICES	116



LIST OF FIGURES

FIGURE	TITLE	PAGE
2.1	A Bulging Effect in a Rubber Isolator Due to a Large Preload	6
2.2	The Embedded Plate in the Rubber Rod	7
2.3	(a)Mass-Damper-Spring of a LR-MS Model (b) Free-Body-Diagram for LR-MS Model	8
2.4	Transmissibility of LR-MS from Lumped Parameter Model with Numbers of Layers of Plate N=1	10
2.5	Transmissibility of LR-MS from Lumped Parameter Model with Numbers of Layers of Plate N=2	10
2.6	Transmissibility of LR-MS from Lumped Parameter Model with Numbers of Layers of Plate N=5	11
2.7	LR-MS with 1 Embedded Plate Assembly	13
2.8	Vibration Mode and Natural Frequency for a Plate	18
3.1	Part Design Option	23
3.2	Sketching Option	24
3.3	Assembly Design Option	24
3.4	Assembly Design Part Component	25

3.5	Drawing Save Format Option	25
3.6	Part Design Option	26
3.7	x-y Plane Property Option	26
3.8	Profile Option and Constrain Definition for Sketch	27
3.9	Exit Workbench Property Option	27
3.10	Pad Definition Property Option	28
3.11	Model of the Nature Rubber Rod	28
3.12	LR-MS Model Assembly	32
3.13	Engineering Data Option	35
3.14	Connection between Engineering Data and Modal Analysis	35
3.15	Set-Up New Material for the Nature Rubber	36
3.16	Physical Properties for the New Material	36
3.17	Isotropic Elasticity Toolbox Option	37
3.18	Tensile Yield Strength Toolbox Option	37
3.19	Engineering Data for General Material Option	38
3.20	Geometry Browse Option	38
3.21	Material for Geometry Part Option	39
3.22	Generate Mesh Option	39
3.23	Fix Support for the Model Option	40
3.24	Mode Option	40

3.25	Create Mode Shape Result Option	41
3.26	Result for the Mode Option	41
3.27	Connection Between Modal and Harmonic Analysis Option	42
3.28	Input Force Option	42
3.29	Insert the Frequency Response for Deformation Option	43
3.30	Frequency Range for the Model Option	43
3.31	Solve Option to Run the Analysis	44
4.1	Result of Analysis	45
4.2	Assembly Type 1	46
4.3	Assembly Type 2	49
4.4	Assembly Type 3	51
4.5	Assembly Type 4	53
4.6	Assembly Type 5	55
4.7	Graph Stress Vs Frequency Response for Force 200 N of 1 Embedded plate	58
4.8	Graph Stress Vs Frequency Response for Force 400 N of 1 Embedded plate	59
4.9	Graph Stress Vs Frequency Response for Force 600 N of 1 Embedded plate	60
4.10	Graph Stress Vs Frequency Response for Force 800 N of 1 Embedded plate	61
4.11	Graph Stress Vs Frequency Response for Force 1000 N of 1 Embedded plate	62



4.12	Result of Five Different Data with Different Value of Force Due to the 1 Embedded Plate Due to the Natural Rubber Rod for Stress Frequency Response	63
4.13	Graph Deformation Vs Frequency Response for Force 200 N of 1 Embedded plate	64
4.14	Graph Deformation Vs Frequency Response for Force 400 N of 1 Embedded plate	65
4.15	Graph Deformation Vs Frequency Response for Force 600 N of 1 Embedded plate	66
4.16	Graph Deformation Vs Frequency Response for Force 800 N of 1 Embedded plate	67
4.17	Graph Deformation Vs Frequency Response for Force 1000 N of 1 Embedded plate	68
4.18	Result of Five Different Data with Different Value of Force Due to the 1 Embedded Plate Due to the Natural Rubber Rod for Deformation Frequency Response	69
4.19	Graph Stress Vs Frequency Response for Force 200 N of 2 Embedded plate	70
4.20	Graph Stress Vs Frequency Response for Force 400 N of 2 Embedded plate	71
4.21	Graph Stress Vs Frequency Response for Force 600 N of 2 Embedded plate	72
4.22	Graph Stress Vs Frequency Response for Force 800 N of 2 Embedded plate	73
4.23	Graph Stress Vs Frequency Response for Force 1000 N of 2 Embedded plate	74
4.24	Result of Five Different Data with Different Value of Force Due to the 2 Embedded Plate Due to the Natural Rubber Rod for Stress Frequency Response	75
4.25	Graph Deformation Vs Frequency Response for Force 200 N of 2 Embedded plate	76

4.26	Graph Deformation Vs Frequency Response for Force 400 N of 2 Embedded plate	77
4.27	Graph Deformation Vs Frequency Response for Force 600 N of 2 Embedded plate	78
4.28	Graph Deformation Vs Frequency Response for Force 800 N of 2 Embedded plate	79
4.29	Graph Deformation Vs Frequency Response for Force 1000 N of 2 Embedded plate	80
4.30	Result of Five Different Data with Different Value of Force Due to the 2 Embedded Plate Due to the Natural Rubber Rod for Deformation Frequency Response	81
4.31	Graph Stress Vs Frequency Response for Force 200 N of 3 Embedded plate	82
4.32	Graph Stress Vs Frequency Response for Force 400 N of 3 Embedded plate	83
4.33	Graph Stress Vs Frequency Response for Force 600 N of 3 Embedded plate	84
4.34	Graph Stress Vs Frequency Response for Force 800 N of 3 Embedded plate	85
4.35	Graph Stress Vs Frequency Response for Force 1000 N of 3 Embedded plate	86
4.36	Result of Five Different Data with Different Value of Force Due to the 3 Embedded Plate Due to the Natural Rubber Rod for Stress Frequency Response	87
4.37	Graph Deformation Vs Frequency Response for Force 200 N of 3 Embedded plate	88
4.38	Graph Deformation Vs Frequency Response for Force 400 N of 3 Embedded plate	89
4.39	Graph Deformation Vs Frequency Response for Force 600 N of 3 Embedded plate	90

4.40	Graph Deformation Vs Frequency Response for Force 800 N of 3 Embedded plate	91
4.41	Graph Deformation Vs Frequency Response for Force 1000 N of 3 Embedded plate	92
4.42	Result of Five Different Data with Different Value of Force Due to the 3 Embedded Plate Due to the Natural Rubber Rod for Deformation Frequency Response	93
4.43	Graph Stress Vs Frequency Response for Force 200 N of 4 Embedded plate	94
4.44	Graph Stress Vs Frequency Response for Force 400 N of 4 Embedded plate	95
4.45	Graph Stress Vs Frequency Response for Force 600 N of 4 Embedded plate	96
4.46	Graph Stress Vs Frequency Response for Force 800 N of 4 Embedded plate	97
4.47	Graph Stress Vs Frequency Response for Force 1000 N of 4 Embedded plate	98
4.48	Result of Five Different Data with Different Value of Force Due to the 4 Embedded Plate Due to the Natural Rubber Rod for Stress Frequency Response	99
4.49	Graph Deformation Vs Frequency Response for Force 200 N of 4 Embedded plate	100
4.50	Graph Deformation Vs Frequency Response for Force 400 N of 4 Embedded plate	101
4.51	Graph Deformation Vs Frequency Response for Force 600 N of 4 Embedded plate	102
4.52	Graph Deformation Vs Frequency Response for Force 800 N of 4 Embedded plate	103
4.53	Graph Deformation Vs Frequency Response for Force 1000 N of 4 Embedded plate	104

4.54	Result of Five Different Data with Different Value of Force Due to the 4 Embedded Plate Due to the Natural Rubber Rod for Deformation Frequency Response	105
4.55	Combination of Graph of the Different Types of Modality with the Frequency	106
4.56	a) Graph of Comparison for the Stress Frequency Response for 200N (b) Graph of Comparison for the Deformation Frequency Response for 200N	109



LIST OF TABLES

TABLE	TITLE	PAGE
3.1	Material Properties of Natural Rubber for Analysis	21
3.2	Material Properties of Aluminium Alloy for Analysis	21
3.3	Component of the LR-MS Model	29
4.1	Result of the Modal Analysis for Type 1	47
4.2	Result of the Modal Analysis for Type 2	49
4.3	Result of the Modal Analysis for Type 3	51
4.4	Result of the Modal Analysis for Type 4	53
4.5	Result of the Modal Analysis for Type 5	55
4.6	Result of the Frequency Response Due Stress for Force 200 N of 1 Embedded Plate	57
4.7	Result of the Frequency Response Due Stress for Force 400 N of 1 Embedded Plate	59
4.8	Result of the Frequency Response Due Stress for Force 600 N of 1 Embedded Plate	60
4.9	Result of the Frequency Response Due Stress for Force 800 N of 1 Embedded Plate	61

4.10	Result of the Frequency Response Due Stress for Force 1000 N of 1 Embedded Plate	62
4.11	Result of the Frequency Response Due Deformation for Force 200 N of 1 Embedded Plate	64
4.12	Result of the Frequency Response Due Deformation for Force 400 N of 1 Embedded Plate	65
4.13	Result of the Frequency Response Due Deformation for Force 600 N of 1 Embedded Plate	66
4.14	Result of the Frequency Response Due Deformation for Force 800 N of 1 Embedded Plate	67
4.15	Result of the Frequency Response Due Deformation for Force 1000 N of 1 Embedded Plate	68
4.16	Result of the Frequency Response Due Stress for Force 200 N of 2 Embedded Plate	70
4.17	Result of the Frequency Response Due Stress for Force 400 N of 2 Embedded Plate	71
4.18	Result of the Frequency Response Due Stress for Force 600 N of 2 Embedded Plate	72
4.19	Result of the Frequency Response Due Stress for Force 800 N of 2 Embedded Plate	73
4.20	Result of the Frequency Response Due Stress for Force 1000 N of 2 Embedded Plate	74
4.21	Result of the Frequency Response Due Deformation for Force 200 N of 2 Embedded Plate	76

4.22	Result of the Frequency Response Due Deformation for Force 400 N of 2 Embedded Plate	77
4.23	Result of the Frequency Response Due Deformation for Force 600 N of 2 Embedded Plate	78
4.24	Result of the Frequency Response Due Deformation for Force 800 N of 2 Embedded Plate	79
4.25	Result of the Frequency Response Due Deformation for Force 1000 N of 2 Embedded Plate	80
4.26	Result of the Frequency Response Due Stress for Force 200 N of 3 Embedded Plate	82
4.27	Result of the Frequency Response Due Stress for Force 400 N of 3 Embedded Plate	83
4.28	Result of the Frequency Response Due Stress for Force 600 N of 3 Embedded Plate	84
4.29	Result of the Frequency Response Due Stress for Force 800 N of 3 Embedded Plate	85
4.30	Result of the Frequency Response Due Stress for Force 1000 N of 3 Embedded Plate	86
4.31	Result of the Frequency Response Due Deformation for Force 200 N of 3 Embedded Plate	88
4.32	Result of the Frequency Response Due Deformation for Force 400 N of 3 Embedded Plate	89
4.33	Result of the Frequency Response Due Deformation for Force 600 N of 3 Embedded Plate	90

4.34	Result of the Frequency Response Due Deformation for Force 800 N of 3 Embedded Plate	91
4.35	Result of the Frequency Response Due Deformation for Force 1000 N of 3 Embedded Plate	92
4.36	Result of the Frequency Response Due Stress for Force 200 N of 4 Embedded Plate	94
4.37	Result of the Frequency Response Due Stress for Force 400 N of 4 Embedded Plate	95
4.38	Result of the Frequency Response Due Stress for Force 600 N of 4 Embedded Plate	96
4.39	Result of the Frequency Response Due Stress for Force 800 N of 4 Embedded Plate	97
4.40	Result of the Frequency Response Due Stress for Force 1000 N of 4 Embedded Plate	98
4.41	Result of the Frequency Response Due Deformation for Force 200 N of 4 Embedded Plate	100
4.42	Result of the Frequency Response Due Deformation for Force 400 N of 4 Embedded Plate	101
4.43	Result of the Frequency Response Due Deformation for Force 600 N of 4 Embedded Plate	102
4.44	Result of the Frequency Response Due Deformation for Force 800 N of 4 Embedded Plate	103
4.45	Result of the Frequency Response Due Deformation for Force 1000 N of 4 Embedded Plate	104
4.46	Natural Frequency for Plate Model from FE Method	107



LIST OF ABBEREVATIONS

NR	Nature Rubber
FE	Finite Element
FEA	Finite Element Analysis
3D	Three Dimensional
LR-MS	Laminated Rubber-Metal Spring
DOF	Degree-of-Freedom
CAD	Computer Aided Design



LIST OF SYMBOLS

ω_n	=	Natural frequency
f	=	Frequency
n	=	Mode
k	=	Stiffness
m	=	Mass
c	=	Damper
T	=	Transmissibility
F_e	=	Force Input
F_t	=	Transmitted Force
ρ	=	Density
E	=	Modulus of Elasticity
A	=	Area
r	=	Radius



CHAPTER 1

INTRODUCTION

1.1 Background

This project was chosen Natural Rubber (NR) as the main element to be analysis. The model of the Laminated Rubber-Metal Spring (LR-MS) is creating to investigate the NR by using the Finite Element Analysis (FEA). Nowadays the NR was being the most importance substance that can generate the economic resources for our country. Another name for the NR is elastomers. The bark of the HAVEA tree produced the latex and will be going the series of the process before it produces to be a product such as preservation, concentration, coagulation, dewatering, drying, cleaning, and blending. NR consists of isoprene, polymers, and a litter bit of water. NR is between the famous productions in our country.

In our country, the history of the NR was beginning when the rubber has been brought in by the British to smuggle rubber tree seeds from Amazonia, Brazil to the botanical gardens in London and then planted in colonies, especially in Malaysia and Singapore. The NR usually sold based on the grades. The grades depended on the purity, viscosity, viscosity stability, oxidation resistance, and rate of cure. At the latex stage, the modified process also can have carried out with the treatment at the latex stage.

The NR is the unique material that was used in a lot of engineering application and manufacturing. This incredibly material has been used in the application of automotive industries, electrical industries, toys, balls, and a lot. The flexibility of the rubber was used in vehicles tire, and rollers industries, while the elasticity of the NR made that substance is

suitable for the shock absorbers and for the machinery. The mounting will design to reduce the vibration and noise of the machines. The higher resistance of the rubber made the rubber is good as the insulation for the cable wire, protective gloves, and shoes because it has the higher electrical resistance.

The analysis that will be made in this project are to study the relationship of the NR due to the force, the deformation of the rubber, and the natural frequency of the rubber. NR can be deflected to larger deformation such as they perform as springs or seals. When deflected, they will provide energy lost. The tensile strength of an elastomer or another name for it is an ultimate tensile strength is less than a metal material, but, its capacity to store energy is greater than a metal substances. The tensile strength of an elastomer is 3000Psi at 600% elongation. The natural rubber only loss the strength due to increasing the temperature and increasing of stiffness with lower temperature.

The software ANSYS 16.0 FEA will run the process of the analysis for this project. This software is related to every site such as manufacturing, automotive, aerospace, and so on. The process to develop the model is used the CATIA V5R20 software start from the part design drawing, assembly the drawing and after the step was finished, import the drawing into the ANSYS software, for analyse the result. The result will obtain in the Microsoft Excel to show more detail about the data that collect from the analysis.

1.2 Problem Statement

NR is the most important substances and a lot of application commonly used in the industry. So, that it was the importance things for us to know the strength properties of the rubber. By used the FEA technique, we will obtain the result of the natural frequency of the rubber rod on the LR-MS model with or without the embedded aluminium plates, the deformation of the rubber rod due to the force, and the frequency response of the rubber rod due to the number of the embedded aluminium alloy plates.

1.3 Objective

The objectives of this project are as follows:

1. To develop laminated rubber-metal spring models using numerical approach.
2. To investigate the force distribution effects in laminated rubber-metal spring.

1.4 Scope of Project

This project work is discussing the analysis of the LR-MS modelling by using the FEA. The analysis will consist of the five-different rubber rod model with the embedded aluminium alloy on the rubber with the same diameter.

1.5 Report Outline

Chapter 1 was introduced into the flow of the project. In this chapter, the basic explanation about this project was introduced. This chapter was consisting in 4 parts starting with background introduction, problem statement, objective, and scope of the project.

Chapter 2 is literature review from the past project were taken and will review. The past project is very importance as the references due to our project and the comparison will carry out to get the better understanding about our project.

Chapter 3 is methodology. This part will explain the flow of this project to obtain the result. This part is the most importance part because we need to determine how this project came to be.

Chapter 4 is the part that shows the result and discussion on this project. To more detail, the result that we obtain from the analysis must be generated in graph and table form. With this form, we can easily to understand the detail.

Chapter 5 is the last part of this report. In this section, the conclusion and recommendation are placed. The suggestion and recommendation were made to improve another project in the future.



CHAPTER 2

LITERATURE REVIEW

2.1 Introduction

In this chapter, there will focus on the theory of the NR and the transmissibility of the LR-MS model. This literature review will use to help the reader to understand the concept and the objective with more clearly.

2.2 Transmissibility of a Laminated Rubber-Metal Spring

In this day, the development of the vibration isolator made from rubber material is still in progress. To reduce the vibration transmission, the vibration isolators must be applying in the vehicles, building for protecting the structure from the earthquake happen. Besides that, the rubber material has the very high damping that can cause the sufficient dissipation of vibration energy from the seismic waves. To reduces the performance of the isolator as well as its durability and to prevent the rubber block of the conventional isolator from excessive bulging effect, the embedded metal plates were applied to the rubber structure. The design was related to the earthquake protection that to provide the isolation when subjected to a shear force at the low frequency. The application of the engine mounting, isolation of building from ground-borne vibration near railways lines or train vehicles suspension, the input of force comes from the vertical direction and can extend up to higher frequencies.

2.2.1 Lumped Parameter Model

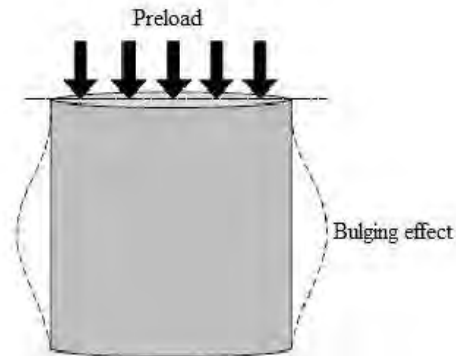


Figure 2.1: A Bulging Effect in a Rubber Isolator Due to a Large Preload (Azli Salim et al., 2013)

Transmissibility of an LR-MS model was carried out by using a lumped parameter model, that consist of the mass, spring, and damper component. The model was loaded with a lumped mass M with a harmonic force F_e at the spring to assess the vibration isolation performance. The rubber is modelled as a massless component with a constant stiffness k and damping coefficient c . The embedded plate in the rubber was defined as a rigid solid mass m without any damping coefficient.

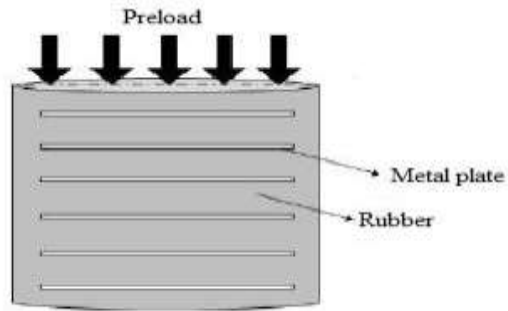
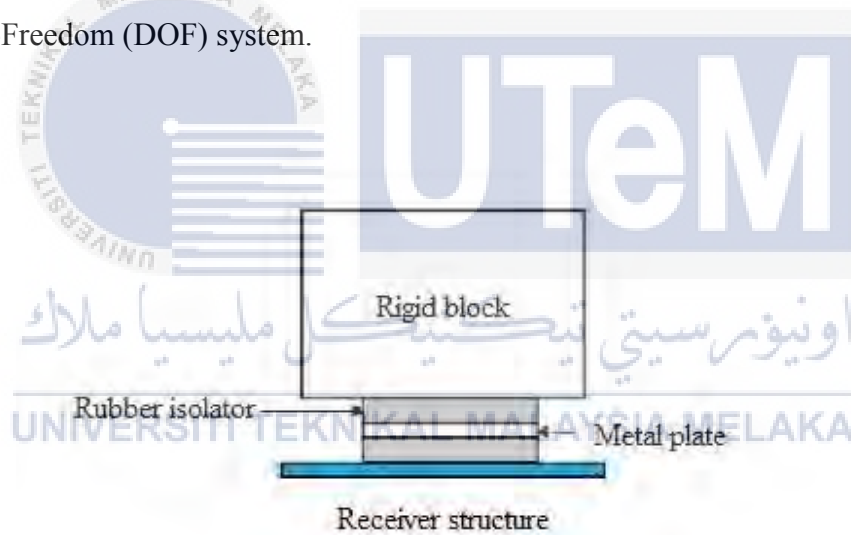
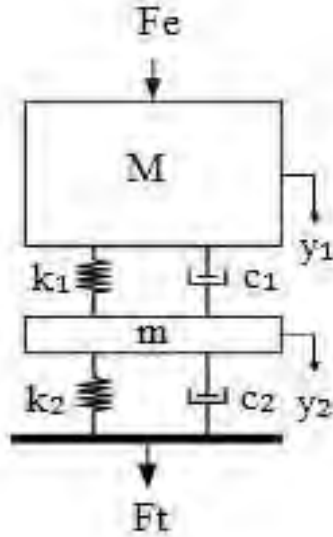


Figure 2.2: The Embedded Plate in the Rubber (Azli Salim et al., 2013)

The laminated spring is attached to the structure and next, the transmissibility is derived in vertical motion and neglected the rotational motion. The figure below shows the schematic diagram of the model laminated spring with one layer of a metal plate which creates 2 Degree-of-Freedom (DOF) system.



(a)



(b)

Figure 2.3: (a) Mass-Damper-Spring of a LR-MS Model (b) Free-Body-Diagram for LR-MS Model (Azli Salim et al., 2013)

From the mass-damper-spring model of an LR-MS, the two equations of motion can be derived as below.

$$m_1 \ddot{y}_1 + c_1 (\dot{y}_1 - \dot{y}_2) + k_1 (y_1 - y_2) = F_e \quad (1)$$

$$m_1 \ddot{y}_2 + c_1 (\dot{y}_1 - \dot{y}_2) + k_1 (y_2 - y_1) + k_2 y_2 = 0 \quad (2)$$

Substituting $y = Y e^{j\omega t}$ in equation (1) and (2) with Y the complex amplitude and ω the frequency, the equations of motion can be expressed in matrix form as below.

$$\left(-\omega^2 \begin{vmatrix} M & 0 \\ 0 & M \end{vmatrix} + j\omega \begin{vmatrix} c_1 & -c_1 \\ -c_1 & c_1 + c_2 \end{vmatrix} + \begin{vmatrix} k_1 & -k_1 \\ -k_1 & c_1 + k_2 \end{vmatrix} \right) \begin{pmatrix} Y_1 \\ Y_2 \end{pmatrix} = \begin{pmatrix} F_e \\ 0 \end{pmatrix}$$

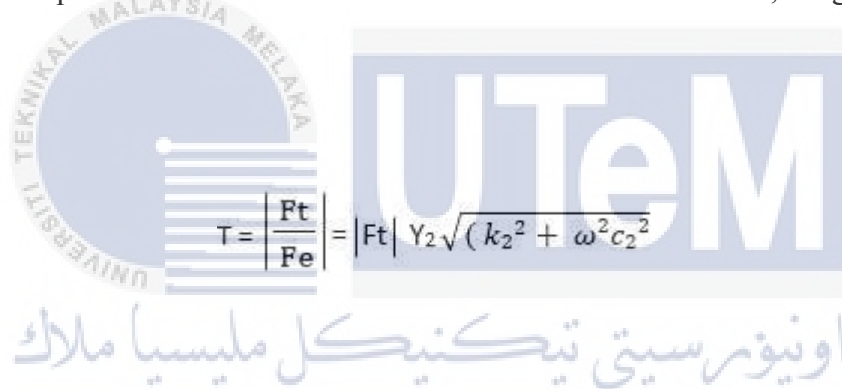
Equation of motion express in general form

$$[-\omega^2 M + j\omega C + K] \tilde{Y} = F$$

where M is the mass matrix, C is the damping matrix, K is the stiffness matrix, Y and F are the vectors of complex displacement amplitude and force, respectively. The displacements Y1 and Y2 at each frequency ω , therefore be obtained the equation below.

$$\tilde{Y} = [-\omega^2 M + j\omega C + K]^{-1} F$$

where A^{-1} indicates the inverse of matrix A. For the case of the system in figure 2.2, the force transmitted to the receiver structure can be written as a function of the displacement of the bottom metal layer. For an excitation force of unit amplitude $F_e = 1$, the transmissibility, for example, the amplitude ratio of transmitted force to excitation force, is given by below equation.



$$T = \left| \frac{F_t}{F_e} \right| = |F_t| Y_2 \sqrt{(k_2^2 + \omega^2 c_2^2)}$$

2.2.2 Result for Different Number of Layer Embedded

For the result, the transmissibility for a different number of layer N of embedded in the metal plate was plotted. By assuming the mass of each plate is the same as the loaded mass and assuming the damping is very small value, the calculation is made. The peak on the graph is indicated the amplified of the injection of the injected force to the receiver structure can be seen at low frequencies, for example at 9 Hz and 23 Hz in the figure below, which appear at the natural frequencies of the system. The addition of the number of plates embedded in the rubber will cause the increasing in a number of DOF and natural frequency in the system. At the 25 Hz of the frequency, the isolation region can be seen roughly. This is because the LR-MS can improve the vibration isolation at high frequency.

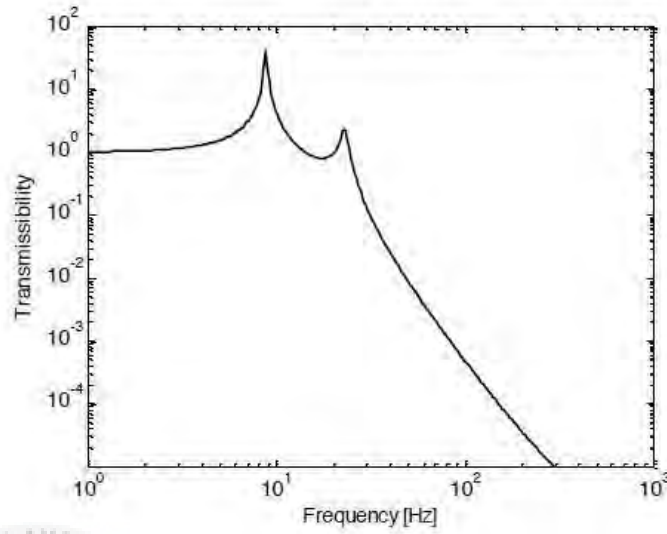


Figure 2.4: Transmissibility of LR-MS from Lumped Parameter Model with Numbers of Layers of Plate $N=1$ (Azli Salim et al., 2013)

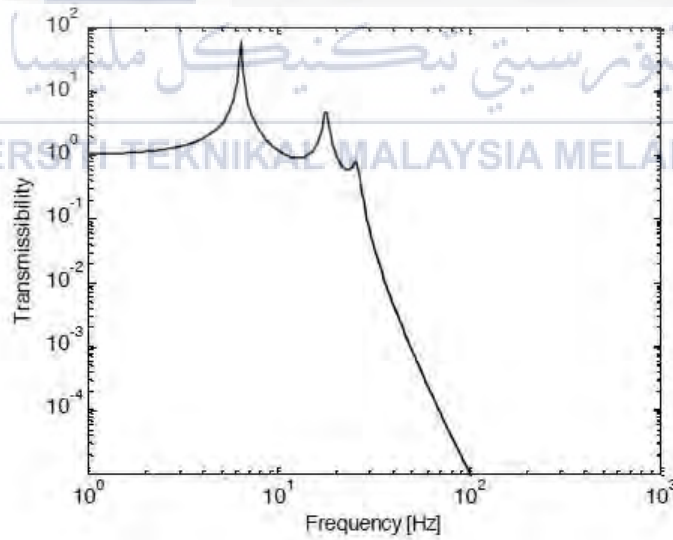


Figure 2.5: Transmissibility of LR-MS from Lumped Parameter Model with Numbers of Layers of Plate $N=2$ (Azli Salim et al., 2013)

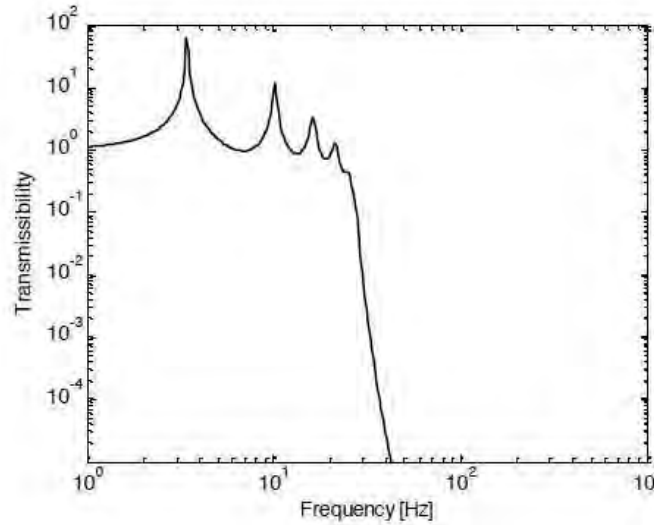


Figure 2.6: Transmissibility of LR-MS from Lumped Parameter Model with Numbers of Layers of Plate $N=5$ (Azli Salim et al., 2013)

As the conclusion, the transmissibility of an LR-MS has been modelled using a lumped parameter system assuming only transverse vibration in the spring. This simple model shows improvement of isolation performance of the spring when more layers of plates are included, but creates more resonances towards low frequency. However, an extended model is required to consider the mass of the rubber, the layer width and various directions of wave propagation inside the spring including the rotational motion for comprehensive analysis.

2.3 Dynamic Analysis of Laminated Rubber-Metal Spring Using Finite Element Method

LR-MS is widely applied in buildings, vehicles and to protect sensitive equipment. The purpose of this analysis is to determine the axial vibration transmissibility performance of the solid rubber isolator and LR-MS using dynamic analysis of FEA. The transmissibility frequency is defining the vibration characteristic of the isolator and to prove the experimental result study, the FEA software is used in this analysis. Based on this study, the dynamic

performance of the isolator was analysed. By using the Finite Element (FE) method, the five model of the rubber based isolator with the different number of layer metal plate was analysed and the transmissibility ratio of the model was determined from the displacement changes of the isolator. The result showed the rubber bearing with embedded metal plate layers can improve the transmissibility ratio at high frequency.

2.3.1 Isolator Model

The isolator model is made with the cylindrical sandwiched mounts shape consists of the steel layer and rubber discs. The diameter, D of each isolator model is same which is 0.1m and 0.1m and the flange plate located at both isolator ends is 5mm in thickness. The metal plate embedded inside the isolator model with the length t_S of 3mm and radius of 0.05m. The thickness of the rubber disc was changed according to the changes of the metal plate number, while, the total length of the isolator and the metal plate are maintained for this whole analysis. The length, t_R for the rubber section for the solid rubber to 4 metal plates isolator were 0.1m, 0.049m, 0.031m, 0.023m and 0.018m respectively while the isolator without metal plate was labelled as solid rubber while LR-MS were labelled based on the number of plate layers exist which were LR-MS with 1 embedded plate to LR-MS with 4 embedded plates on it. The figure below shows the example of the LR-MS with 1 embedded plate assembly.

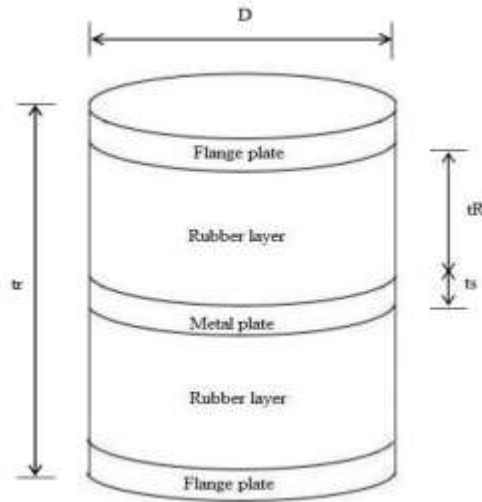


Figure 2.7: LR-MS with 1 Embedded Plate Assembly (Azli Salim et al., 2016)

2.3.2 Material Properties for Isolator Model

For the material properties, the material of the NR has Young Modulus, $E = 1.4 \text{ MPa}$ and density, $\rho = 920 \text{ kgm}^{-3}$, while for the metal plate, the material properties involved are $E = 211 \text{ GPa}$ and $\rho = 7850 \text{ kgm}^{-3}$. The part of the metal plate was defined as the rigid body and rigid mass of 0.3 kg was applied to that body.

2.3.3 Finite Element Analysis Method

The FE modelling of the rubber bearing was analysed by using the ABAQUS FEA software. For the rubber section, it was modelled by using fully integrated axisymmetric solid elements which are CAX8H, while for the both metal end plate used the CAX8. At the given frequency, the direct steady-state dynamic analysis will provide the steady-state amplitude of the response of a system due to harmonic excitation and the transmissibility result was obtained from the ratio of the displacement response of the output end plate to the input

displacement excitation applied to the input end plate. The figure below was shown the results obtain from the ABAQUS FEA due to the solid rubber and the LR-MS isolator. The different types of lines on the result indicate the experimental result for the dashed black line and the solid grey line was representing the FEA result. Based on the result, the observation is the FEA result have good agreement with the experimental data and the presented methodology has good accuracy for analysing solid rubber and LR-MS isolator.

2.3.4 Comparison for Finite Element Analysis Result

The natural frequency for all the isolators was maintained at the low-frequency while frequency while exhibiting better high-frequency performance for the bigger number of metal plates. Between the tested model, the LR-MS 4 was indicated the best dynamic performance among all the tested model because of the stiffness changes of isolator structure with the presence of interlayer metal plates. The better isolation performance, especially at high frequency is the greater stiffness.

For the conclusion, the dynamic analysis of solid rubber isolator and LR-MS was carried out using finite element method in ABAQUS was shown more interlayer metal plate inside LR-MS has better transmissibility performance at the higher frequency and the FEA method has good accuracy for analysing cylindrical solid rubber and LR-MS isolators.

2.4 Parameters Assessment on Laminated Rubber-Metal Spring

The most important part of a vehicle is the internal combustion engine part. When the system is running, it will produce the noise and the vibration. This noise and the vibration that generated from this system cannot be neglected because it is the natural reaction. The engine mounting basically only can absorb up to 30 percent of the vibration amplitude that produces by the vehicle engine and the other 70 percent will transfer to the body of the vehicle. From

this 70 percent of the vibration, it will disturb the driver and the passenger on the car and adding with by another source of vibration such as from the tyres and road surface.

2.4.1 Parameters Selection

In this study, the selected parameter is the mass, Young's Modulus, and the radius. From this three-selected parameter, the mass is chosen as the importance parameter because it can to influenced the point of the natural frequency ω_n . The statement will prove by the equation below.

$$\omega_n = \sqrt{\frac{k}{m}}$$

where k is the stiffness of the system and m is mass.

From this equation, we know the natural frequency is influenced by the stiffness k and the mass m. It means the value of the natural frequency will be reduced when the mass is increase. The second importance parameter is Young's modulus. This will be simplified by the equation below.

$$k = \frac{EA}{L}$$

where E is Young's modulus, A is the area and L is the length.

From this equation, the value of the stiffness is directly proportional to Young's modulus and it will prove if the area and the length of the material are set in the same value. The stiffness value will increase the elasticity of the material increased. The other importance parameter is the value of the radius that used to determine the quantum of an area of a material. The equation below is used to determines the area of the material.

$$A = \pi r^2$$

where r is a radius. From the above equation, the value of an area is directly proportional to the radius. By increasing the radius, the area of the material also increase.

2.4.2 Analysis Result of Laminated Rubber-Metal Spring

Results obtained showed that for the effect of mass on the transmissibility, the value of internal resonance will be closer to unity after the value of mass become decreased and it will be further when the mass volume increased. By increasing the number of degree of freedom, the transmissibility is directly proportional to the quantum of mass and it is inversely proportional. The results also indicate that Young's modulus parameter does not directly affect the transmissibility value for this material. Finally, the effect of the radius was also obtained which revealed that when the smaller radius is used, then the LR-MS will be further away from the unity and by increasing the number of degree of freedom, then the LR-MS will be more ideal in terms of its transmissibility.

2.5 Finite Element Analysis for Leaf Spring

In commercial vehicles, the leaf spring is one of the importance parts of suspension component. The purpose of the leaf spring is to absorb shock load and vibration in the automobiles like heavy duty truck and in the rail system. To meet the needs of the natural resource conservation, energy, and economy, recently the automobile manufacturers have been attempting to minimise the weight of the vehicle.

This study has been carried out on a multi-leaf spring consists of seven leaves of given specification by using the Static structure and the Harmonic Response analysis using ANSYS to find the stress and deformation of the material. The objective of this study is to study the multi-leaf steel leaf spring and verification of the results within the desirable limits. The model of the leaf spring is done and imported into the ANSYS Finite Element Analysis workbench to analyse. This analysis was carried out by using three different materials, namely AISI 6150

Steel, Ti-6Al-4V alloy and S-Glass Fibre Composite for the static analysis as well as for harmonic response analysis.

2.5.1 Harmonic Response Analysis

Harmonic response analysis is a technique used to determine the steady-state response of a linear structure to loads that vary harmonically with time. The main motive is to calculate the structure's response at several frequencies and obtain a graph of displacement versus frequency. The leaf spring based on S-Glass Fiber Composite and Ti-6Al-4V alloy has a lower mass compared to AISI 6150 Steel. The total mass of S-Glass Fiber Composite, Ti-6Al-4V alloy and AISI 6150 steel based multi-leaf spring is 10.278 Kg, 18.318 Kg and 32.532 Kg respectively. Reducing the leaf spring mass in automobiles, we can achieve better riding comfort against hard braking and acceleration. Under the same static load conditions, the stresses in leaf springs are found with the great difference. Stress in S-Glass Fiber Composite is found to be more as compared to conventional AISI 6150 steel. Titanium alloy based leaf spring, under same static loading conditions, shows lesser stress than S-Glass Fiber composite and AISI 6150 steel based leaf spring.

2.6 Modal Analysis Study

Modal analysis is used to determine the vibration characteristics (natural frequencies and mode shapes) of a vibration system. The results from modal analysis may be further applied for another dynamic analysis via mode superposition method.

2.6.1 Vibration Mode Shape Frequency and Natural Frequency

Figure 4.1 shows the results obtained through the modal analysis made by using FE analysis. This figure shows six vibration modes based on the analysis that was carried out to a plate. Based on the FE analysis shown in Figure 4.1, it is shown that a simulation using FE modelling not only extract the natural frequencies but also to show the form of frequency vibration modes. For example, the first modes, or can be also called as bending modes, it has

the natural frequency of 32.775 Hz. Meanwhile, for the second vibration modes, or also known as torsional modes, the natural frequency was 52.996 Hz. Then, for the third vibration modes, or also called as double bending modes with 91.547 Hz of natural frequency. For the fourth vibration modes, it has the natural frequency of 113.69 Hz and called as double twisting modes. Meanwhile, for the fifth vibration modes and also known as triple bending modes, the natural frequency was 179.75 Hz. Lastly, for the sixth vibration modes, or also called as triple twisting modes, it has the natural frequency of 188.7 Hz.

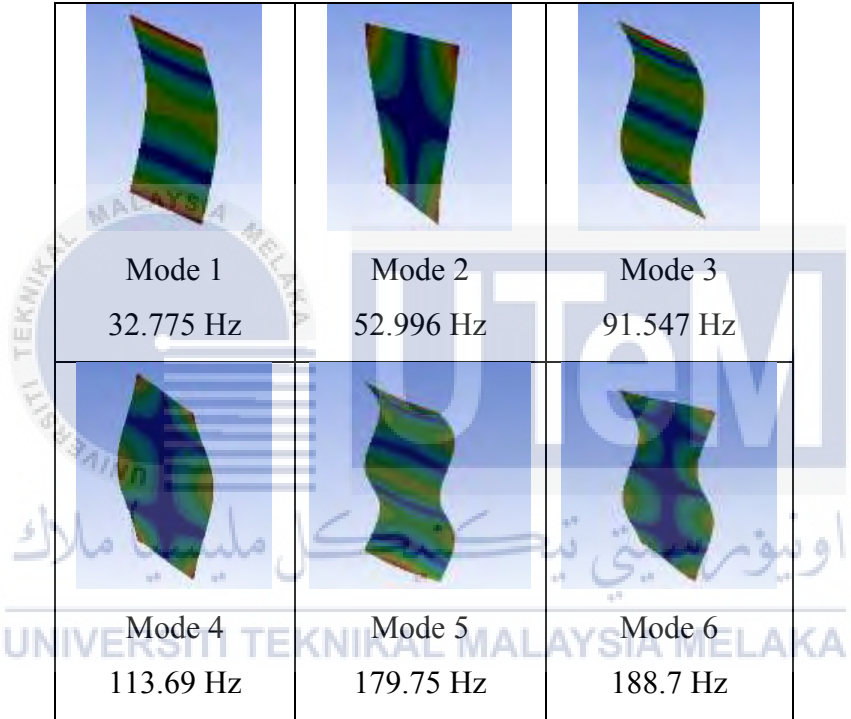


Figure 2.8: Vibration Mode and Natural Frequency for a Plate.

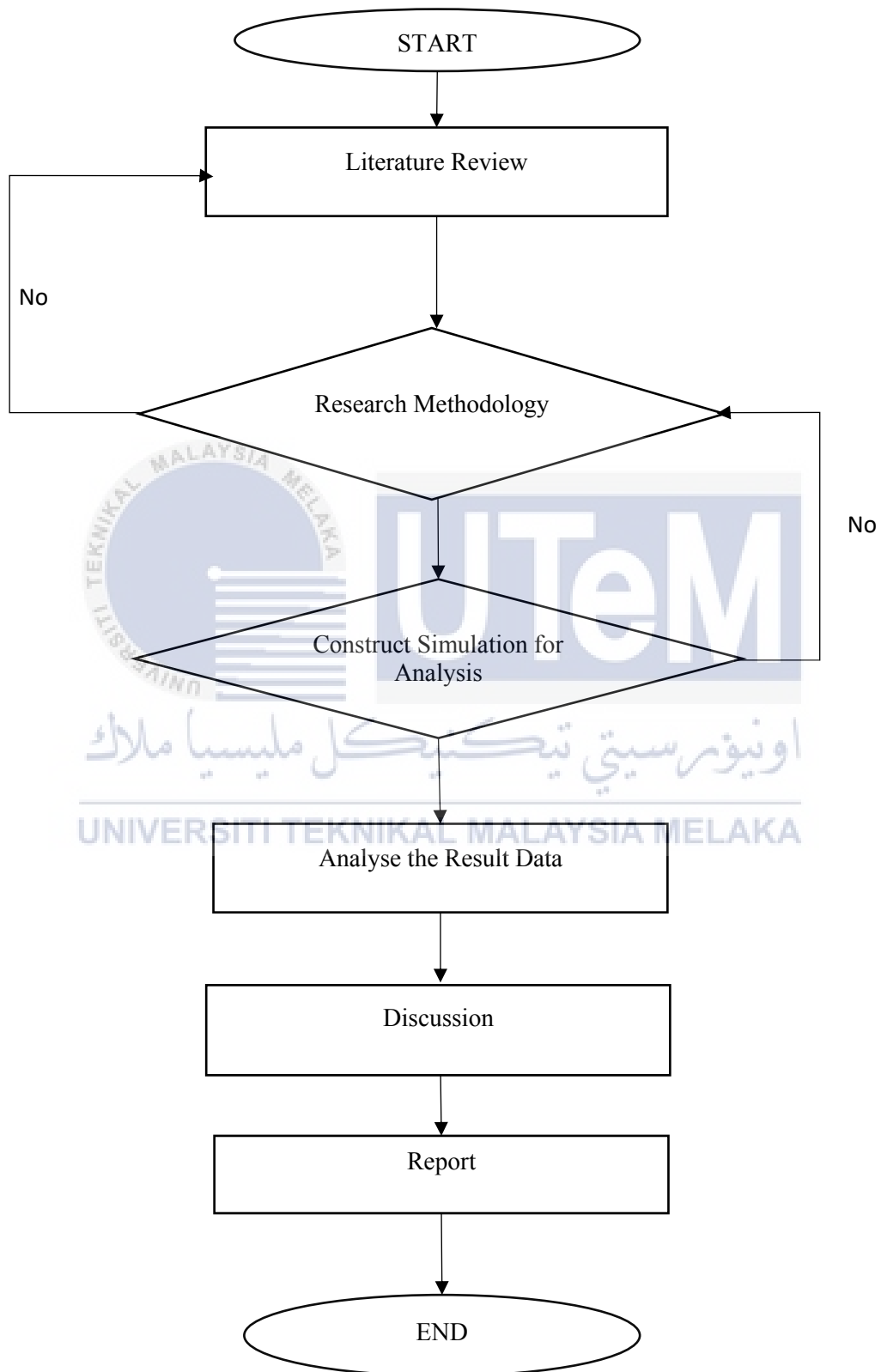
CHAPTER 3

RESEARCH METHODOLOGY

3.1 Introduction

This chapter will describe and cover the detail explanation methodology method that we will use in this project to obtain the data. For the first step in the methodology, we need to identify the literature review about this project. The literature review is an evaluative report and information finding from previous research that can get from any source such as at the book, journal, laboratory report, internet, or others. The importance of the literature review is to make sure the information that found for the literature review related to the area of study in this project. Then, from the literature review, we can get the information to perform analysis, we can run the project analysis by following the step procedure. Static structure analysis is a method to analysis for the laminated rubber and metal due to the force was given. By study and understanding the function of the static structure, this project will be easier to start. The static structure analysis divided into four part which is the engineering data, geometry, model, setup, solution and the last one is the result. Make sure all this part is right before running the analysis to avoid the problem while the analysis is running. The flow of the method used in this project will show with more detail on next part in this chapter.

3.2 Overall Flowchart



3.3 Data Collection

The literature review is a step to find the information and the data collection that related to this project. By using this method, the getting information is easy to analyse, describe and evaluate to use for analysis the model in this project. All the writing that identify related with the study field must be read to get the data collection to use in the project. The literature review is a method to find the information, definition and solution based on previous research. From the collected data, the needed value for starting the analyse was identified as shown in the table below.

Table 3.1: Material Properties of Natural Rubber for Analysis

Mass density	920 kg/m ⁻³
Young's modulus	1.4 MPa
Poison Ratio	0.49
Tensile Strength	6900000 Pa

Table 3.2: Material Properties of Aluminium Alloy for Analysis

Mass density	2770 kg/m ⁻³
Young's modulus	7.1 x 10 ¹⁰ Pa
Poison Ratio	0.33
Tensile Strength	2.8 x 10 ⁸ Pa

3.4 Computer Aided Design

3-dimension (3D) Computer Aided Design (CAD) is a process to define the design process by using the information technology. The system consists of information technology hardware and specialised software. The application is depending based on the area of application because the certain application is more specialised. The computer aided design software is a way to use the graphic application with easily modified the graphical to represent the product. With the short time, the user can perform the complex design model by nearly view the actual product or representations of the real part on the screen and easily make any changes and modification to the model. This way usually uses at the early stages of the product making process because of it able to show the idea about the product design without any prototype.

The 3D modelling becomes popular in any industries such as aerospace and automotive industries because the system can represent the body of the product and today the use of CAD system was expanded to all industries sector such as electronics, textiles, packaging, clothing, and shoe. CAD system is applied to many industries application such as sports-were, computers, equipment, and complex part for the automobile industries. It performs the initial concept before the creation of the manufacturing of the product by using the combination of the digital sketching without enabling the traditional tools to perform the experimentation. So, the user is easy to evaluation and review the quality, accuracy, and precision to integration with engineering concept and the manufacturing process by transfer the data to the CAD systems. The most popular systems in the industries design are Alias/Wavefront, Maya, CDRS, and CATIA.

3.4.1 Step in 3-D Modelling by CATIA.

Step 1: Open the V5R20 CATIA software. Click to “Start” and select the “Part Design” option.

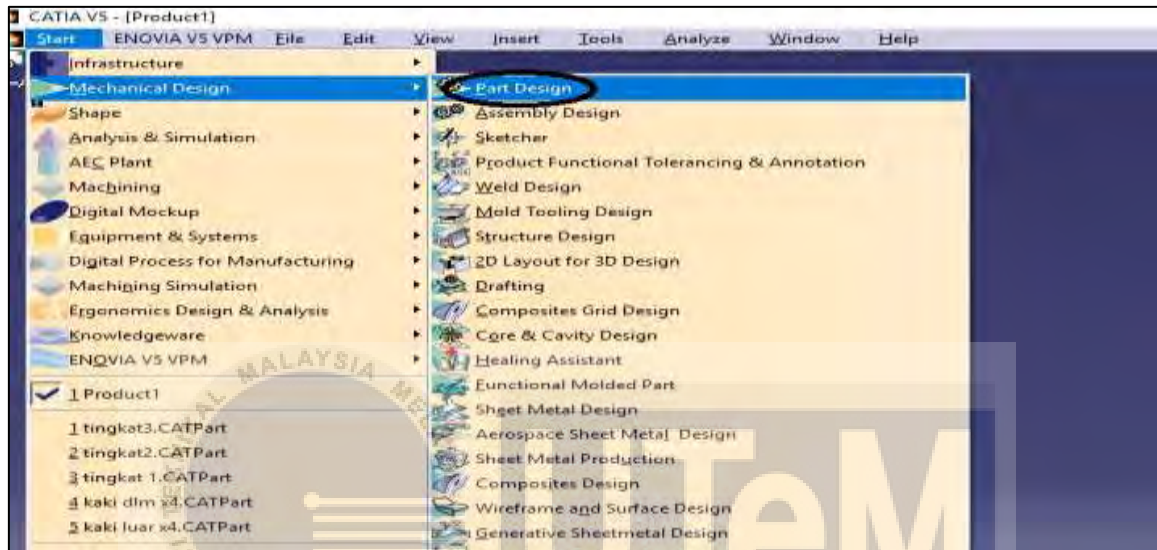


Figure 3.1: Part Design Option

Step 2: Select the axis on the screen and draw the component follow the correct dimension by using the “Profile, User Selection Filter, Operation, and Constrain” option.

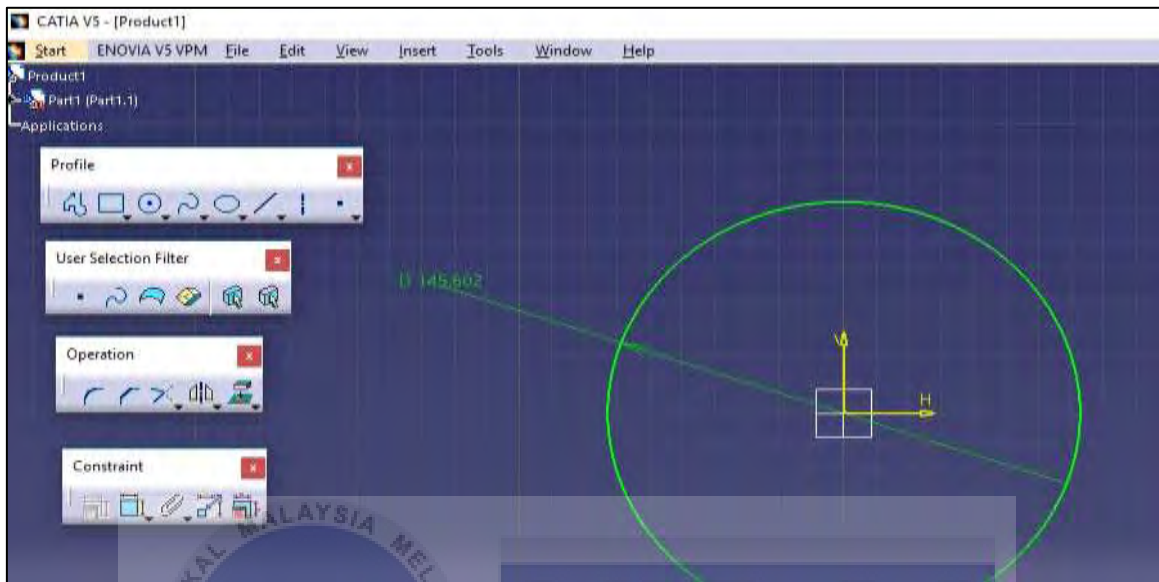


Figure 3.2: Sketching Option

Step 3: Save all the component drawing in a folder. Click to “Start” and select the “Assembly Design” option.

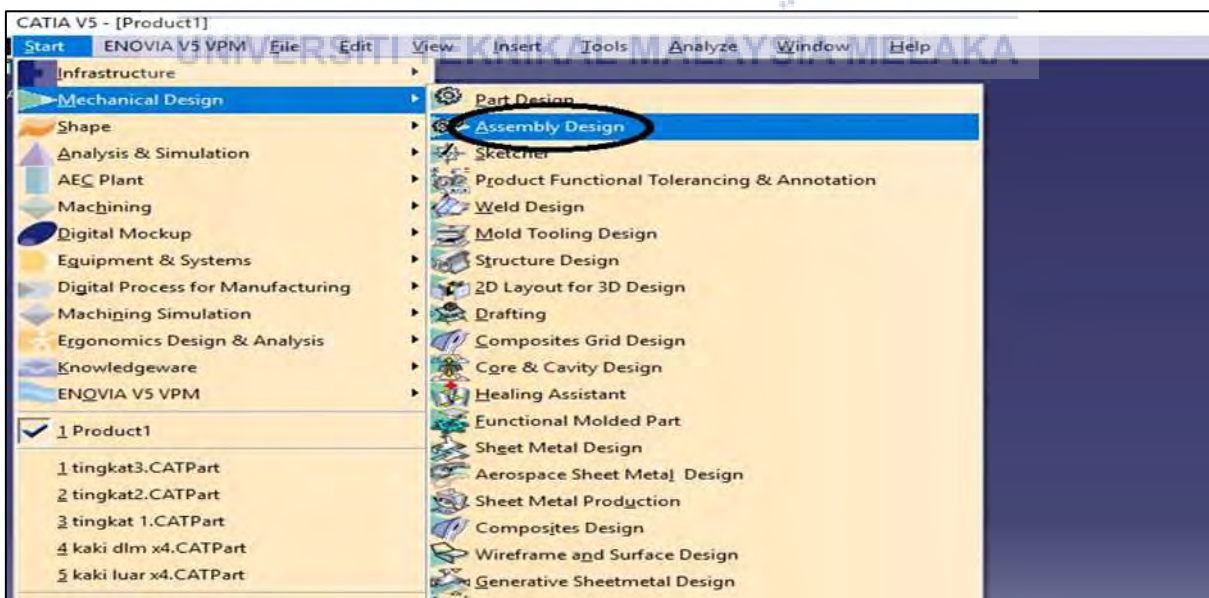


Figure 3.3: Assembly Design Option

Step 4: On the property screen, select the “Existing Component” option to import the component geometry. Select the “Manipulation” option to move the component.

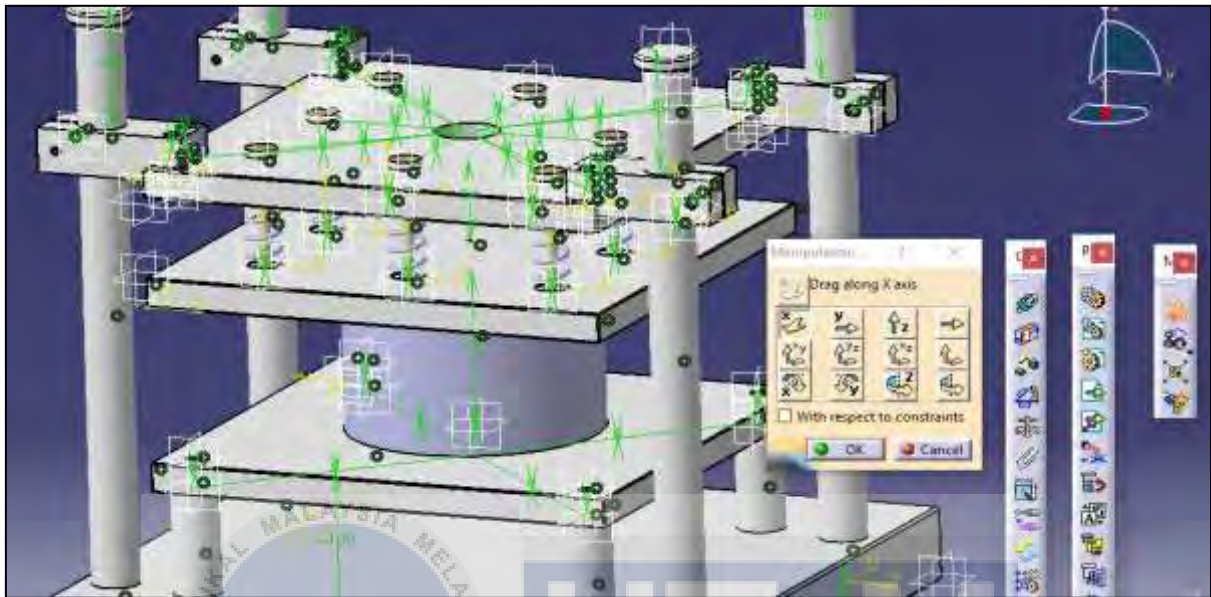


Figure 3.4: Assembly Design Part Component

Step 5: After finish the step, click the “File” and select the “Save As” to save the drawing. Save as the drawing in “.stp” format.

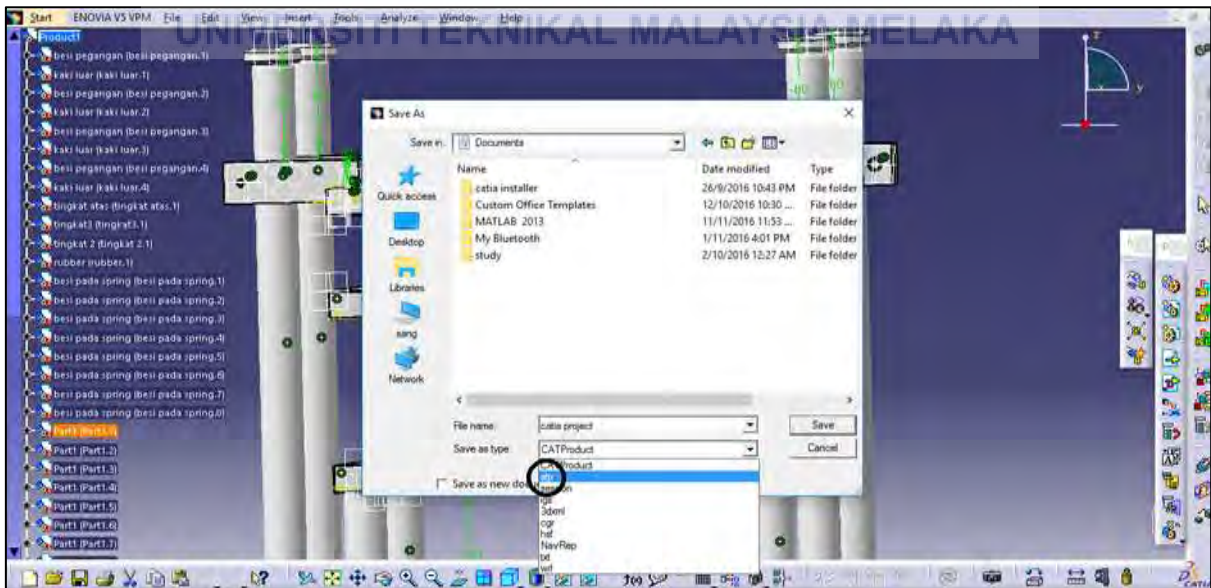


Figure 3.5: Drawing Save Format Option

3.4.2 Step for Design a Part by CATIA.

Step 1: Open the V5R20 CATIA software. Click to “Start” and select the “Part Design” option.

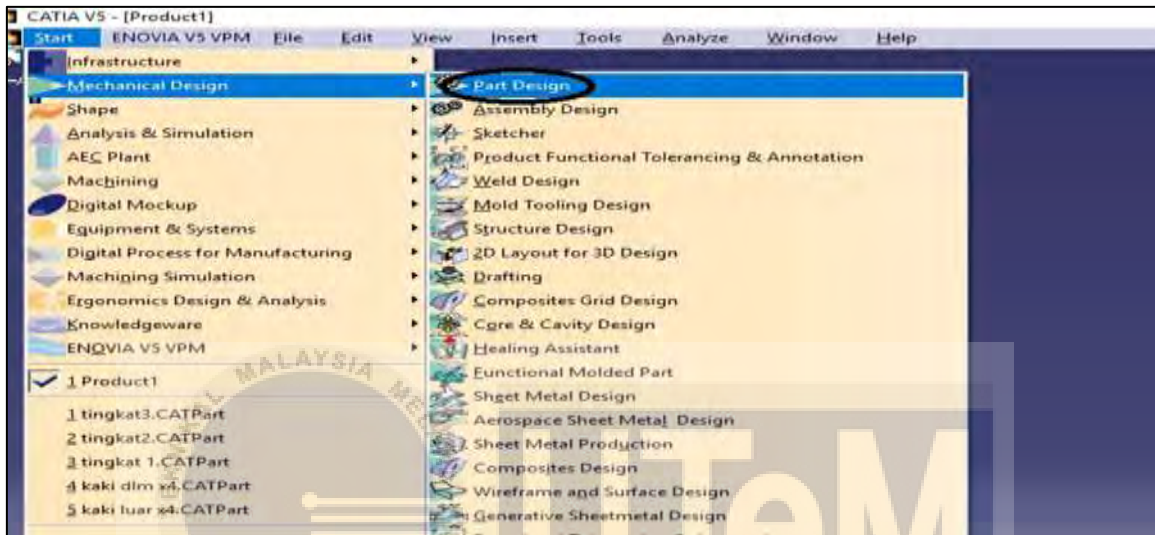


Figure 3.6: Part Design Option

Step 2: Click at the “xy-plane” on the screen, and select the “Sketch” option.

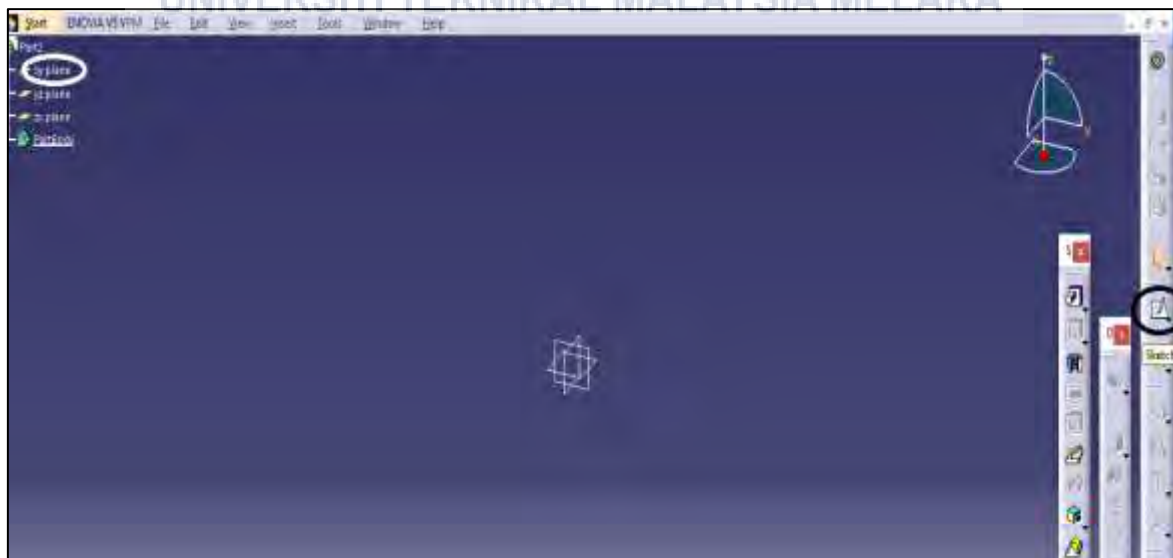


Figure 3.7: x-y Plane Property Option

Step 3: Use the “Profile” option and select “Circle” shape to draw the circle. And then, to set the radius, use the “Constrain” option. Set the needed diameter at the diameter constrain definition column.

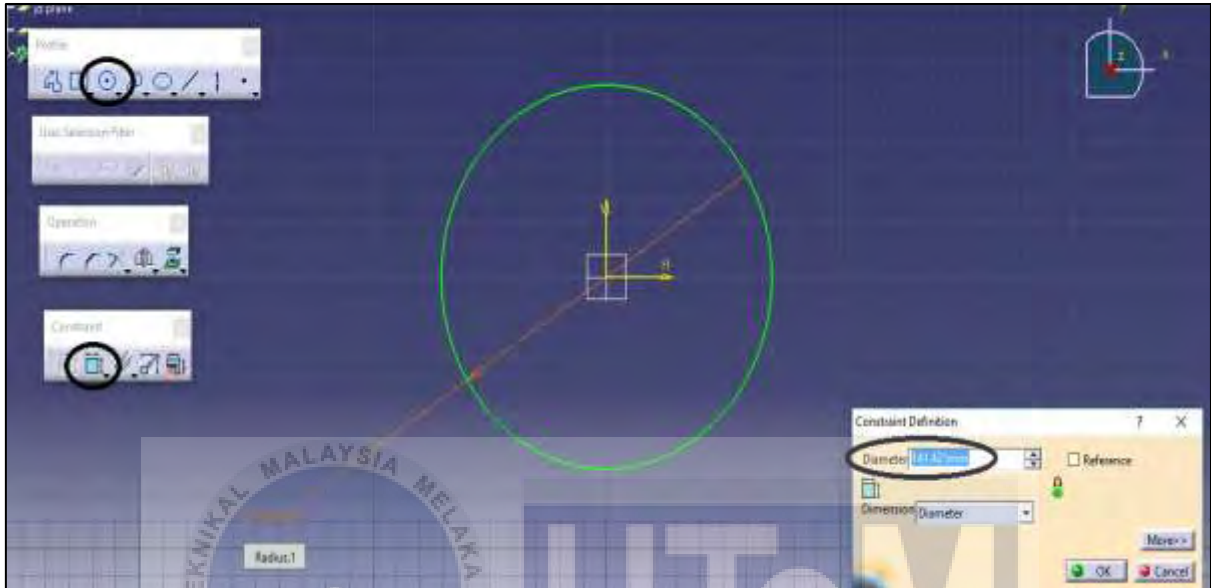


Figure 3.8: Profile Option and Constrain Definition for Sketch

Step 4: After done the step 3, click on the “Exit Workbench” option.

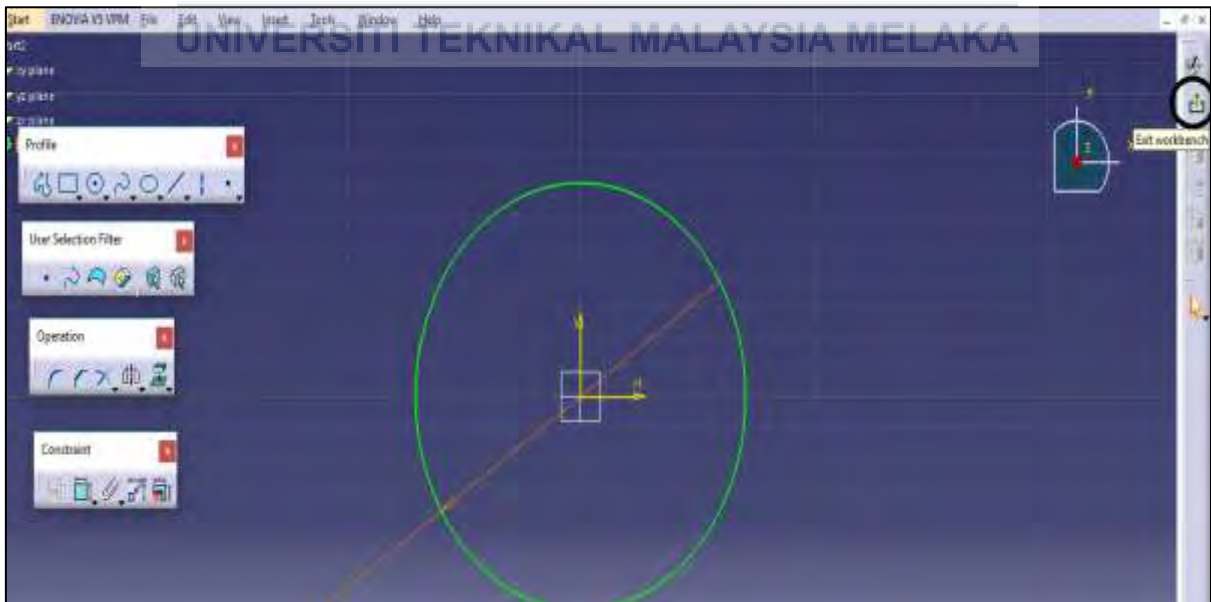


Figure 3.9: Exit Workbench Property Option

Step 5: Click on the “Pad” option, and change the length of the sketch on the pad definition column.



Figure 3.10: Pad Definition Property Option

Step 6: After that, click “OK” and the model will appear on the workbench:

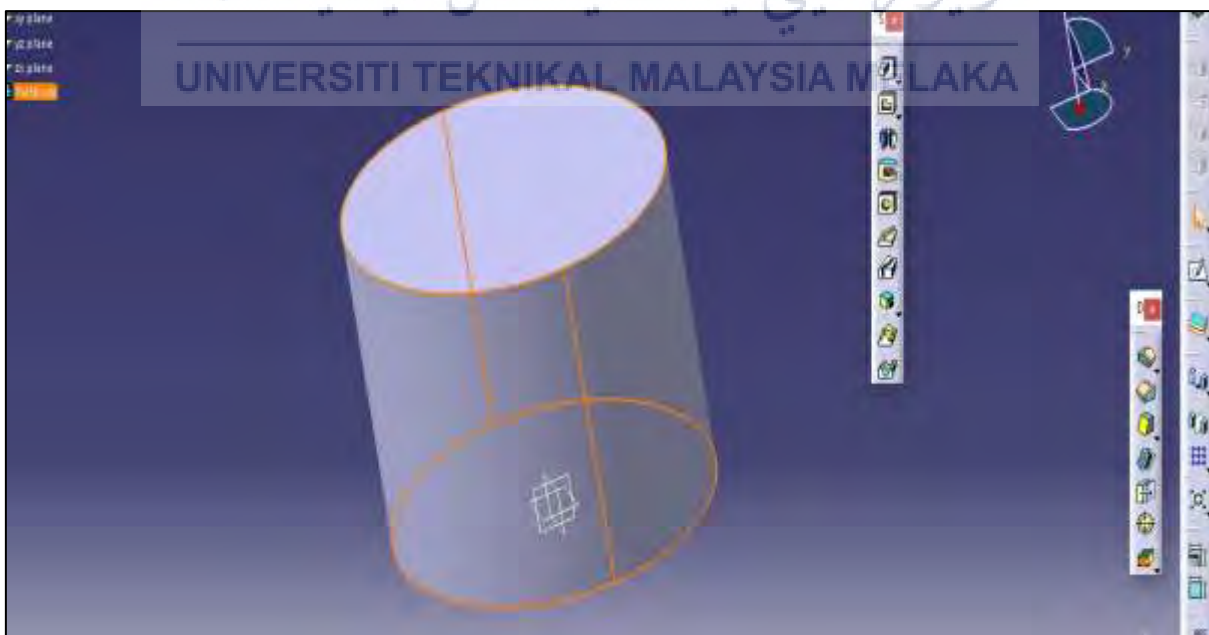
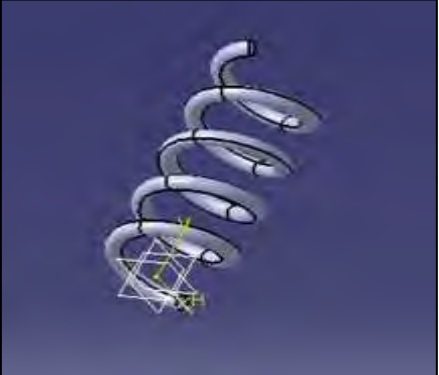


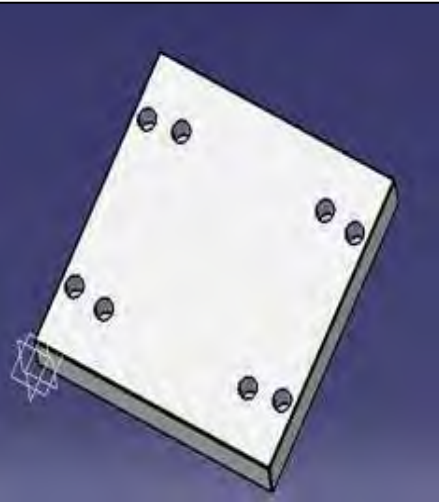
Figure 3.11: Model of the Nature Rubber Rod

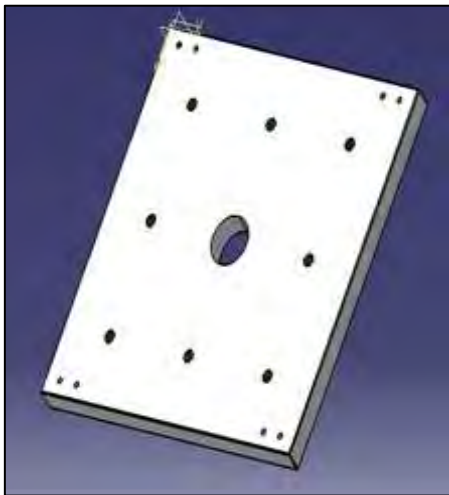
3.4.3 Laminated Rubber – Metal Spring Component

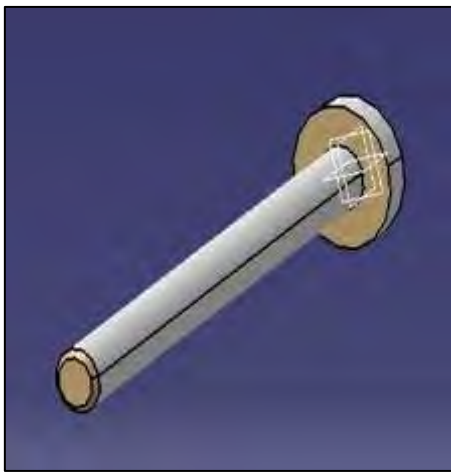
Table below is to show the details of parts component of the LR-MS model after the sketching and drawing process by using the CATIA CAD.

Table 3.3: Component of the LR-MS Model

Name	Part	Specifications
Rubber		Material: Rubber Quantity: 1
Holder		Material: Aluminium Alloy Quantity: 4
Spring		Material: Aluminium Alloy Quantity: 8

<p>Outer Shaft</p>		<p>Material: Aluminium Alloy Quantity: 4</p>
<p>Inner Shaft</p>		<p>Material: Aluminium Alloy Quantity: 4</p>
<p>Structure Base</p>		<p>Material: Aluminium Alloy Quantity: 1</p>

<p>Rubber Base</p>		<p>Material: Aluminium Alloy Quantity: 1</p>
<p>Lower Spring Holder</p>		<p>Material: Aluminium Alloy Quantity: 1</p>
<p>Upper Spring Holder</p>		<p>Material: Aluminium Alloy Quantity: 1</p>

<p>Spring Holder</p>		<p>Material: Aluminium Alloy Quantity: 8</p>
----------------------	--	--

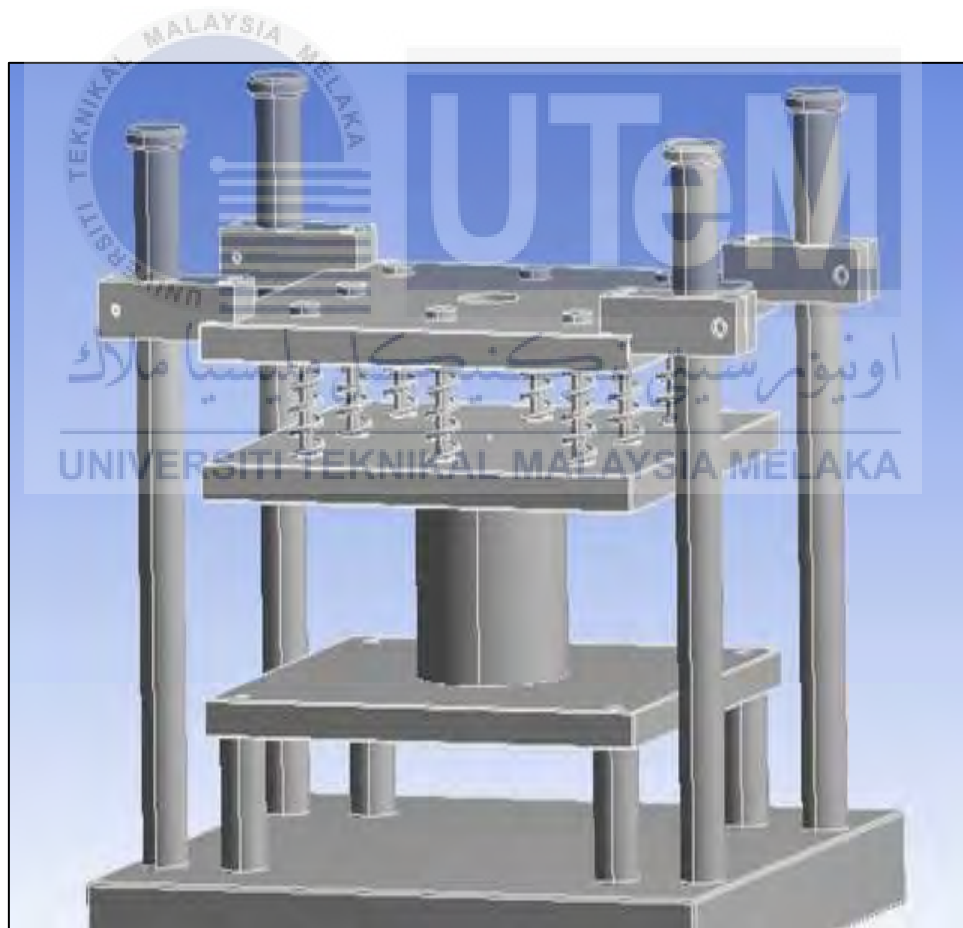


Figure 3.12: LR-MS Model Assembly

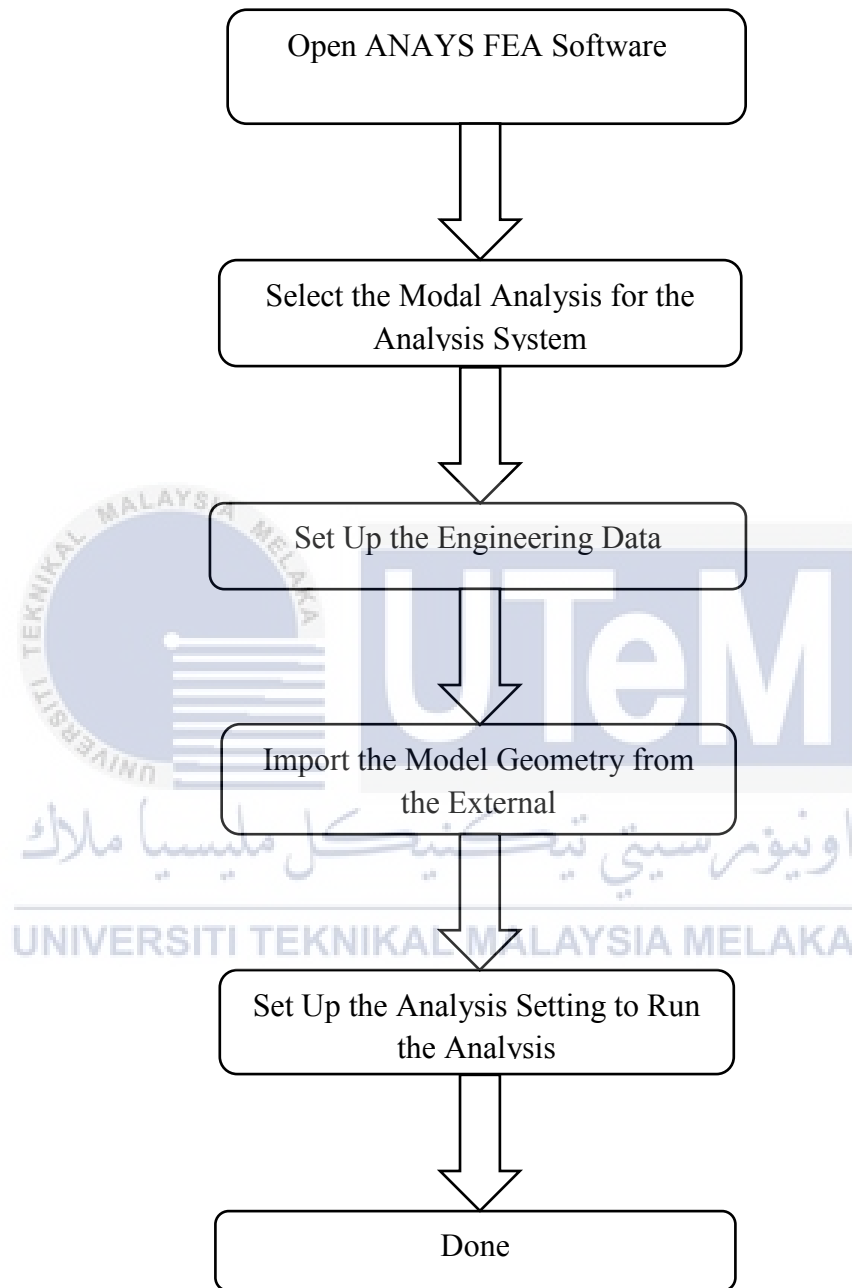
3.5 Finite-Element Analysis

In engineering application, the most famous of the numerical analysis process is the FEA. With FEA, the user easily analyses and study the performance of a product or object by dividing the object into several small building blocks, called FE.

The example of the functional performance of an object is structure stresses and deflection that can be predicted by using this FEA. To forms the model of the real object, the product will have divided into a grid of an element. The element usually has the simple shape such as a square, triangle, cube or any other shape that was related to the FEA program. With the shape, the finite-element analysis program can convey the information to write the governing information's in the form of a stiffness matrix. The unknown parameters for each element are the displacements at the node points, which are the points at which the elements are connected.

With the FEA program, it will assemble the stiffness matrices for the element to the global stiffness form for the whole model. By giving the known force and the boundary condition, the FEA program will solve the stiffness matrix of the unknown displacement. By analysing the displacement of the object at the nodes, the stress of each element can be calculated. Today, for engineering analysis program, the software package was developed for covering a wide range of application. The engineering analysis application is including the static analysis, transient dynamic analysis, natural frequency analysis, heat transfer analysis, plastic analysis, fluid flow analysis, and so on.

3.5.1 Modal Analysis on Ansys Software



Step 1: Open the Ansys software and select the “Engineering Data” to the “Project Schematic”.

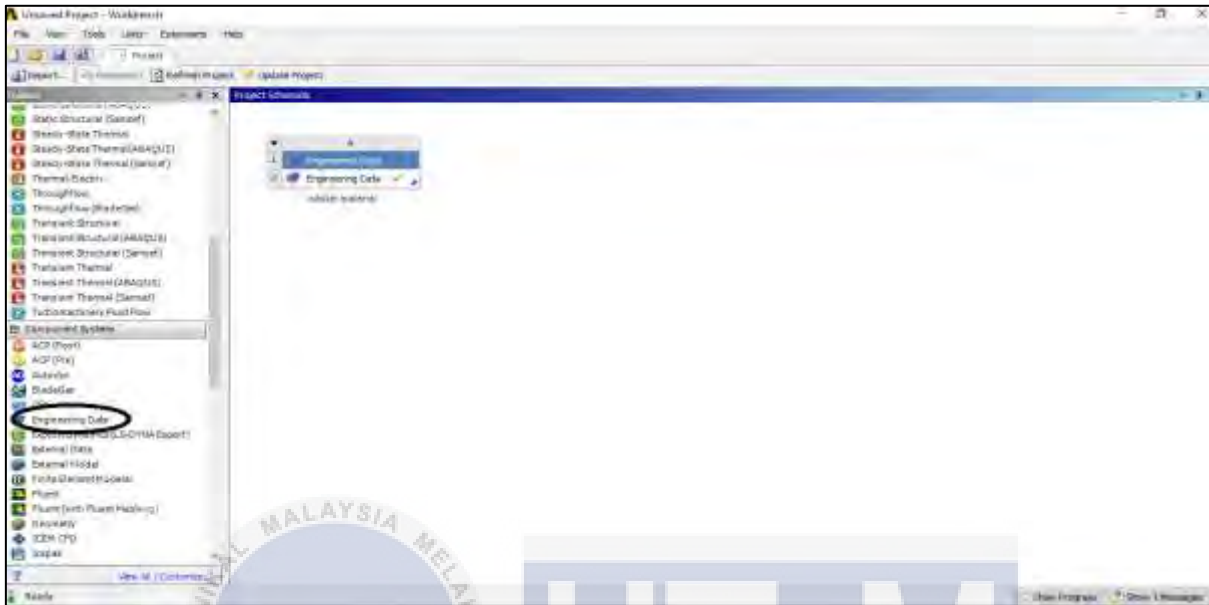


Figure 3.13: Engineering Data Option

Step 2: Select the “Modal” in the “Analysis System” to the “Project Schematic”. And then, share the Engineering Data A and B.



Figure 3.14: Connection between Engineering Data and Modal Analysis

Step 3: To set the rubber material, click the “Engineering Data A” and write down the Rubber in the column “ Click Here To Add a New Material”.

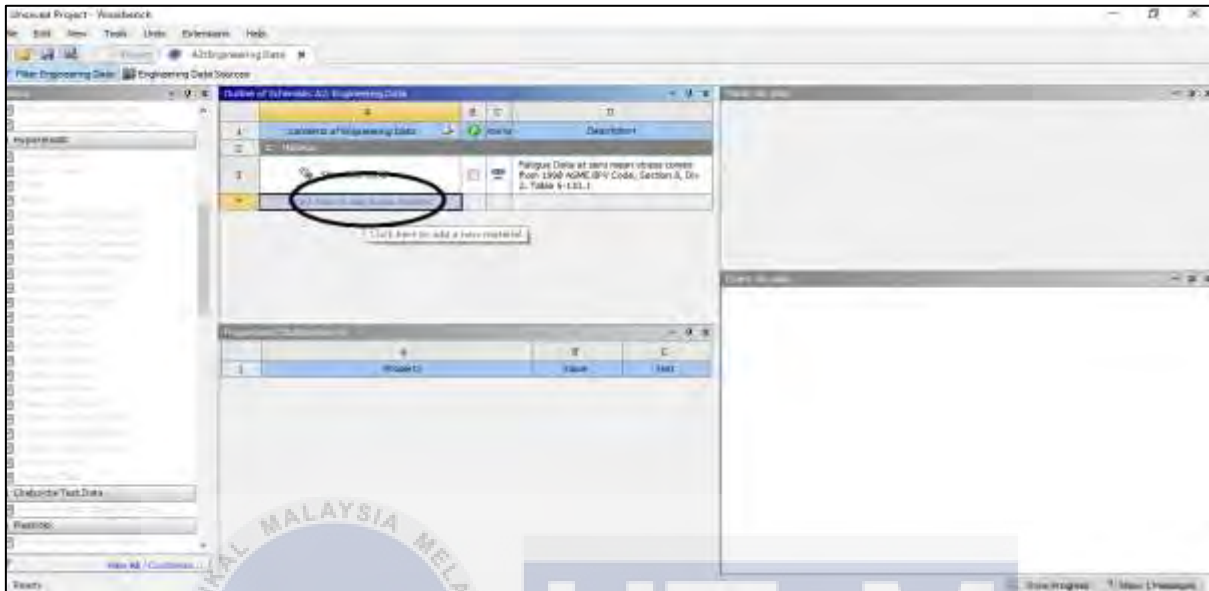


Figure 3.15: Set-Up New Material for the Nature Rubber

Step 4: Double click the “Density” for the “Physical Properties” at the “Toolbox”. Then, set the density for the rubber.

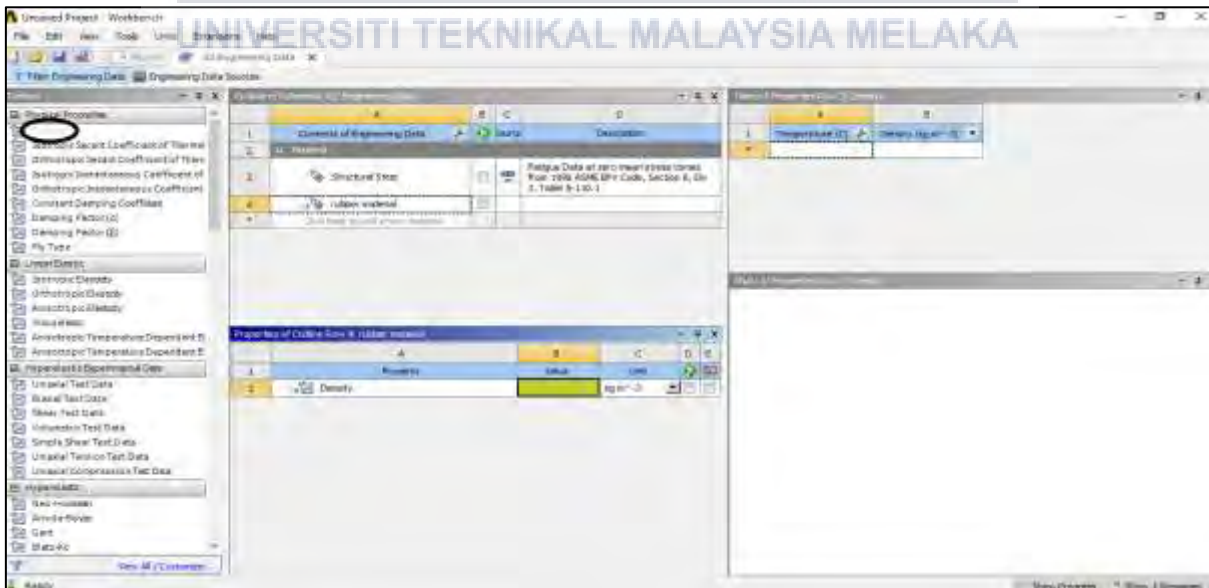


Figure 3.16: Physical Properties for the New Material

Step 5: Double click the “Isotropic Elasticity” for the “Linear Elasticity” at the “Toolbox”. Then, set the Young’s Modulus and the Poisson’s Ratio for the rubber.

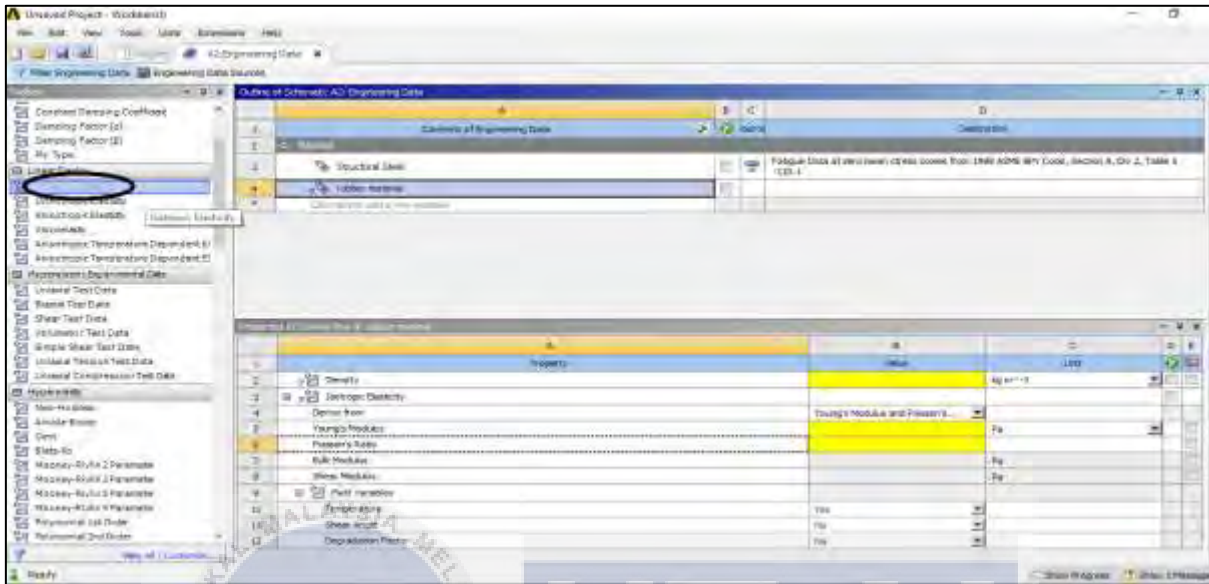


Figure 3.17: Isotropic Elasticity Toolbox Option

Step 6: Double click the “Tensile Yield Strength” for the “Strength” at the “Toolbox”. Then, set the Tensile Yield Strength for the rubber.



Figure 3.18: Tensile Yield Strength Toolbox Option

Step 7: Click the “Engineering Data Source” and click at the “General Material”. Then, choose and click the “Aluminium Alloy” to add in the Engineering Data.

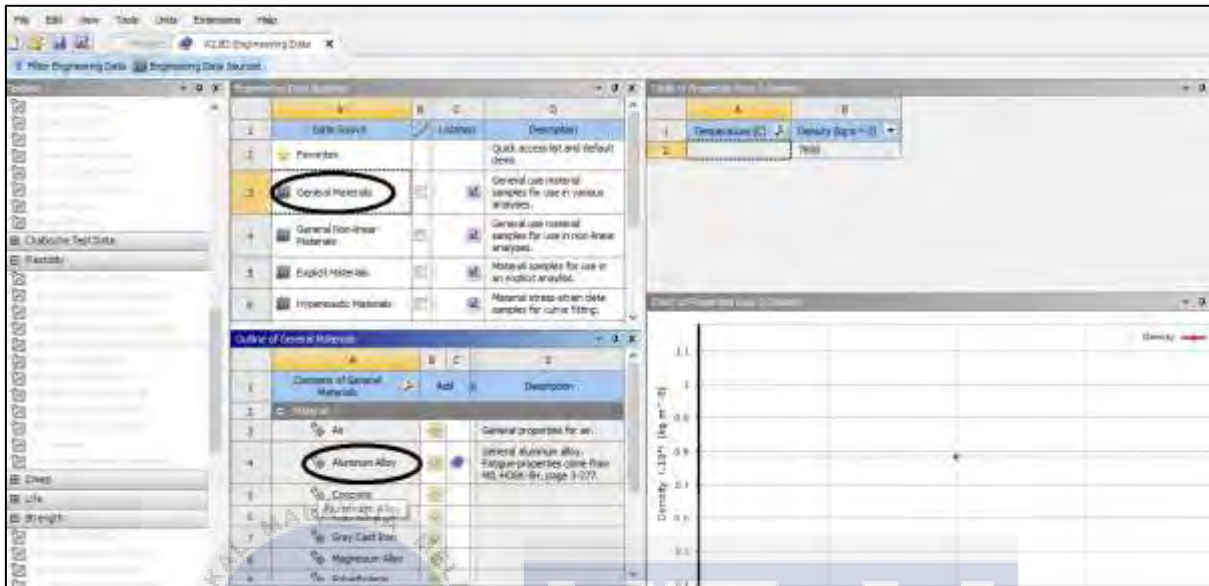


Figure 3.19: Engineering Data for General Material Option

Step 8: Right click on “Geometry” and browse the model from the external.

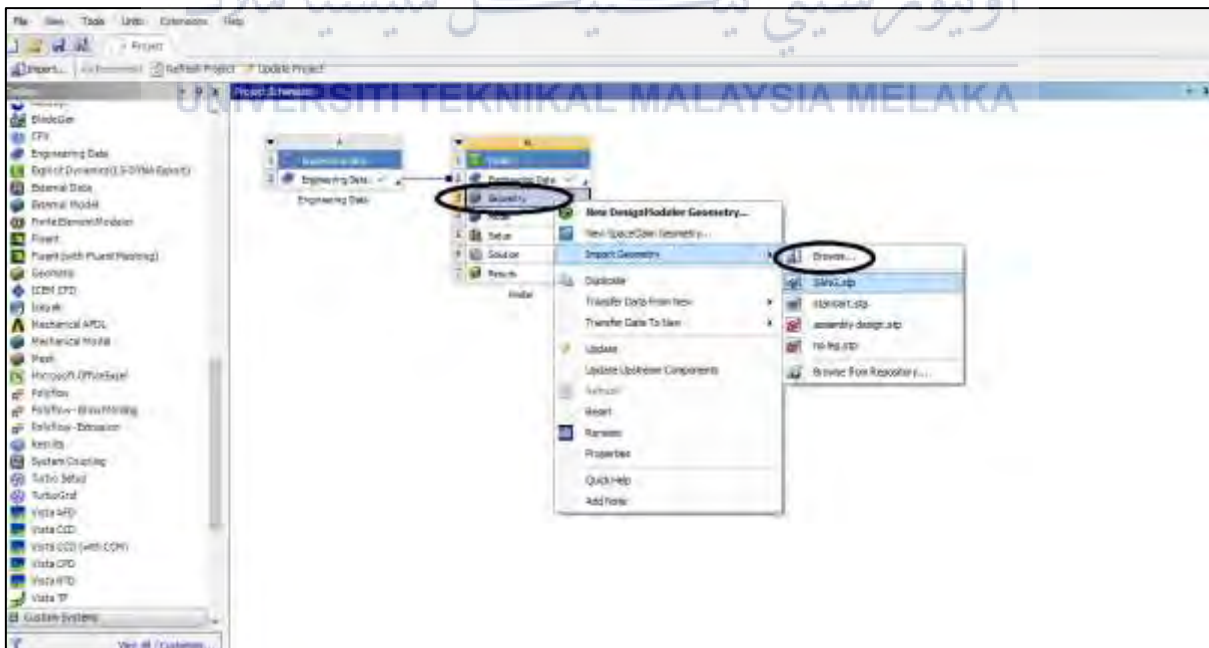


Figure 3.20: Geometry Browse Option

Step 9: Double click the “ Model” on the Work Bench. To change the material of the model, select the geometry part and choose the material.

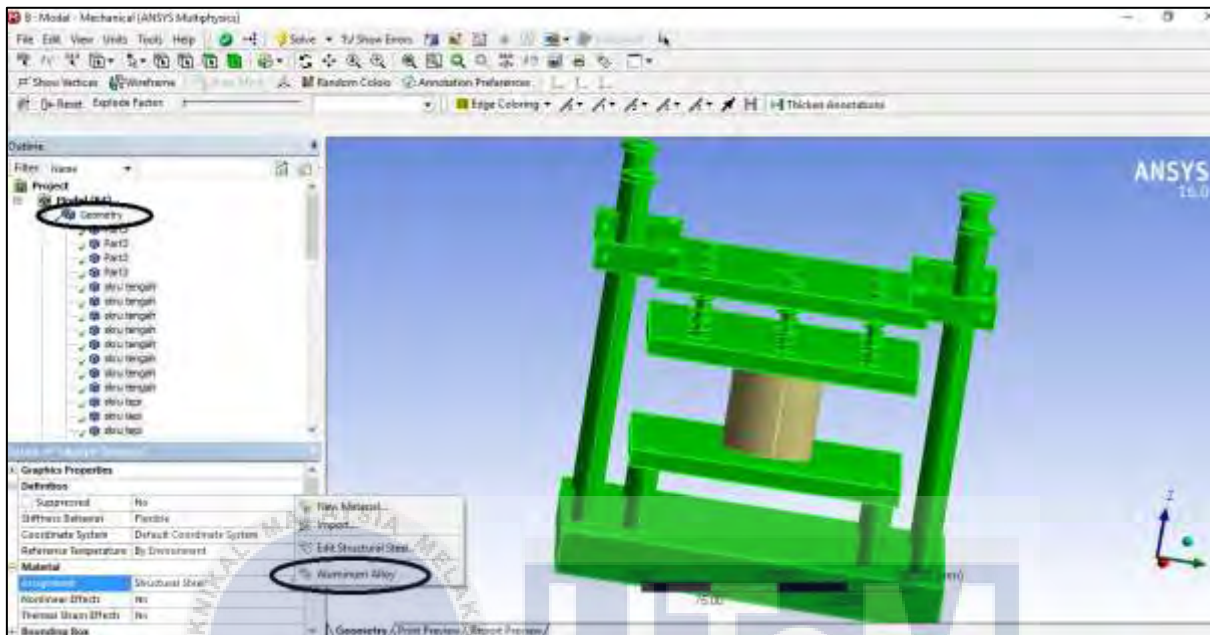


Figure 3.21: Material for Geometry Part Option

Step 10: Right click on “Mesh” and select the “Update” to generate the mesh.

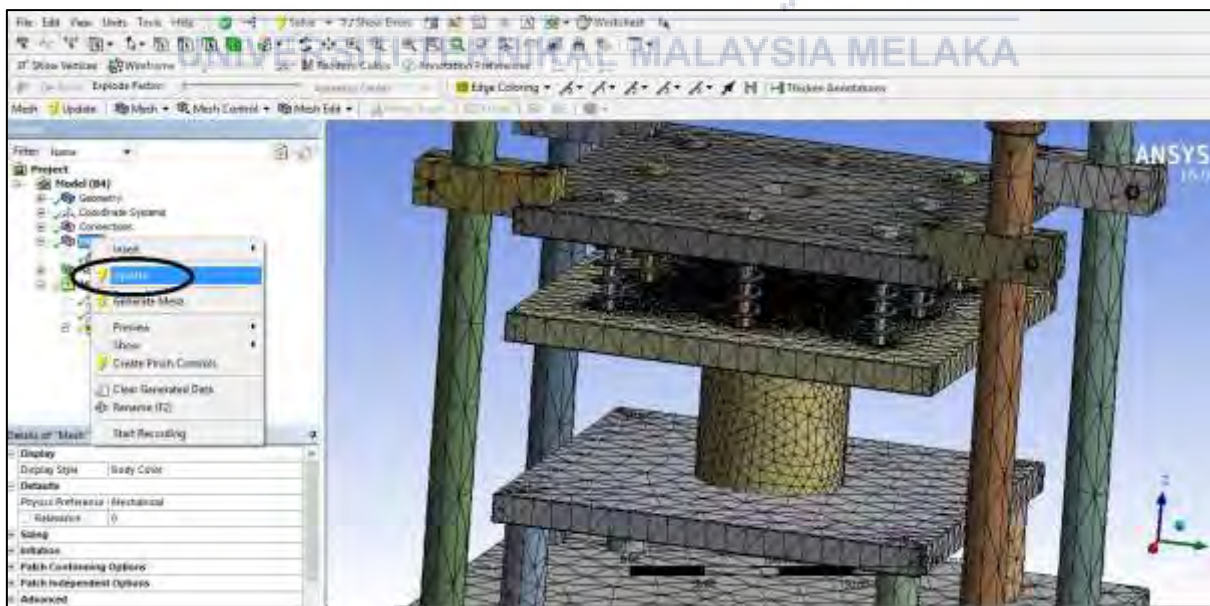


Figure 3.22: Generate Mesh Option

Step 11: Right click on “Modal” and select the “Fixed Support” to build the fix support option to the model. And then, select the “Solve” option to update the project.

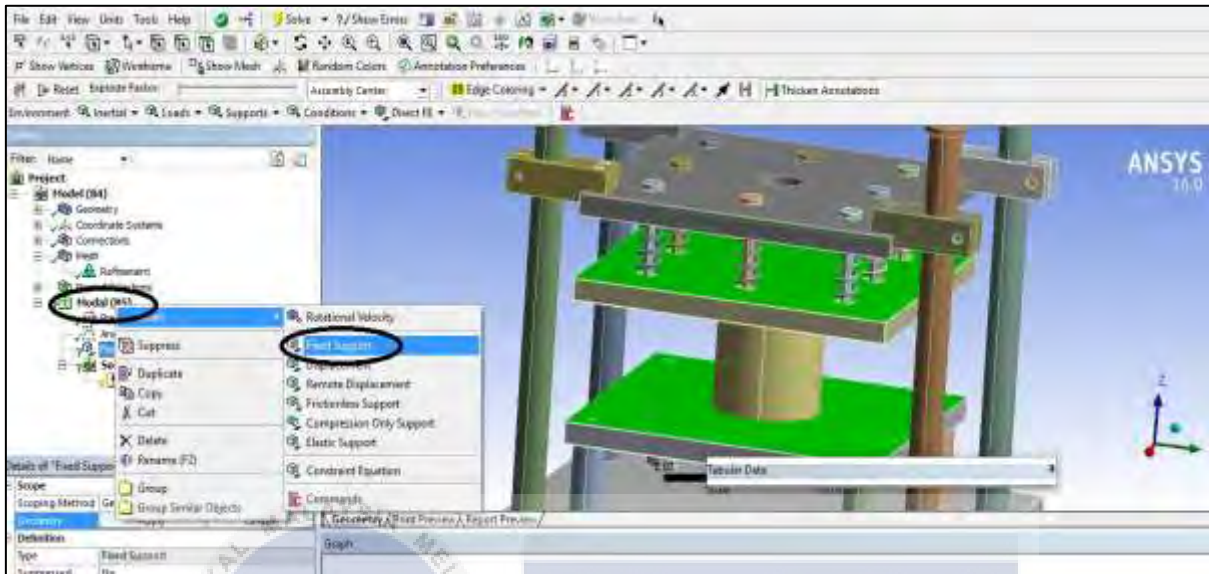


Figure 3.23: Fix Support for the Model Option

Step 12: Right click on “Analysis Setting” and select the “Max Mode to Find” and set the mode for the model.

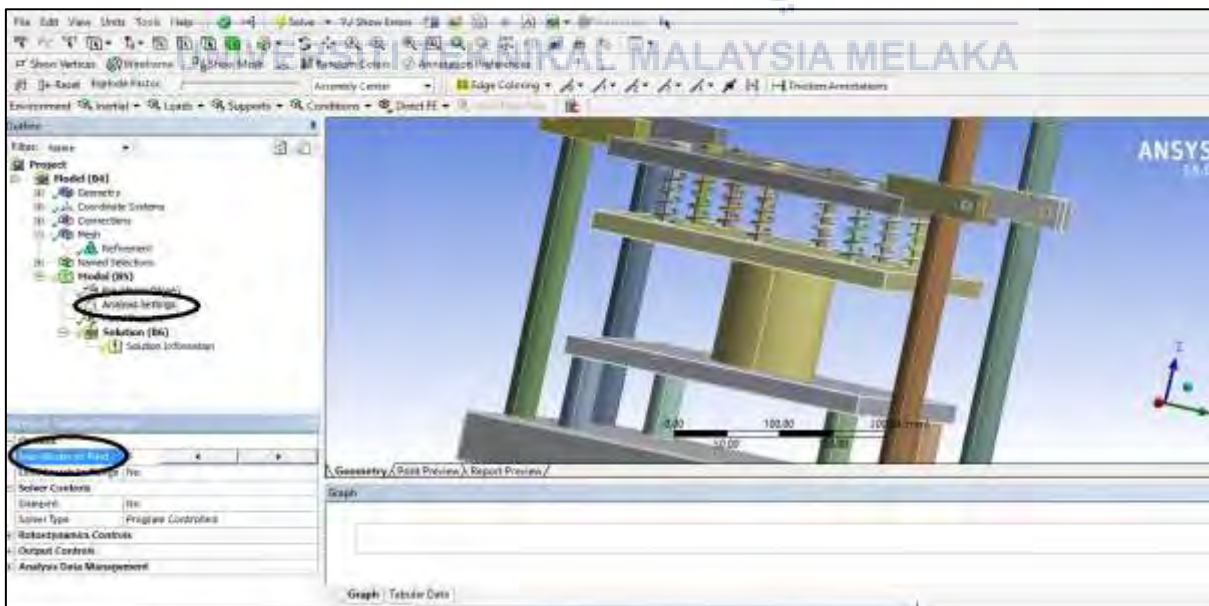


Figure 3.24: Mode Option

Step 13: Right click on “Solution” and select the “Select All” at the graph. Then, at the graph, select the “Create Mode Shape Result”. Then click the “Solve” option to resolve the solution.

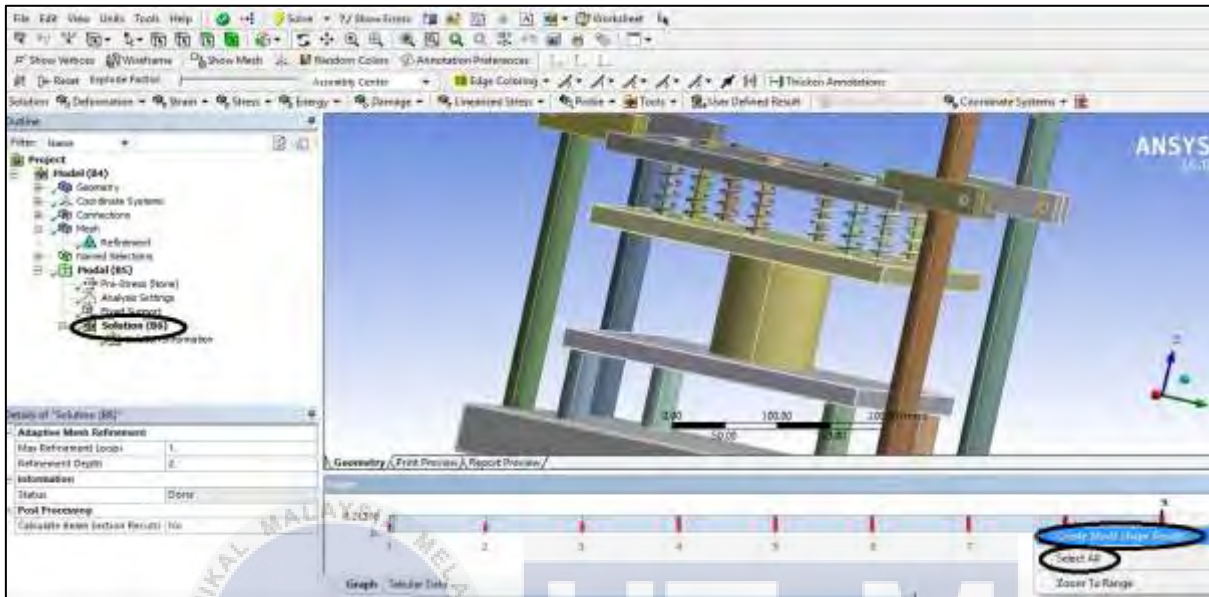


Figure 3.25: Create Mode Shape Result Option

Step 14: Right click on the “Total Deformation” on the “Solution” to know the result of the first “Mode”.

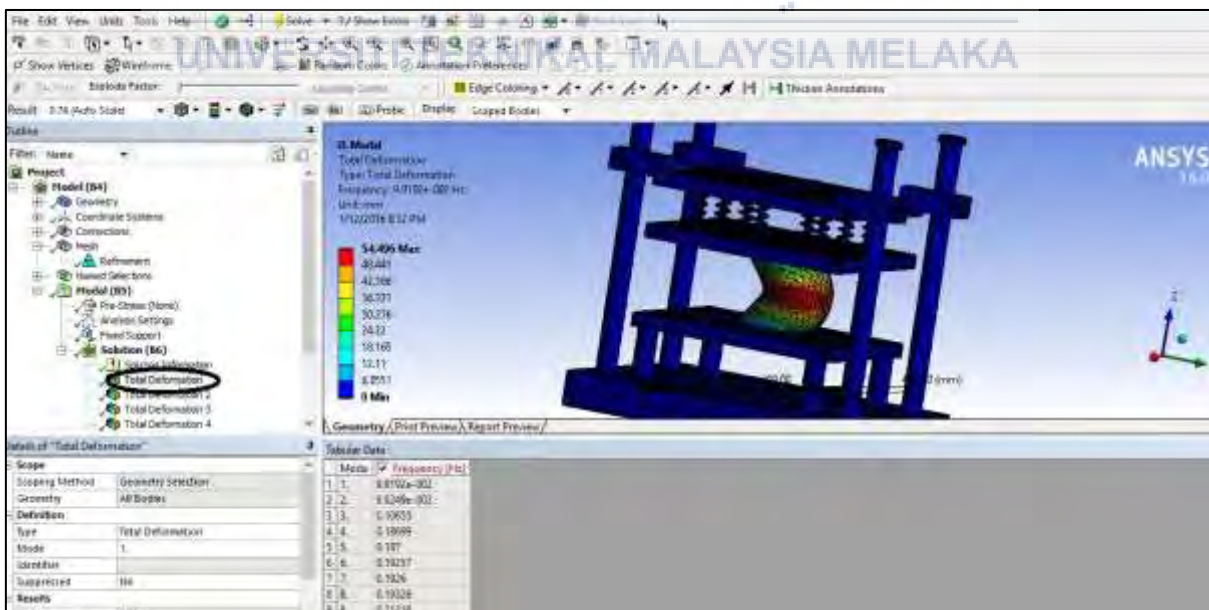


Figure 3.26: Result for the Mode Option

3.5.2 Harmonic Response Analysis on ANSYS Software

Step 1: To set the Harmonic Responses Analysis, choose the “Harmonic Response” and connect with the “Modal Analysis” as shown in figure below.

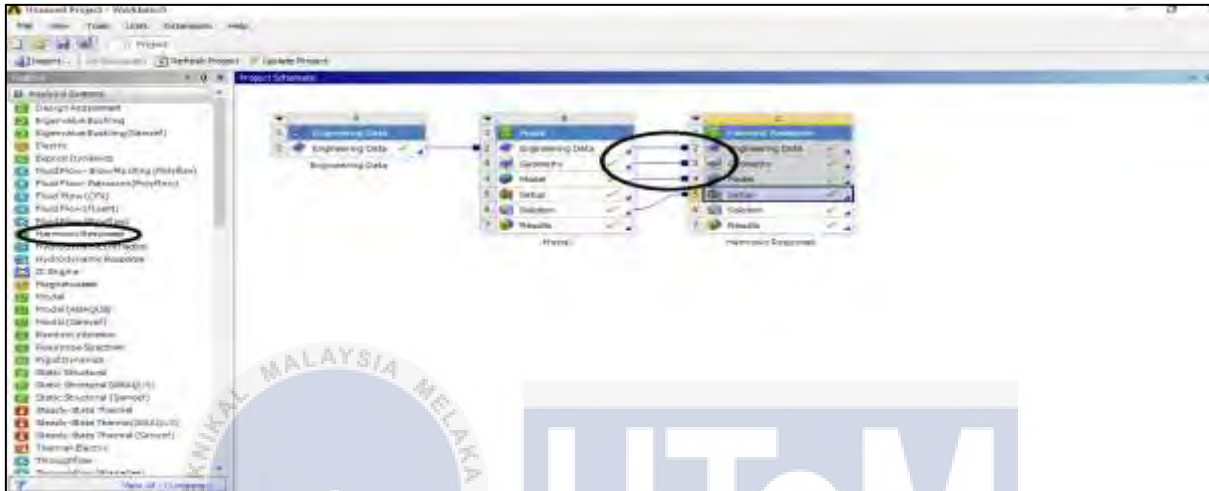


Figure 3.27: Connection Between Modal and Harmonic Analysis Option

Step 2: Select the “Harmonic Response” and click to the “Force” option. On the “Detail of Force” set the needed force due to z-component.

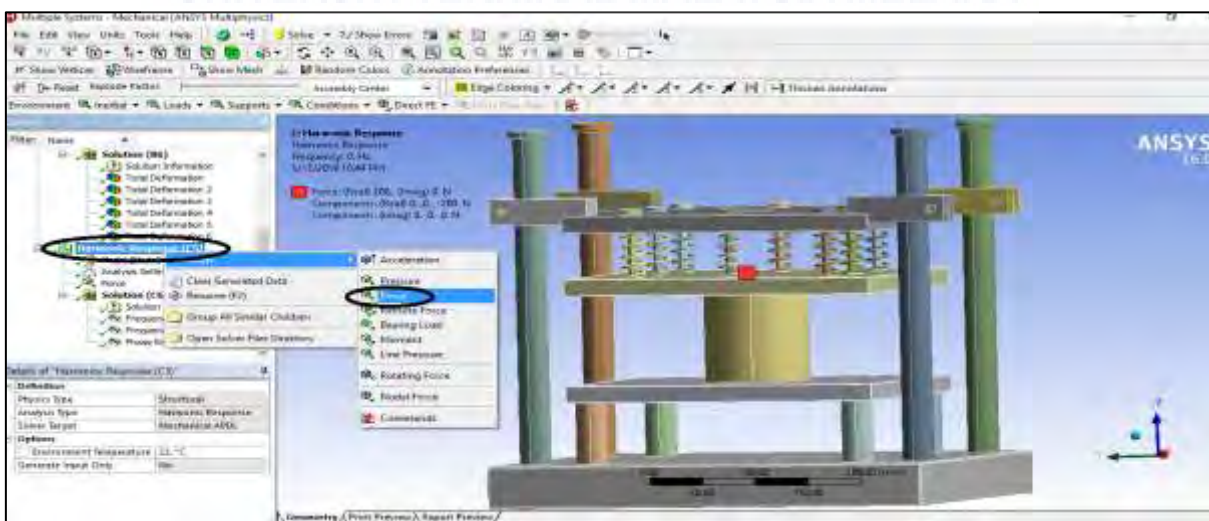


Figure 3.28: Input Force Option

Step 3: Select the “Solution”, click to the “Frequency Response” option, and insert the “Deformation”.

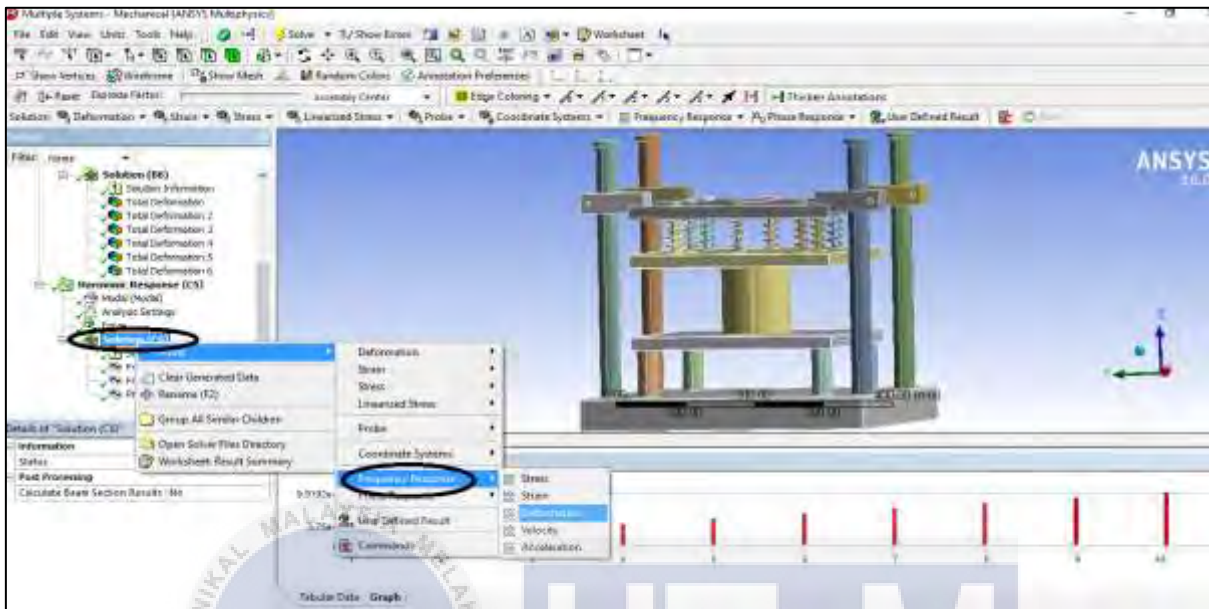


Figure 3.29: Insert the Frequency Response for Deformation Option

Step 4: Select the “Analysis Setting” and go to the “Detail of Analysis Setting”. Set the “Range Maximum” and the “Range Minimum” for the analysis.

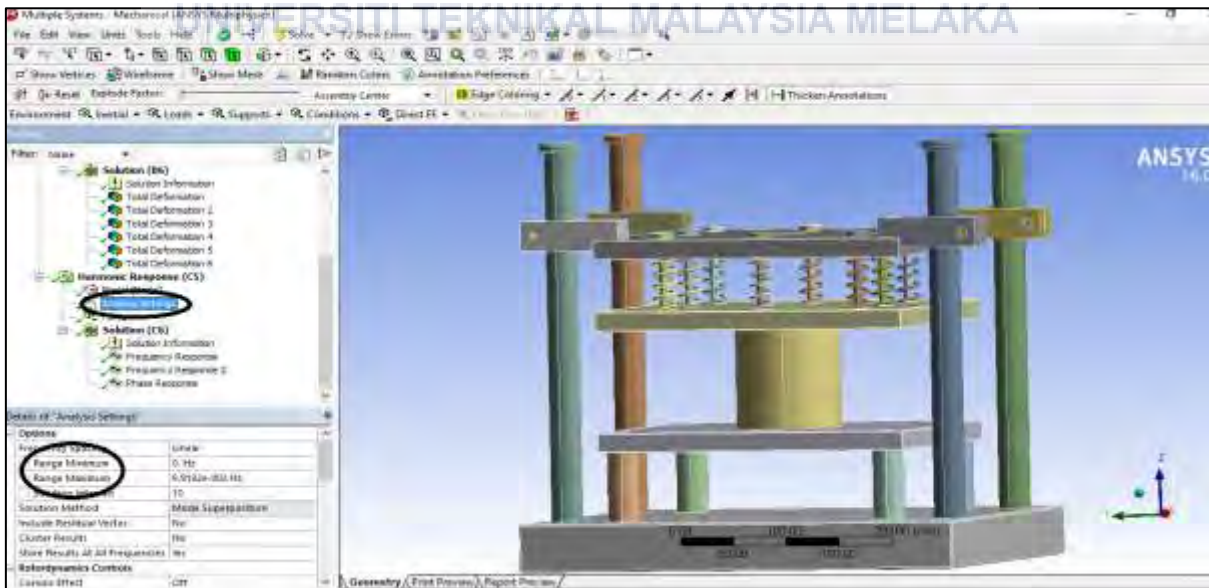


Figure 3.30: Frequency Range for the Model Option

Step 5: After all of the procedure is complete, click the “Solve” to run the analysis.

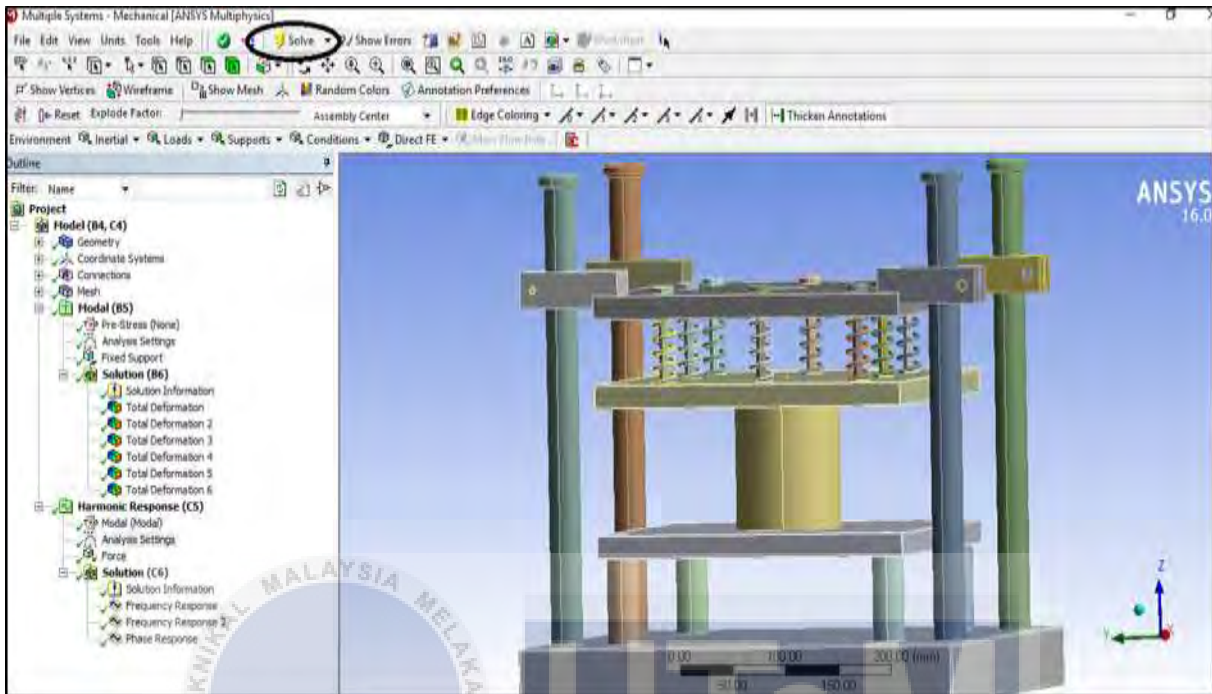


Figure 3.31: Solve Option to Run the Analysis

CHAPTER 4

RESULTS AND DISCUSSION

4.1 Analysis of Nature Rubber Rod by ANSYS Finite Element Analysis

This chapter will generally explain the result from the analysis. By following the required step in the previous chapter, from the analysis, it shows there are different types of colour that generate at all the nature rubber rod. The different colour of the nature rubber rod was represented the different value of the deformation due to the frequency as the Figure 4.1 below. All the data gained from the analysis will be generated in the table and graph in the next part.



Figure 4.1: Result of Analysis

As we can see in Figure 4.1 above, it shows the various type of colour that represent the different value of the minimum deformation and the maximum deformation on the natural rubber rod. The highest value of the deformation was showed the red colour as the indicator. It

shows that the natural rubber rod has been imposed by the highest load and highest deformation was occur on that place. The part that not affected by the deformation will show in the blue colour with the lowest value for the deformation on the natural rubber rod.

4.2 Modal Analysis

From this analysis, the results obtained will show the modal analysis made by using ANSYS Finite Element Analysis (FEA) software. This analysis shows six vibration modes that were carried out to the rubber rod without embedded aluminium alloy on it.

4.2.1 Modal Analysis of the Type 1 Nature Rubber Rod

Based on the FEA is shown in Figure 4.1, it is shown that a simulation using Finite Element (FE) modelling not only extracts the natural frequencies but also to show the form of frequency vibration modes. For example, the first modes, or can be also called as bending modes, it has the natural frequency of 13.951 Hz. Meanwhile, for the second vibration modes, or also known as torsional modes, the natural frequency was 14.039 Hz. Then, for the third vibration modes, or also called as double bending modes with 21.009 Hz of natural frequency. For the fourth vibration modes, it has the natural frequency of 37.949 Hz and called as double twisting modes. Meanwhile for the fifth vibration modes and known as triple bending modes, the natural frequency was 39.925 Hz. Lastly, for the sixth vibration modes, or also called as triple twisting modes, it has natural frequency of 39.947 Hz

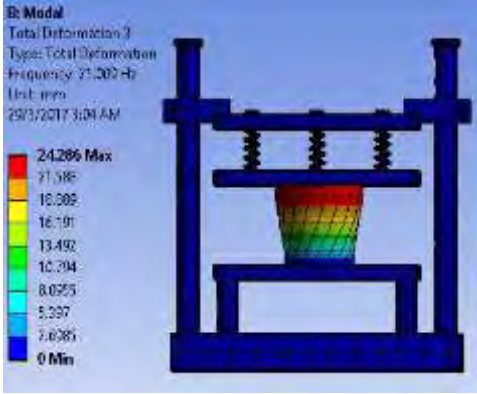
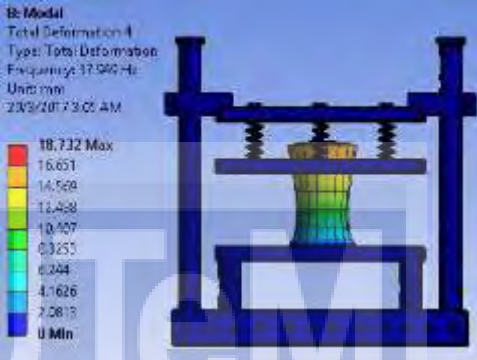
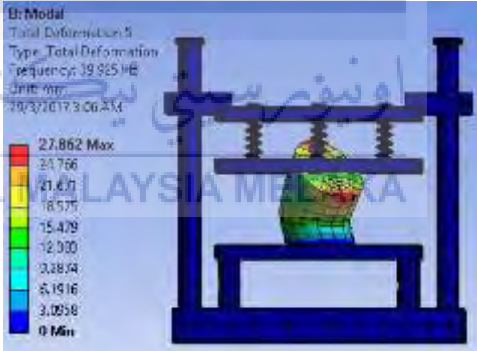
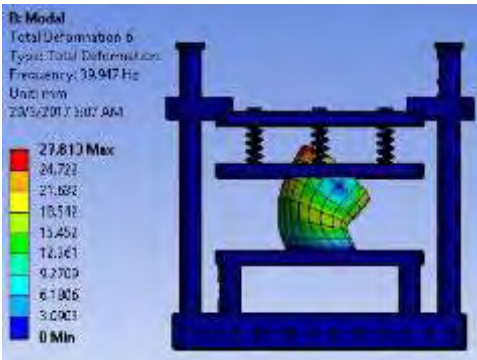
Figure 4.2 below represent the assembly by the CATIA modelling software, for the type without the embedded plate on the nature rubber rod.



Figure 4.2: Assembly Type 1

Table 4.1: Result of the Modal Analysis for Type 1

Modality	Frequency (Hz)	Visual
1	13.951	
2	14.039	

3	21.009	
4	37.949	
5	39.925	
6	39.947	

4.2.2 Modal Analysis of the Type 2 Nature Rubber Rod

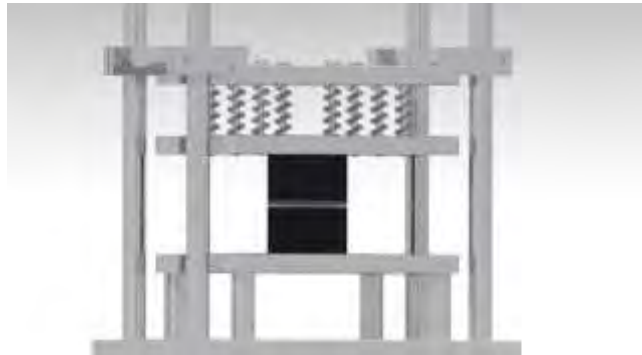
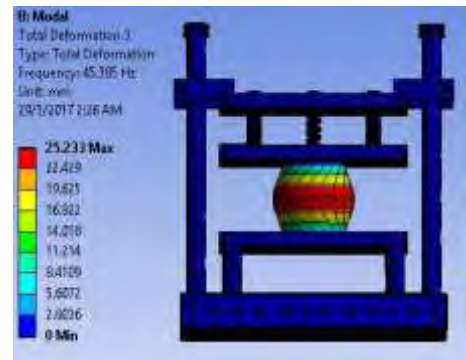
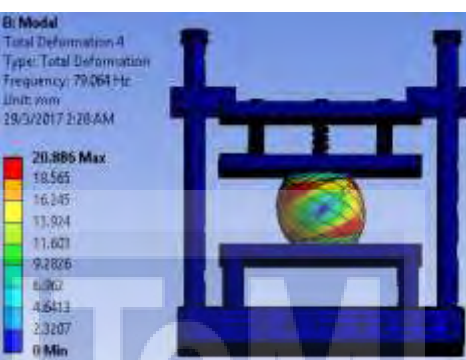


Figure 4.3: Assembly Type 2

Table 4.2: Result of the Modal Analysis for Type 2

Modality	Frequency (Hz)	Visual
1	42.490	
2	42.720	

3	45.385	 <p> Bi Modal Total Deformation 3 Type: Total Deformation Frequency: 45.385 Hz Unit: mm 29/3/2017 2:26 AM 25.233 Max 22.429 19.623 16.817 14.011 11.204 8.4129 5.6072 2.8026 0 Min </p>
4	79.064	 <p> Bi Modal Total Deformation 4 Type: Total Deformation Frequency: 79.064 Hz Unit: mm 29/3/2017 2:28 AM 20.885 Max 18.565 16.245 13.924 11.603 9.2826 6.962 4.6413 2.3207 0 Min </p>
5	79.072	 <p> Bi Modal Total Deformation 5 Type: Total Deformation Frequency: 79.072 Hz Unit: mm 29/3/2017 2:29 AM 20.922 Max 18.597 16.273 13.949 11.627 9.2907 6.974 4.6401 2.3247 0 Min </p>
6	85.246	 <p> Bi Modal Total Deformation 6 Type: Total Deformation Frequency: 85.246 Hz Unit: mm 29/3/2017 2:31 AM 16.983 Max 15.096 13.209 11.322 9.4349 7.5479 5.6609 3.774 1.887 0 Min </p>

4.2.3 Modal Analysis of the Type 3 Nature Rubber Rod

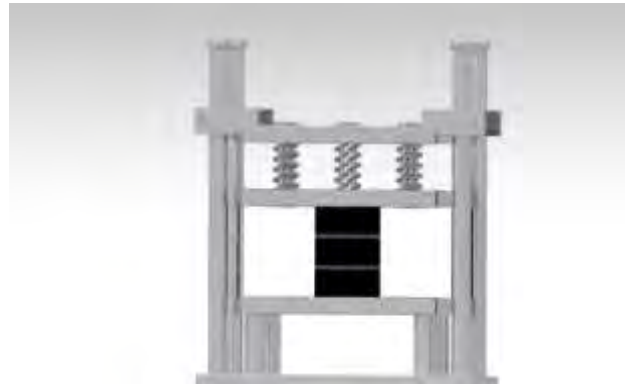
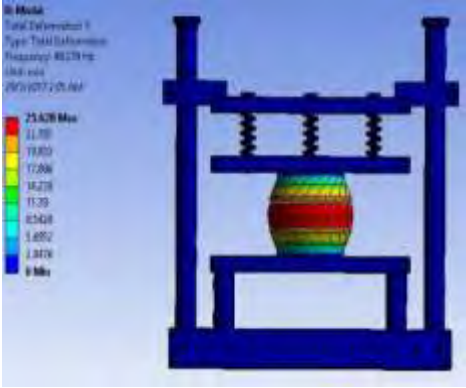
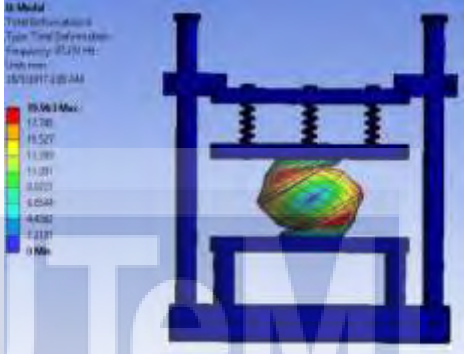
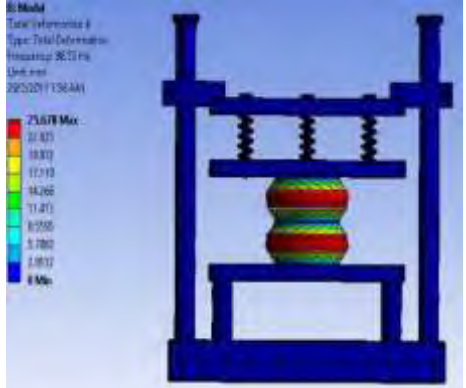


Figure 4.4: Assembly Type 3

Table 4.3: Result of the Modal Analysis for Type 3

Modality	Frequency (Hz)	Visual
1	45.585	
2	45.976	

3	48.274	 <p> St Model Total Deformation 3 Type: Total Deformation Frequency: 48.274 Hz Unit: mm 20/10/2017 1:05:44 PM 25.628 MPa 11.785 7.930 7.206 34.278 11.29 6.5438 1.4872 1.3478 0 MPa </p>
4	87.232	 <p> St Model Total Deformation 3 Type: Total Deformation Frequency: 87.232 Hz Unit: mm 18/10/2017 1:05:44 PM 35.061 MPa 11.785 11.527 11.099 6.6021 4.2549 0.2337 0 MPa </p>
5	87.845	 <p> St Model Total Deformation 3 Type: Total Deformation Frequency: 87.845 Hz Unit: mm 18/10/2017 1:05:44 PM 24.997 MPa 17.376 25.149 21.001 13.029 1.9477 6.5838 4.2238 3.7689 0 MPa </p>
6	96.550	 <p> St Model Total Deformation 3 Type: Total Deformation Frequency: 96.550 Hz Unit: mm 20/10/2017 1:06:44 PM 23.678 MPa 31.473 38.819 17.719 34.266 71.471 8.9266 5.7883 1.8932 0 MPa </p>

4.2.4 Modal Analysis of the Type 4 Nature Rubber Rod



Figure 4.5: Assembly Type 4

Table 4.4: Result of the Modal Analysis for Type 4

Modality	Frequency (Hz)	Visual
1	45.644	
2	45.842	

3	47.839	<p>B: Model Total Deformation 3 Type: Total Deformation Frequency: 47.839 Hz Unit: mm 28/3/2017 3:46 AM</p> <p>25.546 Max 12.707 19.069 17.017 14.100 11.354 8.5153 5.6768 2.8384 0 Min</p>
4	87.704	<p>B: Model Total Deformation 4 Type: Total Deformation Frequency: 87.704 Hz Unit: mm 28/3/2017 3:47 AM</p> <p>55.118 Max 16.894 16.893 11.247 10.621 6.4988 6.3726 4.2484 2.1242 0 Min</p>
5	88.136	<p>B: Model Total Deformation 5 Type: Total Deformation Frequency: 88.136 Hz Unit: mm 28/3/2017 3:48 AM</p> <p>19.074 Max 16.999 14.816 12.716 10.597 8.4775 6.3581 4.2387 2.1194 0 Min</p>
6	95.636	<p>B: Model Total Deformation 6 Type: Total Deformation Frequency: 95.636 Hz Unit: mm 29/3/2017 3:49 AM</p> <p>25.88 Max 23.007 20.129 17.253 14.378 11.502 8.6267 5.7512 2.8756 0 Min</p>

4.2.5 Modal Analysis of the Type 5 Nature Rubber Rod

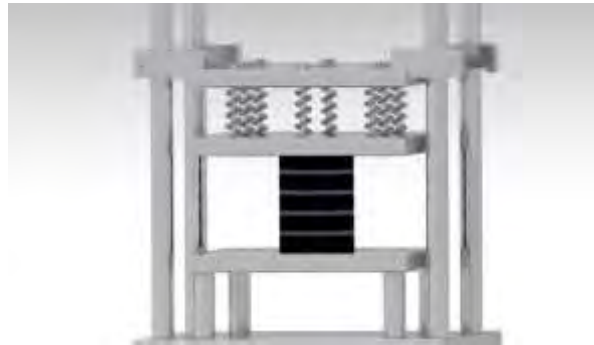
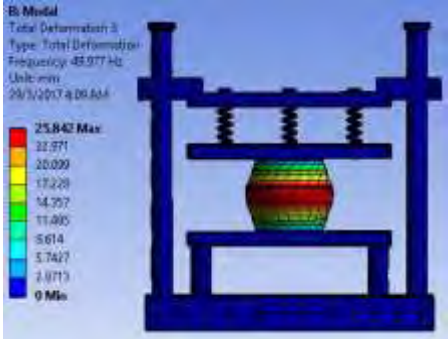
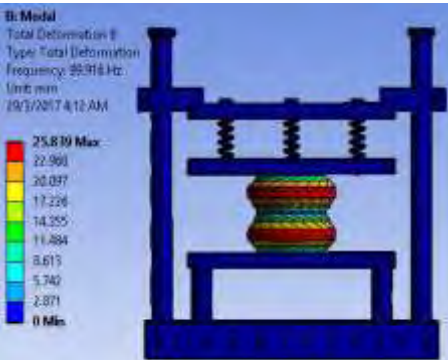


Figure 4.6: Assembly Type 5

Table 4.5: Result of the Modal Analysis for Type 5

Modality	Frequency (Hz)	Visual
1	47.927	
2	48.117	

3	49.977	 <p> B: Model Total Deformation: 3 Type: Total Deformation Frequency: 49.977 Hz Unit: mm 29/3/2017 4:06:44 AM </p> <p> 25.842 Max 22.971 20.099 17.228 14.357 11.485 8.614 5.7427 2.8713 0 Min </p>
4	94.532	 <p> B: Model Total Deformation: 4 Type: Total Deformation Frequency: 94.532 Hz Unit: mm 30/3/2017 4:10: AM </p> <p> 35.388 Max 17.234 15.079 12.925 10.771 8.6168 6.4626 4.3084 2.1542 0 Min </p>
5	94.923	 <p> B: Model Total Deformation: 5 Type: Total Deformation Frequency: 94.923 Hz Unit: mm 29/3/2017 4:11: AM </p> <p> 30.398 Max 17.241 15.086 12.931 10.776 8.6204 6.463 4.310 2.1553 0 Min </p>
6	99.916	 <p> B: Model Total Deformation: 6 Type: Total Deformation Frequency: 99.916 Hz Unit: mm 29/3/2017 4:12: AM </p> <p> 25.839 Max 22.991 20.097 17.226 14.355 11.484 8.613 5.742 2.871 0 Min </p>

4.3 Stress Frequency Response of the Nature Rubber Rod

4.3.1 Stress Frequency Response of the Nature Rubber Rod with 1 Embedded Aluminium Alloy

4.3.1.1 For Force 200 N

Table 4.6 consist of the result of the force 200 N against the LR-MS model. The result of the analysis is represented in the form of graph in Figure 4.7 below.

Table 4.6: Result of the Frequency Response Due Stress for Force 200 N

Frequency [Hz]	Amplitude (MPa)
10	3.9708×10^{-7}
20	4.0281×10^{-7}
30	4.1346×10^{-7}
40	4.4022×10^{-7}
50	4.4091×10^{-7}
60	4.7211×10^{-7}
70	4.9077×10^{-7}
80	3.6803×10^{-6}
90	3.0103×10^{-7}
100	4.0517×10^{-7}

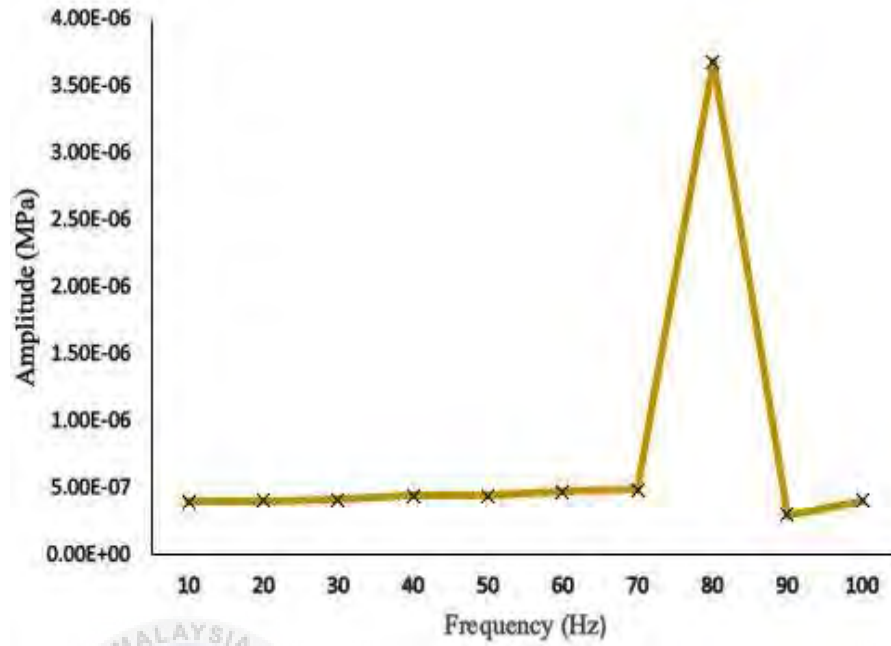
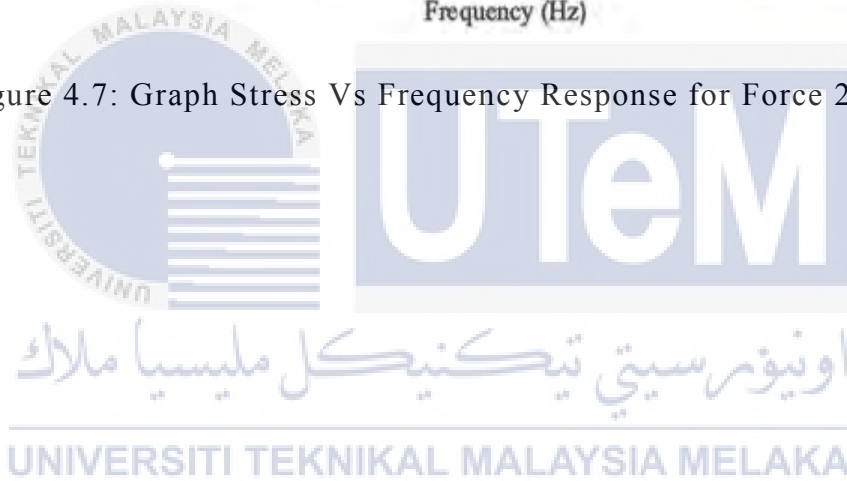


Figure 4.7: Graph Stress Vs Frequency Response for Force 200 N



4.3.1.2 For Force 400 N

Table 4.7 consist of the result of the force 400 N against the LR-MS model. The result of the analysis is represented in the form of graph in figure 4.8 below.

Table 4.7: Result of the Frequency Response Due Stress for Force 400 N

Frequency [Hz]	Amplitude (MPa)
10	7.9415×10^{-7}
20	8.0562×10^{-7}
30	8.2691×10^{-7}
40	8.8044×10^{-7}
50	8.8181×10^{-7}
60	9.4422×10^{-7}
70	9.8154×10^{-7}
80	7.3606×10^{-6}
90	6.0207×10^{-7}
100	8.1034×10^{-7}

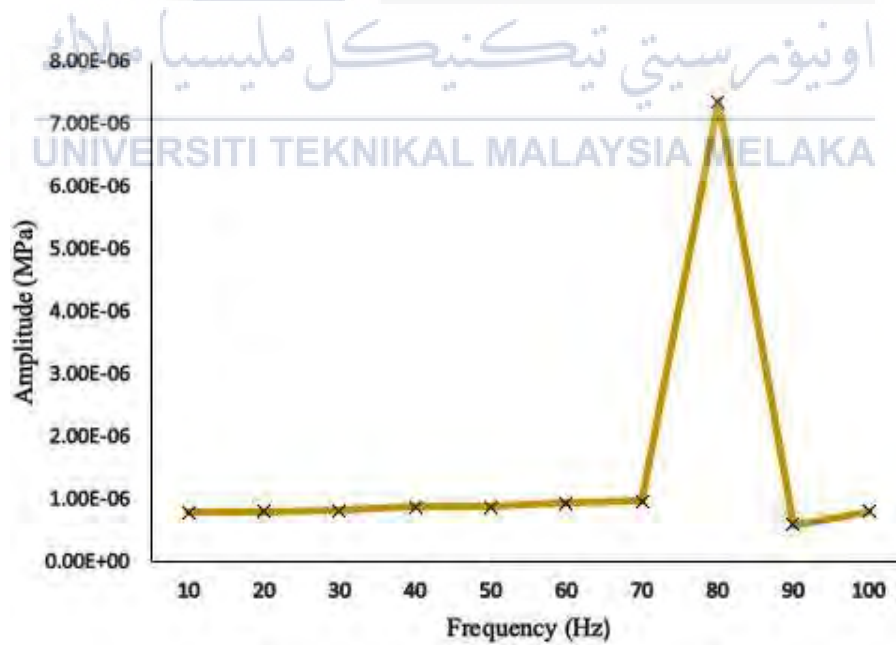


Figure 4.8: Graph Stress Vs Frequency Response for Force 400 N

4.3.1.3 For Force 600 N

Table 4.8 consist of the result of the force 600 N against the LR-MS model. The result of the analysis is represented in the form of graph in Figure 4.9 below.

Table 4.8: Result of the Frequency Response Due Stress for Force 600 N

Frequency [Hz]	Amplitude (MPa)
10	1.1912×10^{-6}
20	1.2084×10^{-6}
30	1.2404×10^{-6}
40	1.3207×10^{-6}
50	1.3227×10^{-6}
60	1.4163×10^{-6}
70	1.4723×10^{-6}
80	1.1041×10^{-5}
90	9.0310×10^{-7}
100	1.2155×10^{-6}

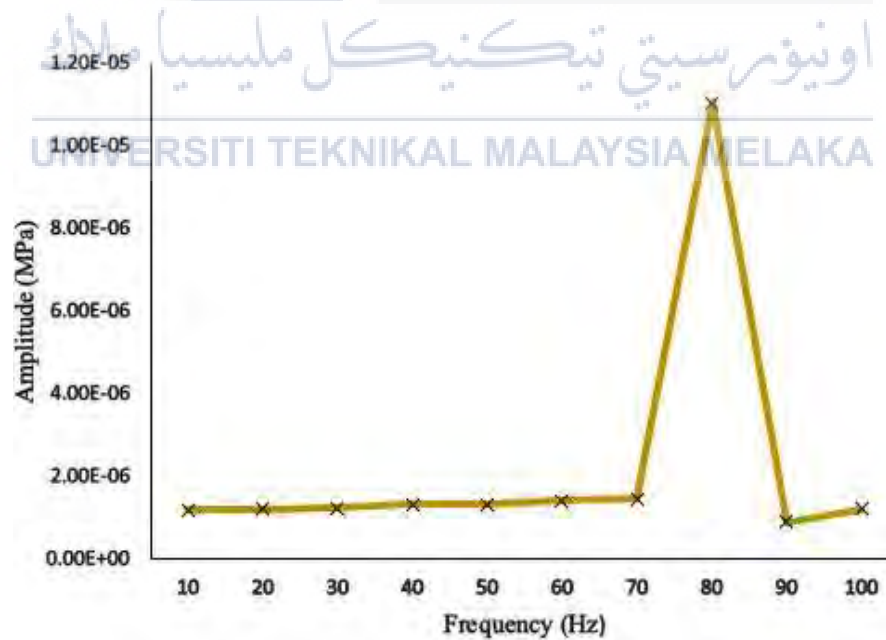


Figure 4.9: Graph Stress Vs Frequency Response for Force 600 N

4.3.1.4 For Force 800 N

Table 4.9 consist of the result of the force 800 N against the LR-MS model. The result of the analysis is represented in the form of graph in Figure 4.10 below.

Table 4.9: Result of the Frequency Response Due Stress for Force 800 N

Frequency [Hz]	Amplitude (MPa)
10	1.5883×10^{-6}
20	1.6112×10^{-6}
30	1.6538×10^{-6}
40	1.7609×10^{-6}
50	1.7636×10^{-6}
60	1.8884×10^{-6}
70	1.9631×10^{-6}
80	1.4721×10^{-5}
90	1.2041×10^{-6}
100	1.6207×10^{-6}

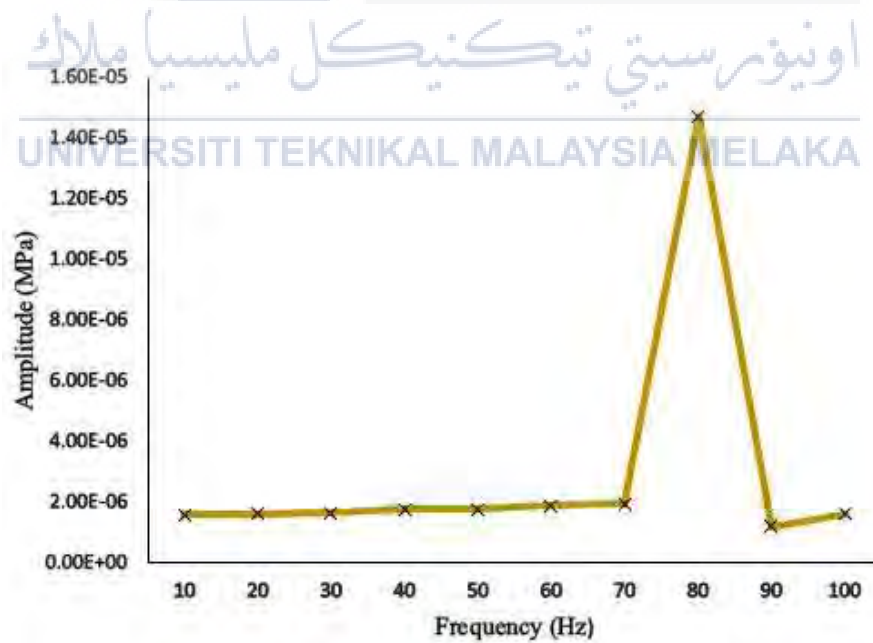


Figure 4.10: Graph Stress Vs Frequency Response for Force 800 N

4.3.1.5 For Force 1000 N

Table 4.10 consist of the result of the Force 1000 N against the LR-MS model. The result of the analysis is represented in the form of graph in Figure 4.11 below.

Table 4.10: Result of the Frequency Response Due Stress for Force 1000 N

Frequency [Hz]	Amplitude (MPa)
10	1.9854×10^{-6}
20	2.0141×10^{-6}
30	2.0673×10^{-6}
40	2.2011×10^{-6}
50	2.2045×10^{-6}
60	2.3605×10^{-6}
70	2.4539×10^{-6}
80	1.8402×10^{-5}
90	1.5052×10^{-6}
100	2.0259×10^{-6}

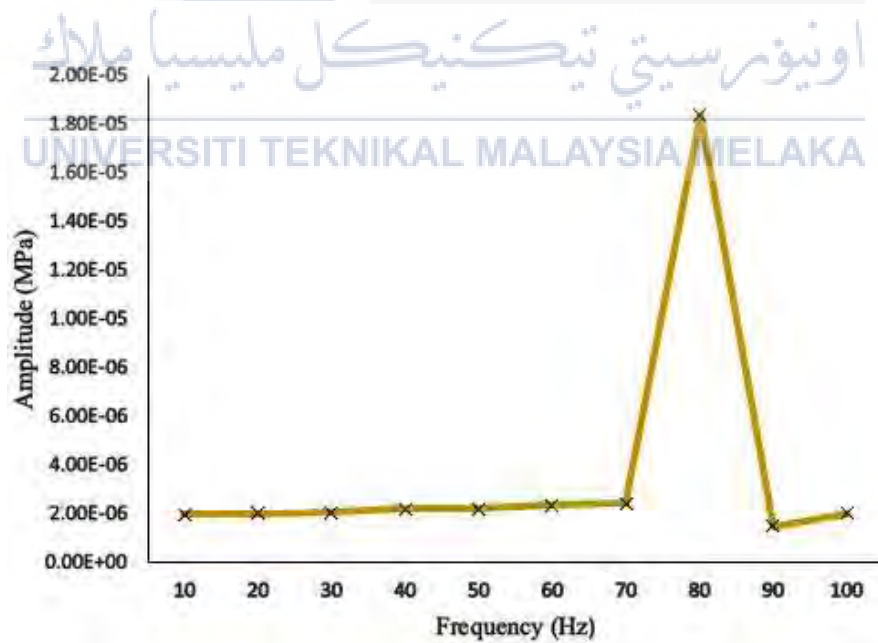


Figure 4.11: Graph Stress Vs Frequency Response for Force 1000 N

Based on Figure 4.12 below, it shows the five-different line that represents the value of each analysis that completely done with the different value of the force due to the four-embedded plate on the natural rubber rod. The value of force is set to be 200N represent the yellow line, 400N represent the brown line, 600N represent the red line, 800N represent the purple line, and lastly, 1000N represent the green line. The data that obtain show that the graph is linearly increasing. The value of the amplitude increases with respectively to the value of the force.

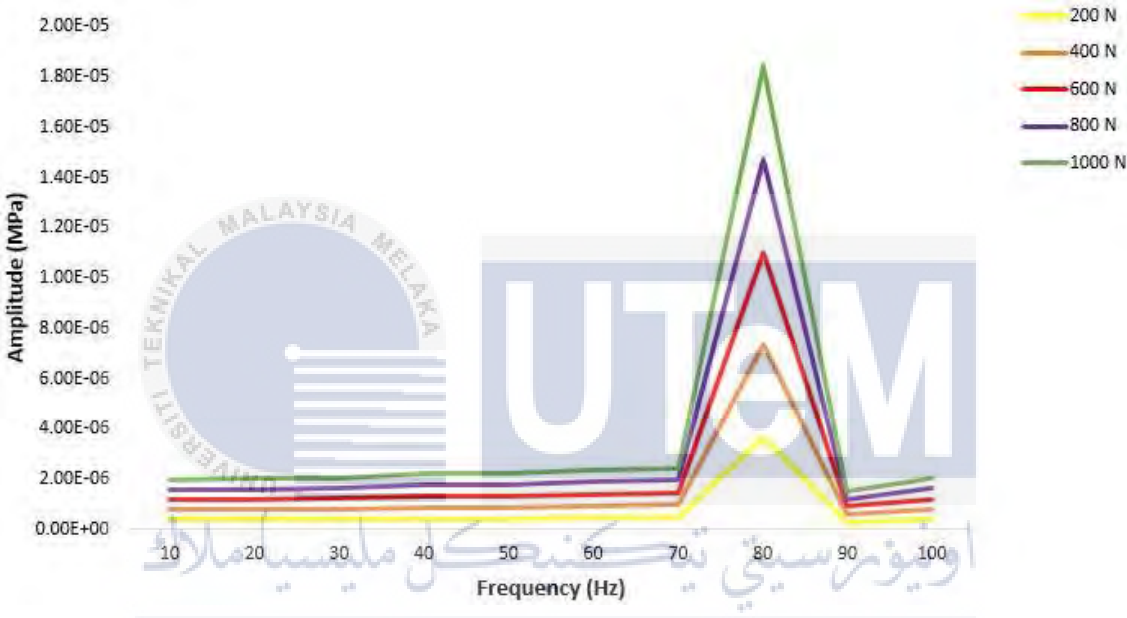


Figure 4.12: Result of Five Different Data with Different Value of Force Due to the 1 Embedded Plate Due to the Natural Rubber Rod for Stress Frequency Response

4.3.2 Deformation Frequency Response of Nature Rubber Rod with 1 Embedded Aluminium Alloy

4.3.2.1 For Force 200 N

Table 4.11 consist of the result of the force 200 N against the LR-MS model. The result of the analysis is represented in the form of graph in Figure 4.13 below.

Table 4.11: Result of the Frequency Response Due Deformation for Force 200 N

Frequency [Hz]	Amplitude (mm)
10	5.5757×10^{-4}
20	5.8221×10^{-4}
30	6.2941×10^{-4}
40	7.2785×10^{-4}
50	8.1789×10^{-4}
60	1.0689×10^{-3}
70	1.6519×10^{-3}
80	4.5724×10^{-3}
90	4.6564×10^{-3}
100	1.4007×10^{-3}

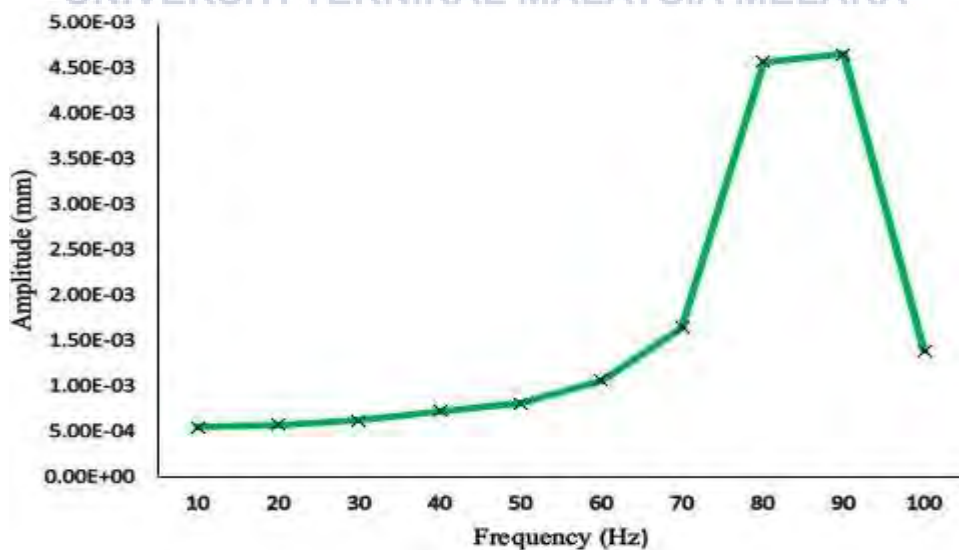


Figure 4.13: Graph Deformations Vs Frequency Response for Force 200 N

4.3.2.2 For Force 400 N

Table 4.12 consist of the result of the force 400 N against the LR-MS model. The result of the analysis is represented in the form of graph in Figure 4.14 below.

Table 4.12: Result of the Frequency Response Due Deformation for Force 400 N

Frequency [Hz]	Amplitude (mm)
10	1.1151×10^{-3}
20	1.1644×10^{-3}
30	1.2588×10^{-3}
40	1.4557×10^{-3}
50	1.6358×10^{-3}
60	2.1379×10^{-3}
70	3.3039×10^{-3}
80	9.1448×10^{-3}
90	9.3128×10^{-3}
100	2.8014×10^{-3}

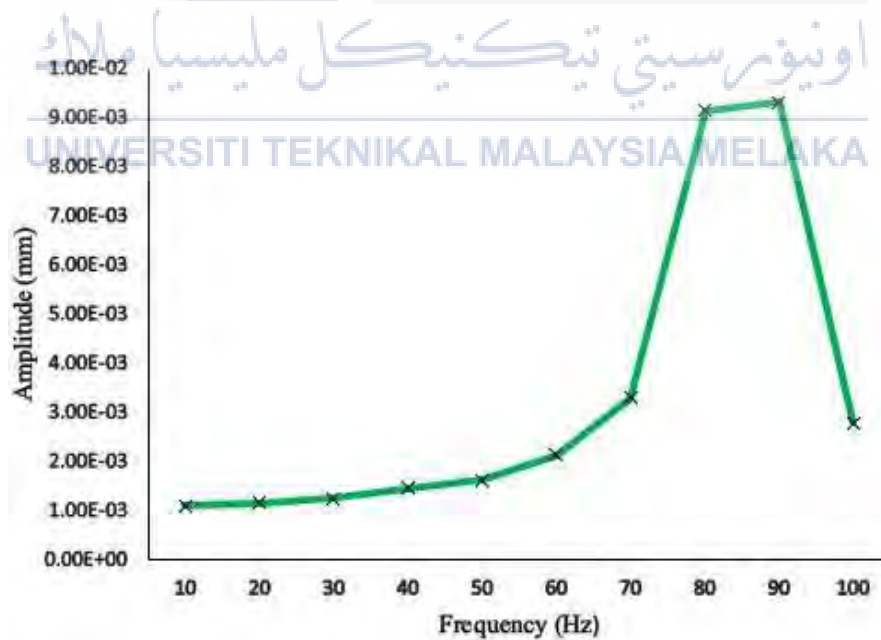


Figure 4.14: Graph Deformations Vs Frequency Response for Force 400 N

4.3.2.3 For Force 600 N

Table 4.13 consist of the result of the force 600 N against the LR-MS model. The result of the analysis is represented in the form of graph in Figure 4.15 below.

Table 4.13: Result of the Frequency Response Due Deformation for Force 600 N

Frequency [Hz]	Amplitude (mm)
10	1.6727×10^{-3}
20	1.7466×10^{-3}
30	1.8882×10^{-3}
40	2.1835×10^{-3}
50	2.4537×10^{-3}
60	3.2068×10^{-3}
70	4.9558×10^{-3}
80	1.3717×10^{-2}
90	1.3969×10^{-2}
100	4.2020×10^{-3}

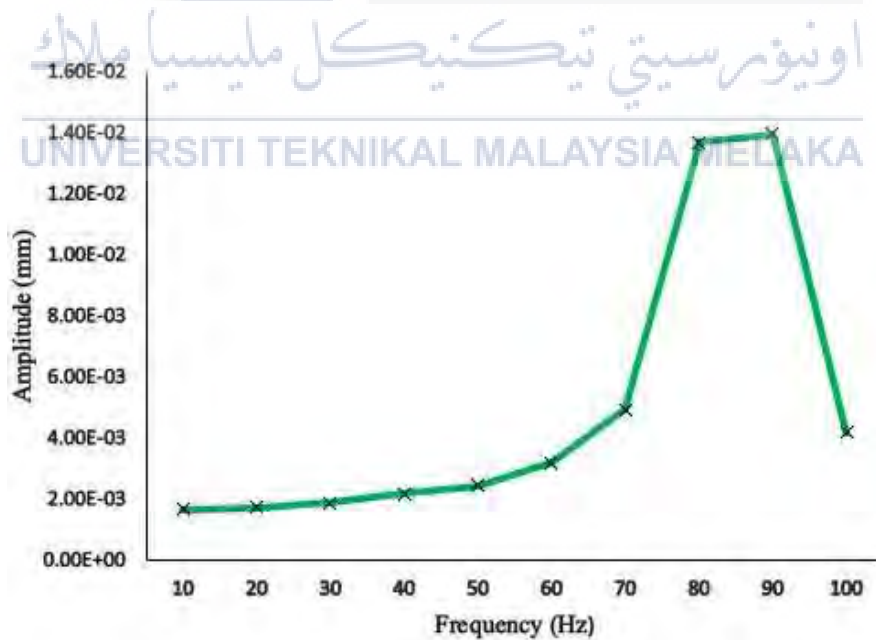


Figure 4.15: Graph Deformations Vs Frequency Response for Force 600 N

4.3.2.4 For Force 800 N

Table 4.14 below consist of the result of the force 800 N against the LR-MS model. The result of the analysis is represented in the form of graph in Figure 4.16.

Table 4.14: Result of the Frequency Response Due Deformation for Force 800 N

Frequency [Hz]	Amplitude (mm)
10	2.2303×10^{-3}
20	2.3288×10^{-3}
30	2.5176×10^{-3}
40	2.9114×10^{-3}
50	3.2716×10^{-3}
60	4.2757×10^{-3}
70	6.6077×10^{-3}
80	1.8290×10^{-2}
90	1.8626×10^{-2}
100	5.6027×10^{-3}

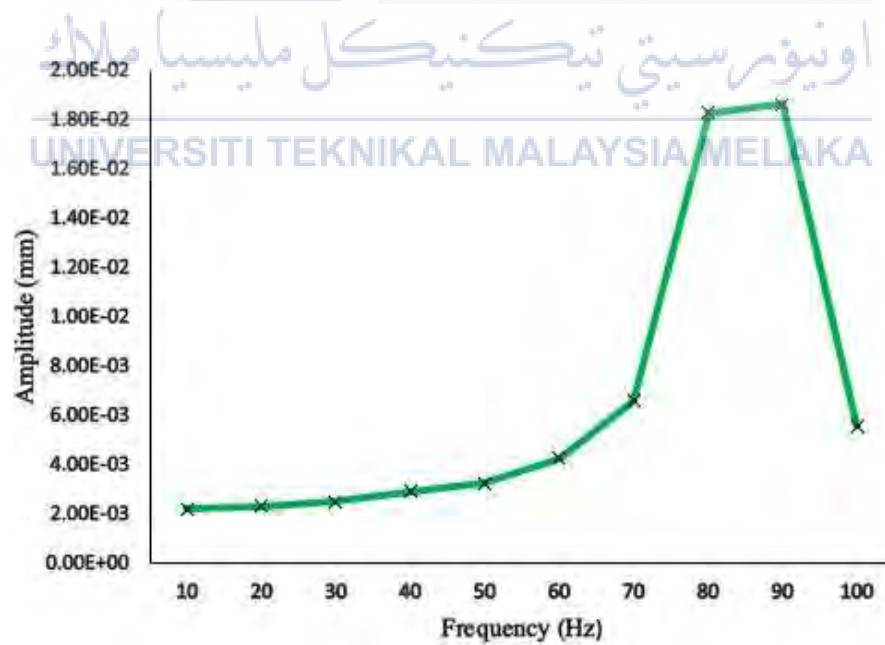


Figure 4.16: Graph Deformations Vs Frequency Response for Force 800 N

4.3.2.5 For Force 1000 N

Table 4.15 consist of the result of the force 1000 N against the LR-MS model. The result of the analysis is represented in the form of graph in Figure 4.17.

Table 4.15: Result of the Frequency Response Due Deformation for Force 1000 N

Frequency [Hz]	Amplitude (mm)
10	2.7879×10^{-3}
20	2.9111×10^{-3}
30	3.1471×10^{-3}
40	3.6392×10^{-3}
50	4.0894×10^{-3}
60	5.3447×10^{-3}
70	8.2597×10^{-3}
80	2.2862×10^{-2}
90	2.3282×10^{-2}
100	7.0034×10^{-3}

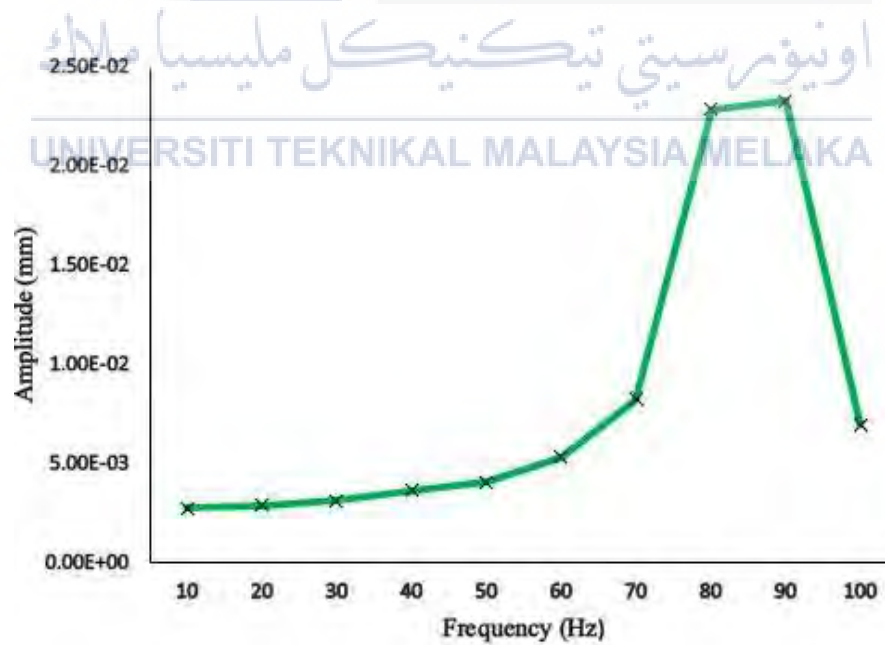


Figure 4.17: Graph Deformations Vs Frequency Response for Force 1000 N

Based on Figure 4.18 below, it shows the five-different line that represents the value of each analysis that completely done with the different value of the force due to the four-embedded plate on the natural rubber rod. The value of force is set to be 200N represent the yellow line, 400N represent the brown line, 600N represent the red line, 800N represent the purple line, and lastly, 1000N represent the green line. The data that obtain show that the graph is linearly increasing. The value of the amplitude increases with respectively to the value of the force.

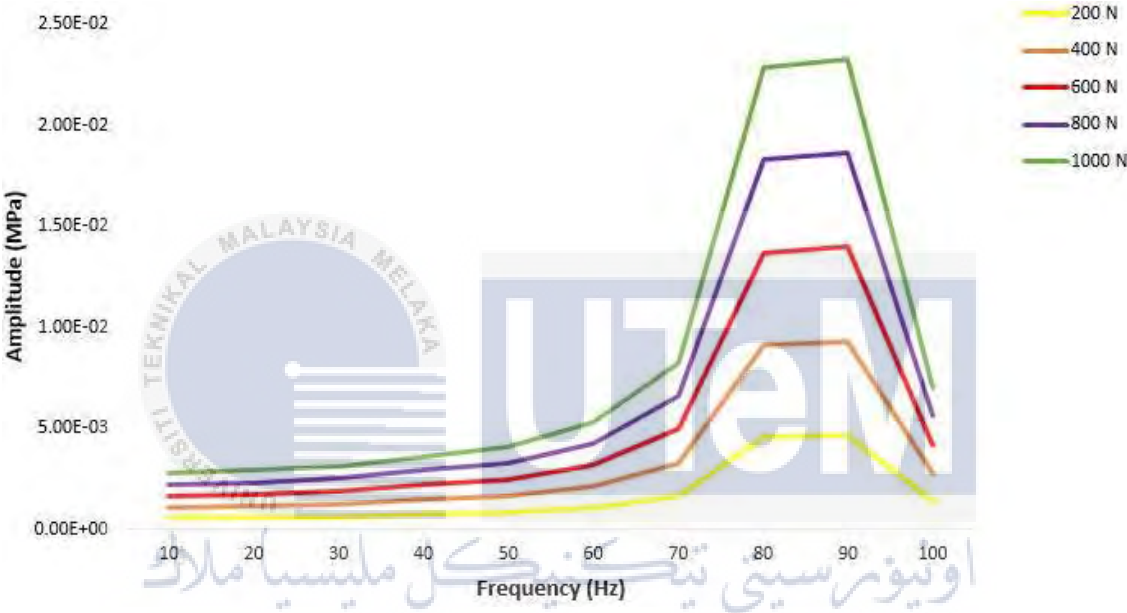


Figure 4.18: Result of Five Different Data with Different Value of Force Due to the 1 Embedded Plate Due to the Natural Rubber Rod for Deformation Frequency Response

4.3.3 Stress Frequency Response of the Nature Rubber Rod with 2 Embedded Aluminium Alloy

4.3.3.1 For Force 200 N

Table 4.16 consist of the result of the force 200 N against the LR-MS model. The result of the analysis is represented in the form of graph in Figure 4.19 below.

Table 4.16: Result of the Frequency Response Due Stress for Force 200 N

Frequency [Hz]	Amplitude (MPa)
10	4.7996×10^{-7}
20	4.9030×10^{-7}
30	5.0839×10^{-7}
40	5.3400×10^{-7}
50	5.8789×10^{-7}
60	6.4536×10^{-7}
70	7.3387×10^{-7}
80	8.2827×10^{-7}
90	2.0089×10^{-6}
100	3.3665×10^{-6}

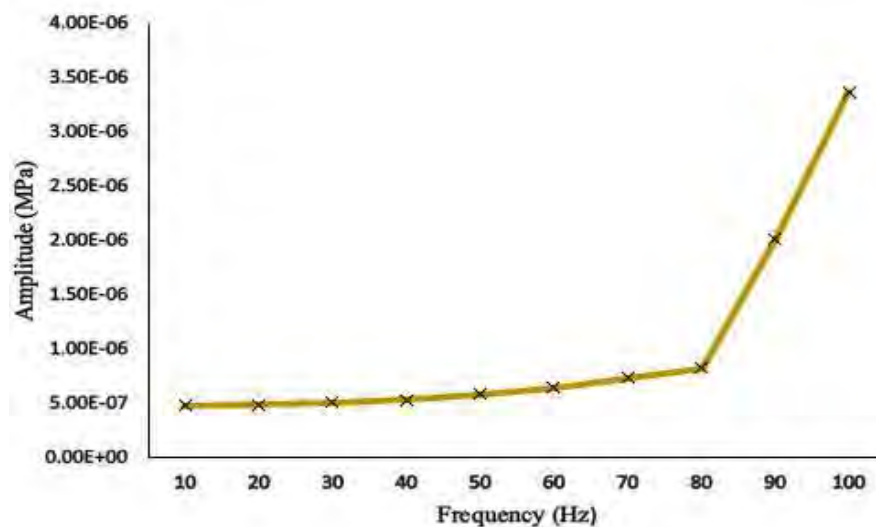


Figure 4.19: Graph Stress Vs Frequency Response for Force 200 N

4.3.3.2 For Force 400 N

Table 4.17 consist of the result of the force 400 N against the LR-MS model. The result of the analysis is represented in the form of graph in Figure 4.20 below.

Table 4.17: Result of the Frequency Response Due Stress for Force 400 N

Frequency [Hz]	Amplitude (MPa)
10	9.5991×10^{-7}
20	9.8060×10^{-7}
30	1.0168×10^{-6}
40	1.0680×10^{-6}
50	1.1758×10^{-6}
60	1.2907×10^{-6}
70	1.4677×10^{-6}
80	1.6565×10^{-6}
90	4.0178×10^{-6}
100	6.7330×10^{-6}

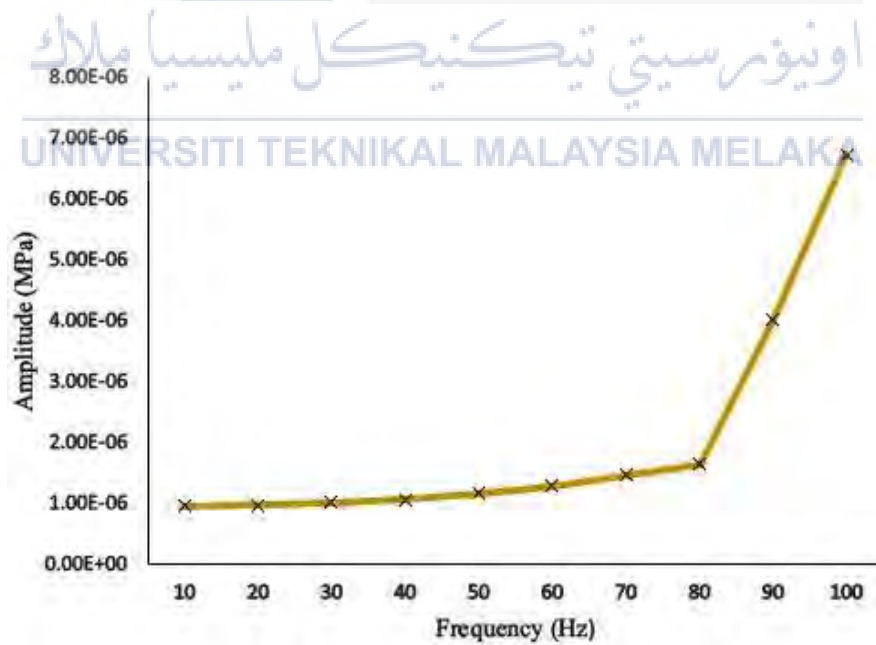


Figure 4.20: Graph Stress Vs Frequency Response for Force 400 N

4.3.3.3 For Force 600 N

Table 4.18 consist of the result of the force 600 N against the LR-MS model. The result of the analysis is represented in the form of graph in Figure 4.21 below.

Table 4.18: Result of the Frequency Response Due Stress for Force 600 N

Frequency [Hz]	Amplitude (MPa)
10	1.4399×10^{-6}
20	1.4709×10^{-6}
30	1.5252×10^{-6}
40	1.6020×10^{-6}
50	1.7637×10^{-6}
60	1.9361×10^{-6}
70	2.2016×10^{-6}
80	2.4848×10^{-6}
90	6.0267×10^{-6}
100	1.010×10^{-5}

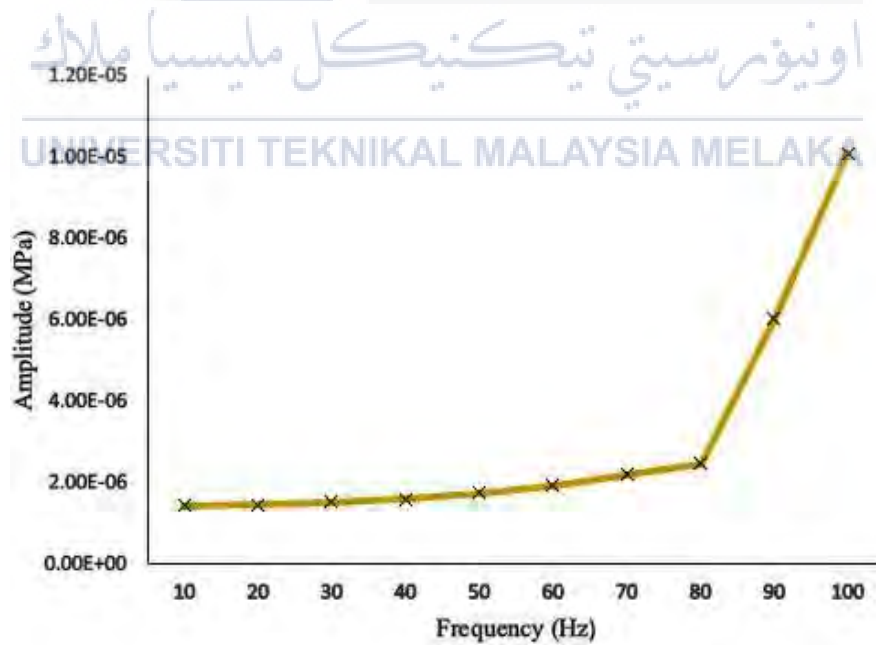


Figure 4.21: Graph Stress Vs Frequency Response for Force 600 N

4.3.3.4 For Force 800 N

Table 4.19 consist of the result of the force 800 N against the LR-MS model. The result of the analysis is represented in the form of graph in Figure 4.22 below.

Table 4.19: Result of the Frequency Response Due Stress for Force 800 N

Frequency [Hz]	Amplitude (MPa)
10	1.9198×10^{-6}
20	1.9612×10^{-6}
30	2.0336×10^{-6}
40	2.1360×10^{-6}
50	2.3516×10^{-6}
60	2.5814×10^{-6}
70	2.9355×10^{-6}
80	3.3131×10^{-6}
90	8.0356×10^{-6}
100	1.3466×10^{-5}

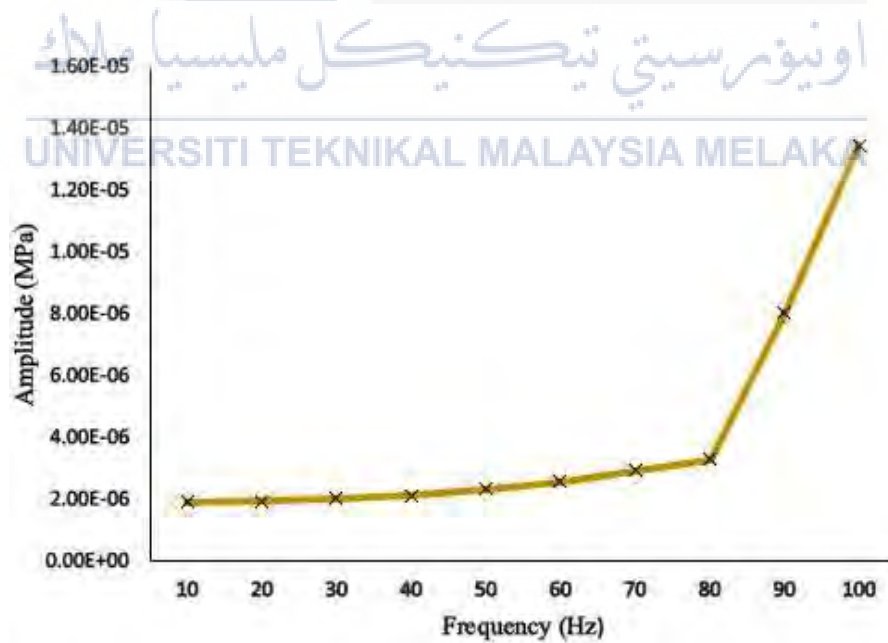


Figure 4.22: Graph Stress Vs Frequency Response for Force 600 N

4.3.3.5 For Force 1000 N

Table 4.20 consist of the result of the Force 1000 N against the LR-MS model. The result of the analysis is represented in the form of graph in Figure 4.23 below.

Table 4.20: Result of the Frequency Response Due Stress for Force 1000 N

Frequency [Hz]	Amplitude (MPa)
10	2.3998×10^{-6}
20	2.4515×10^{-6}
30	2.5419×10^{-6}
40	2.6700×10^{-6}
50	2.9394×10^{-6}
60	3.2268×10^{-6}
70	3.6693×10^{-6}
80	4.1414×10^{-6}
90	1.0045×10^{-5}
100	1.6833×10^{-5}

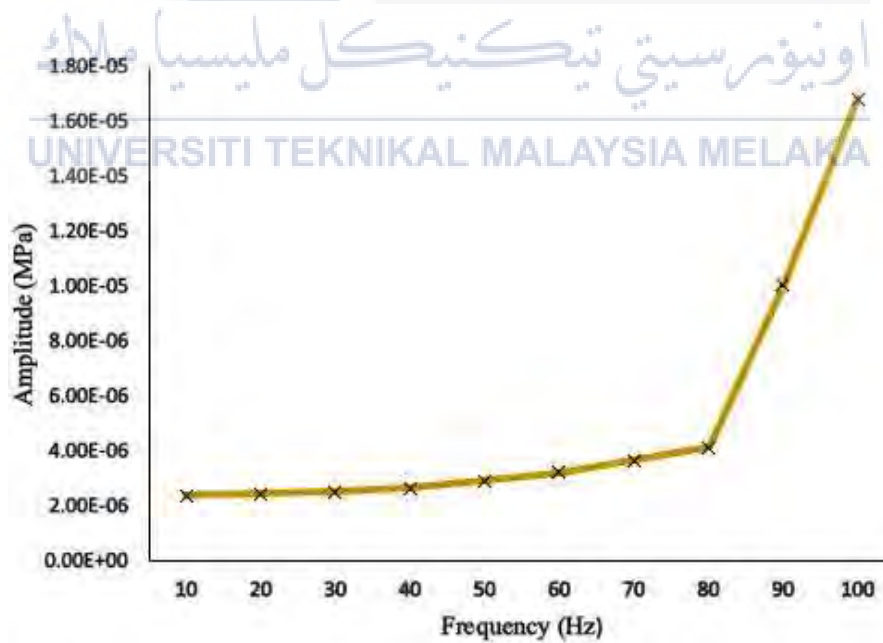


Figure 4.23: Graph Stress Vs Frequency Response for Force 1000 N

Based on figure 4.24 below, it shows the five-different line that represents the value of each analysis that completely done with the different value of the force due to the four-embedded plate on the natural rubber rod. The value of force is set to be 200N represent the yellow line, 400N represent the brown line, 600N represent the red line, 800N represent the purple line, and lastly, 1000N represent the green line. The data that obtain show that the graph is linearly increasing. The value of the amplitude increases with respectively to the value of the force.

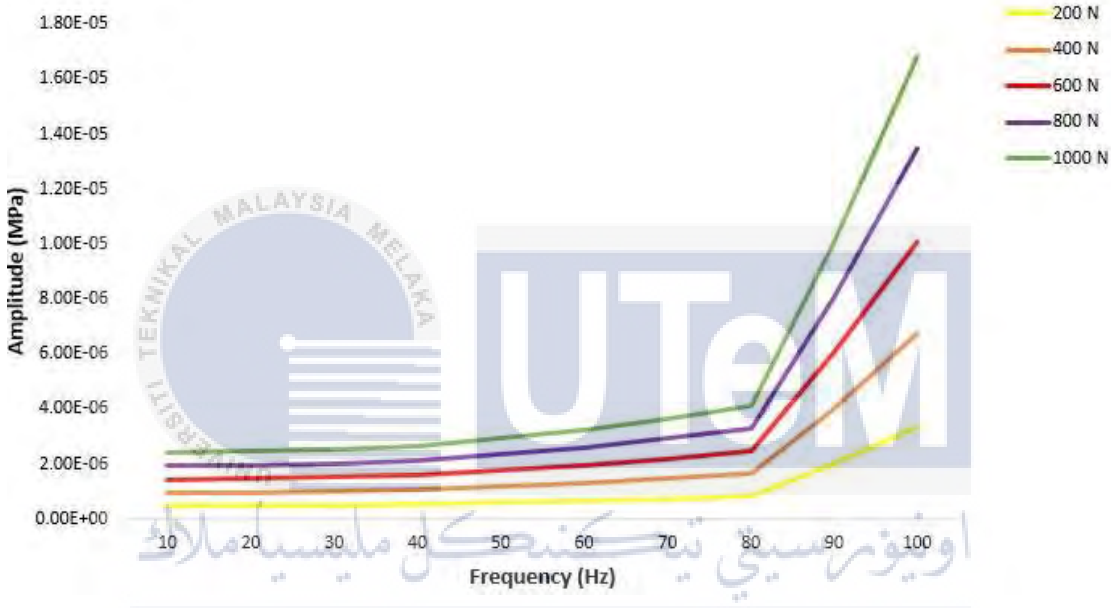


Figure 4.24: Result of Five Different Data with Different Value of Force Due to the 2 Embedded Plate Due to the Natural Rubber Rod for Stress Frequency Response

4.3.4 Deformation Frequency Response of Nature Rubber Rod with 2 Embedded Aluminium Alloy

4.3.4.1 For Force 200 N

Table 4.21 consist of the result of the force 200 N against the LR-MS model. The result of the analysis is represented in the form of graph in Figure 4.25 below.

Table 4.21: Result of the Frequency Response Due Deformation for Force 200 N

Frequency [Hz]	Amplitude (mm)
10	6.0542×10^{-4}
20	6.2264×10^{-4}
30	6.5427×10^{-4}
40	7.1064×10^{-4}
50	7.4638×10^{-4}
60	8.6898×10^{-4}
70	1.0492×10^{-3}
80	1.3794×10^{-3}
90	1.9673×10^{-3}
100	4.8077×10^{-3}

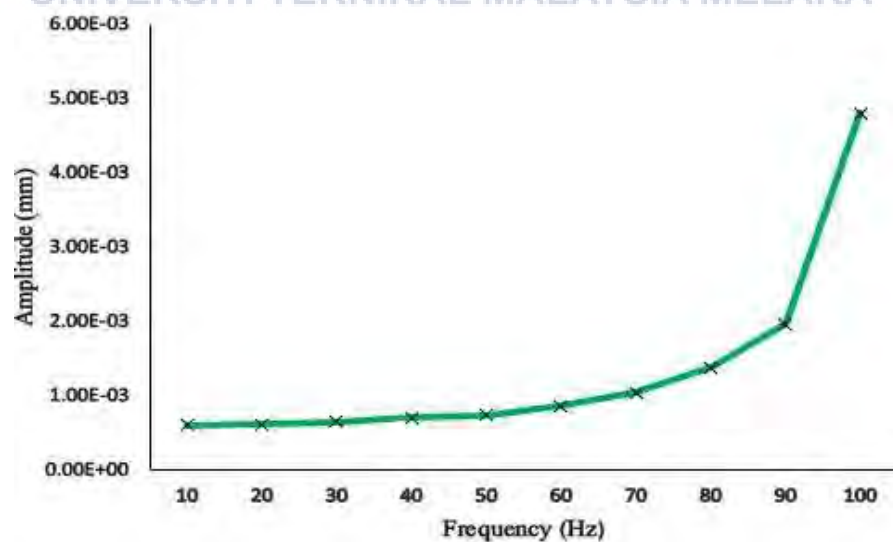


Figure 4.25: Graph Deformations Vs Frequency Response for Force 200 N

4.3.4.2 For Force 400 N

Table 4.22 consist of the result of the force 400 N against the LR-MS model. The result of the analysis is represented in the form of graph in Figure 4.26 below.

Table 4.22: Result of the Frequency Response Due Deformation for Force 400 N

Frequency [Hz]	Amplitude (mm)
10	1.2108×10^{-3}
20	1.2453×10^{-3}
30	1.3085×10^{-3}
40	1.4213×10^{-3}
50	1.4928×10^{-3}
60	1.7380×10^{-3}
70	2.0983×10^{-3}
80	2.7589×10^{-3}
90	3.9345×10^{-3}
100	9.6155×10^{-3}

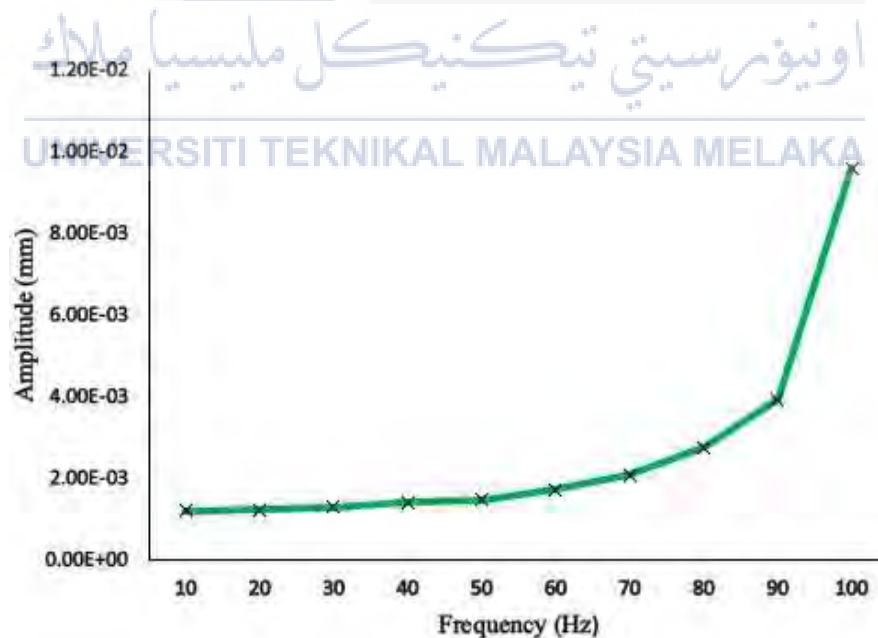


Figure 4.26: Graph Deformations Vs Frequency Response for Force 400 N

4.3.4.3 For Force 600 N

Table 4.23 consist of the result of the force 600 N against the LR-MS model. The result of the analysis is represented in the form of graph in Figure 4.27 below.

Table 4.23: Result of the Frequency Response Due Deformation for Force 600 N

Frequency [Hz]	Amplitude (mm)
10	1.8163×10^{-3}
20	1.8679×10^{-3}
30	1.9628×10^{-3}
40	2.1319×10^{-3}
50	2.2392×10^{-3}
60	2.6069×10^{-3}
70	3.1475×10^{-3}
80	4.1383×10^{-3}
90	5.9018×10^{-3}
100	1.4423×10^{-2}

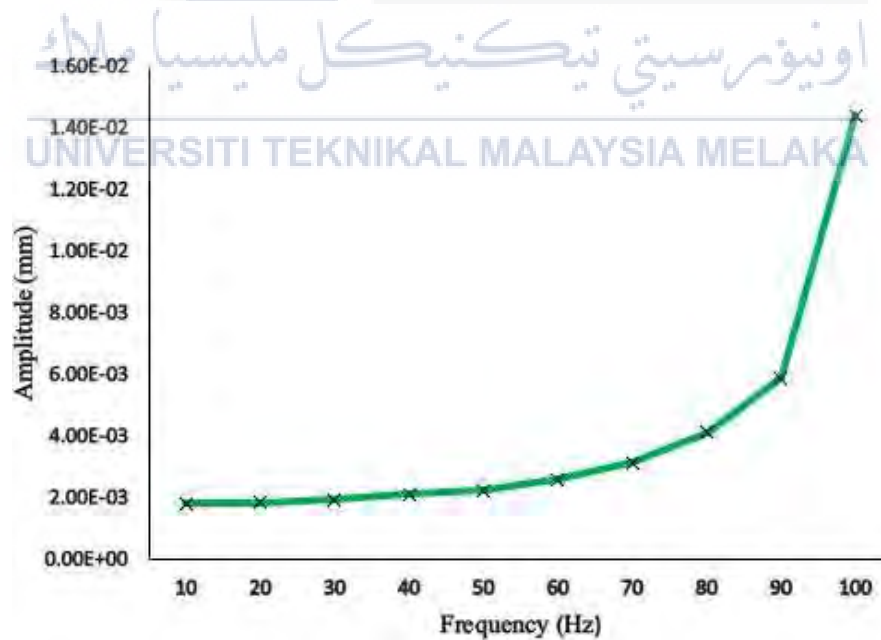


Figure 4.27: Graph Deformations Vs Frequency Response for Force 600 N

4.3.4.4 For Force 800 N

Table 4.24 below consist of the result of the force 800 N against the LR-MS model. The result of the analysis is represented in the form of graph in Figure 4.28.

Table 4.24: Result of the Frequency Response Due Deformation for Force 800 N

Frequency [Hz]	Amplitude (mm)
10	2.4217×10^{-3}
20	2.4906×10^{-3}
30	2.6171×10^{-3}
40	2.8426×10^{-3}
50	2.9855×10^{-3}
60	3.4759×10^{-3}
70	4.1967×10^{-3}
80	5.5178×10^{-3}
90	7.8691×10^{-3}
100	1.9231×10^{-2}

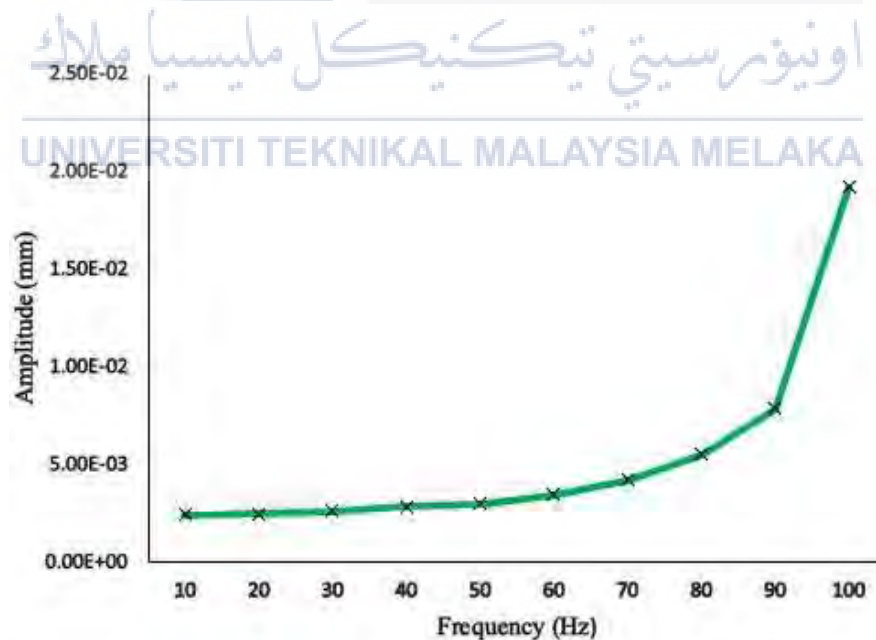


Figure 4.28: Graph Deformations Vs Frequency Response for Force 800 N

4.3.4.5 For Force 1000 N

Table 4.25 consist of the result of the force 1000 N against the LR-MS model. The result of the analysis is represented in the form of graph in Figure 4.29 above.

Table 4.25: Result of the Frequency Response Due Deformation for Force 1000 N

Frequency [Hz]	Amplitude (mm)
10	3.0271×10^{-3}
20	3.1132×10^{-3}
30	3.2713×10^{-3}
40	3.5532×10^{-3}
50	3.7319×10^{-3}
60	4.3449×10^{-3}
70	5.2458×10^{-3}
80	6.8972×10^{-3}
90	9.8363×10^{-3}
100	2.4039×10^{-2}

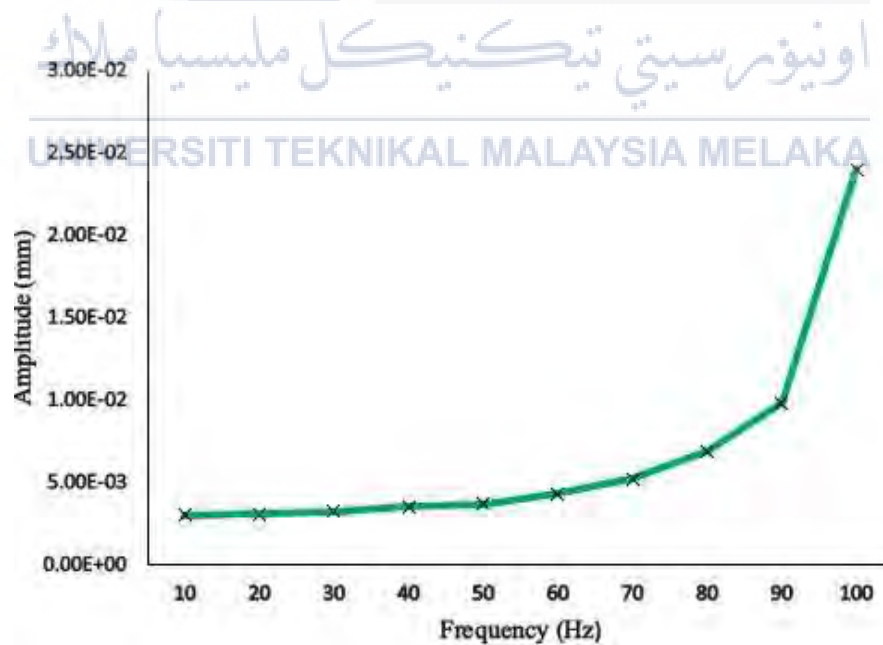


Figure 4.29: Graph Deformations Vs Frequency Response for Force 1000 N

Based on Figure 4.30 below, it shows the five-different line that represents the value of each analysis that completely done with the different value of the force due to the four-embedded plate on the natural rubber rod. The value of force is set to be 200N represent the yellow line, 400N represent the brown line, 600N represent the red line, 800N represent the purple line, and lastly, 1000N represent the green line. The data that obtain show that the graph is linearly increasing. The value of the amplitude increases with respectively to the value of the force.

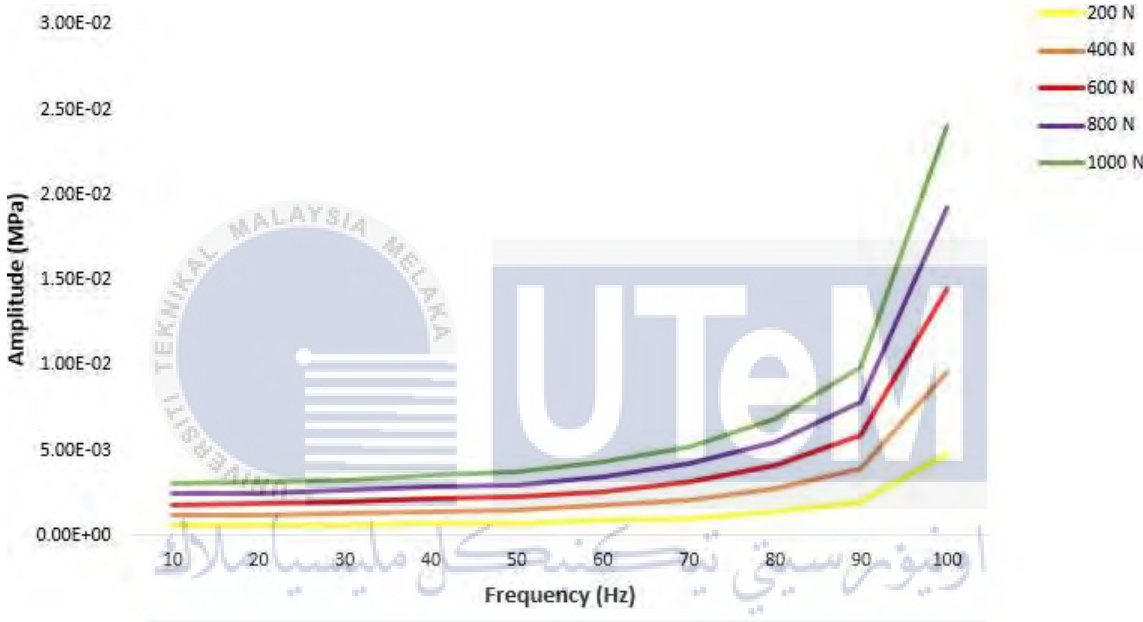


Figure 4.30: Result of Five Different Data with Different Value of Force Due to the 2 Embedded Plate Due to the Natural Rubber Rod for Deformation Frequency Response

4.3.5 Stress Frequency Response of the Nature Rubber Rod with 3 Embedded Aluminium Alloy

4.3.5.1 For Force 200 N

Table 4.26 consist of the result of the force 200 N against the LR-MS model. The result of the analysis is represented in the form of graph in Figure 4.31 below.

Table 4.26: Result of the Frequency Response Due Stress for Force 200 N

Frequency [Hz]	Amplitude (MPa)
10	9.5120×10^{-7}
20	9.2308×10^{-7}
30	9.4026×10^{-7}
40	1.0005×10^{-6}
50	8.2064×10^{-7}
60	9.0224×10^{-7}
70	9.1348×10^{-7}
80	8.7069×10^{-7}
90	1.2751×10^{-6}
100	9.2946×10^{-7}

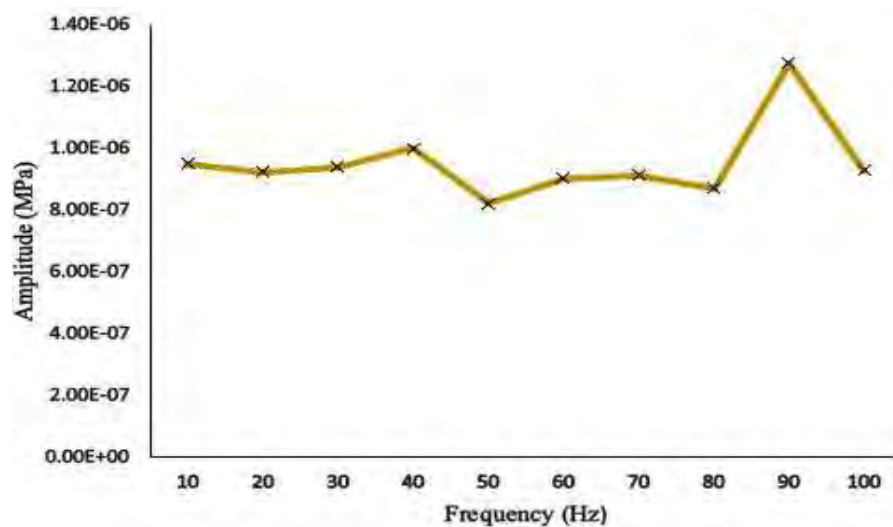


Figure 4.31: Graph Stress Vs Frequency Response for Force 200 N

4.3.5.2 For Force 400 N

Table 4.27 consist of the result of the force 400 N against the LR-MS model. The result of the analysis is represented in the form of graph in Figure 4.32 below.

Table 4.27: Result of the Frequency Response Due Stress for Force 400 N

Frequency [Hz]	Amplitude (MPa)
10	1.8304×10^{-6}
20	1.8462×10^{-6}
30	1.8805×10^{-6}
40	2.0010×10^{-6}
50	1.6413×10^{-6}
60	1.8045×10^{-6}
70	1.8270×10^{-6}
80	1.7414×10^{-6}
90	2.5502×10^{-6}
100	1.8589×10^{-6}

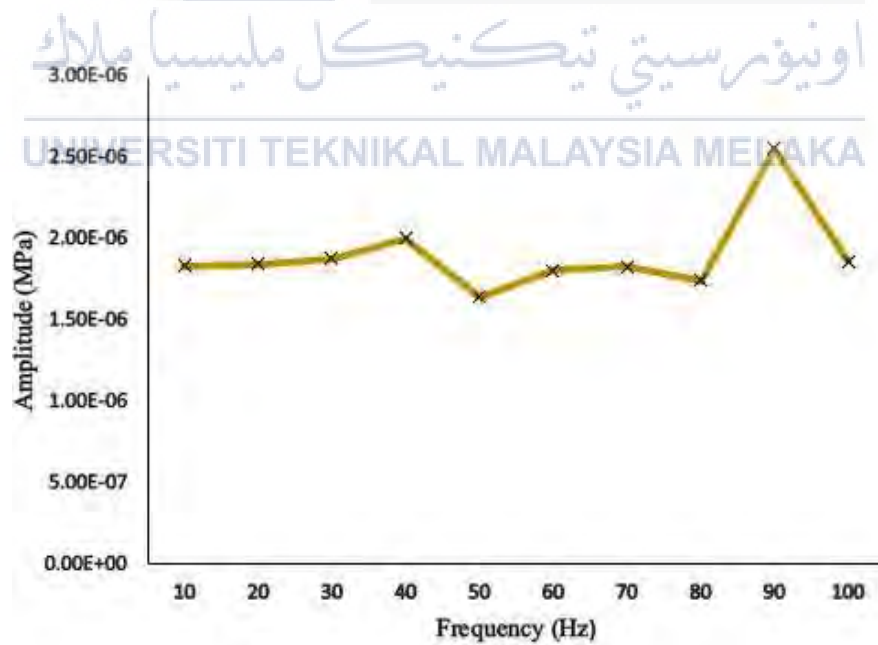


Figure 4.32: Graph Stress Vs Frequency Response for Force 400 N

4.3.5.3 For Force 600 N

Table 4.28 consist of the result of the force 600 N against the LR-MS model. The result of the analysis is represented in the form of graph in Figure 4.33 below.

Table 4.28: Result of the Frequency Response Due Stress for Force 600 N

Frequency [Hz]	Amplitude (MPa)
10	2.7456×10^{-6}
20	2.7692×10^{-6}
30	2.8208×10^{-6}
40	3.0015×10^{-6}
50	2.4619×10^{-6}
60	2.7067×10^{-6}
70	2.7405×10^{-6}
80	2.6121×10^{-6}
90	3.8253×10^{-6}
100	2.7884×10^{-6}

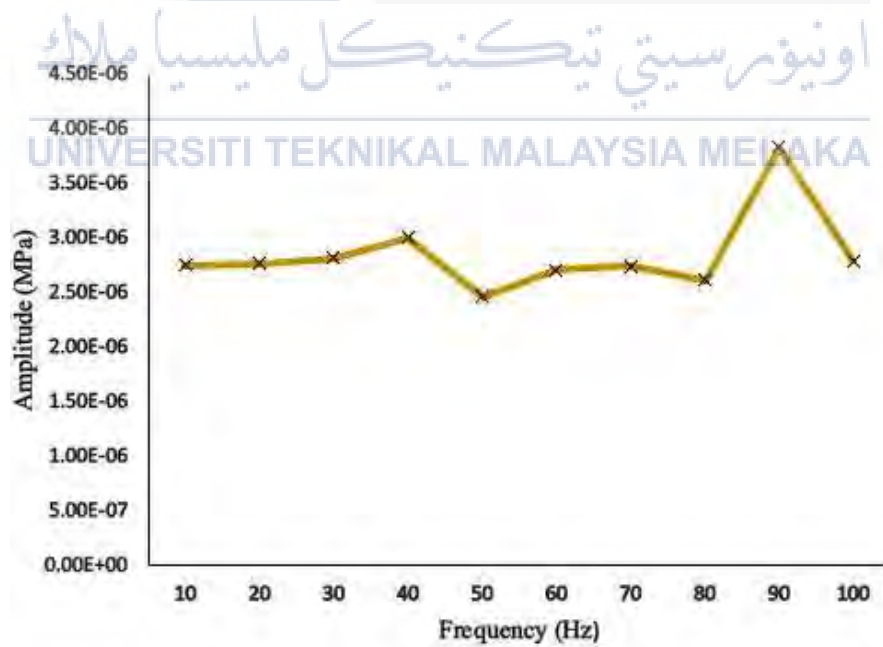


Figure 4.33: Graph Stress Vs Frequency Response for Force 600 N

4.3.5.4 For Force 800 N

Table 4.29 consist of the result of the force 800 N against the LR-MS model. The result of the analysis is represented in the form of graph in Figure 4.34 below.

Table 4.29: Result of the Frequency Response Due Stress for Force 800 N

Frequency [Hz]	Amplitude (MPa)
10	3.6608×10^{-6}
20	3.6923×10^{-6}
30	3.7611×10^{-6}
40	4.0020×10^{-6}
50	3.2826×10^{-6}
60	3.6089×10^{-6}
70	3.6539×10^{-6}
80	3.4828×10^{-6}
90	5.1004×10^{-6}
100	3.7178×10^{-6}

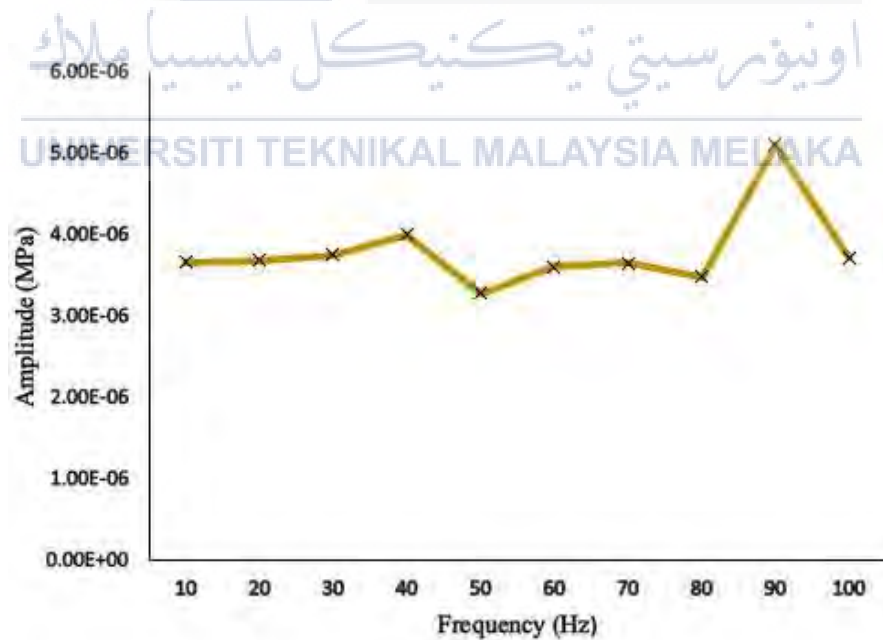


Figure 4.34: Graph Stress Vs Frequency Response for Force 600 N

4.3.5.5 For Force 1000 N

Table 4.30 consist of the result of the Force 1000 N against the LR-MS model. The result of the analysis is represented in the form of graph in Figure 4.35 below.

Table 4.30: Result of the Frequency Response Due Stress for Force 1000 N

Frequency [Hz]	Amplitude (MPa)
10	4.5760×10^{-6}
20	4.6154×10^{-6}
30	4.7013×10^{-6}
40	5.0025×10^{-6}
50	4.1032×10^{-6}
60	4.5112×10^{-6}
70	4.5674×10^{-6}
80	4.3535×10^{-6}
90	6.3755×10^{-6}
100	4.6473×10^{-6}

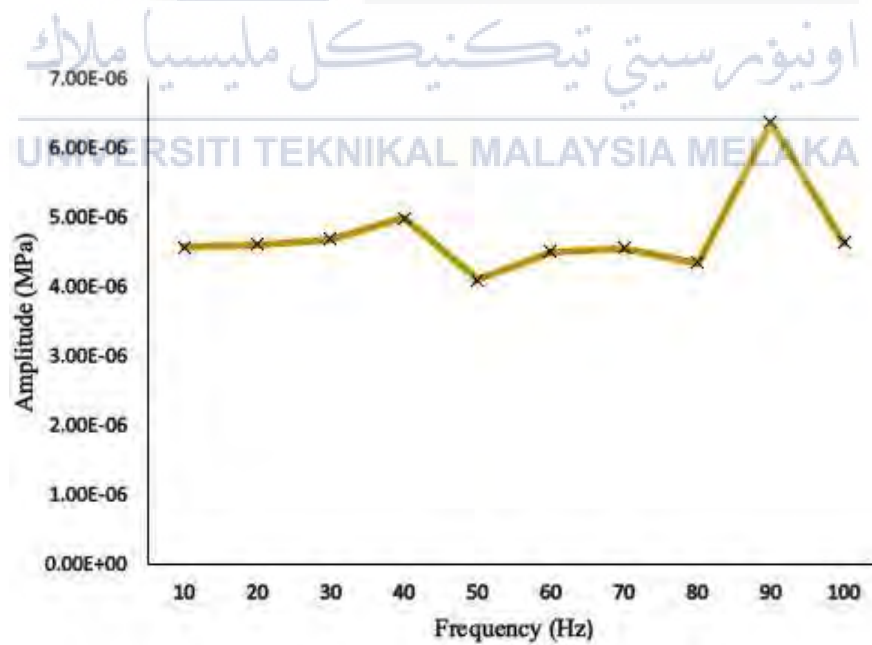


Figure 4.35: Graph Stress Vs Frequency Response for Force 1000 N

Based on Figure 4.36 below, it shows the five-different line that represents the value of each analysis that completely done with the different value of the force due to the four-embedded plate on the natural rubber rod. The value of force is set to be 200N represent the yellow line, 400N represent the brown line, 600N represent the red line, 800N represent the purple line, and lastly, 1000N represent the green line. The data that obtain show that the graph is linearly increasing. The value of the amplitude increases with respectively to the value of the force.

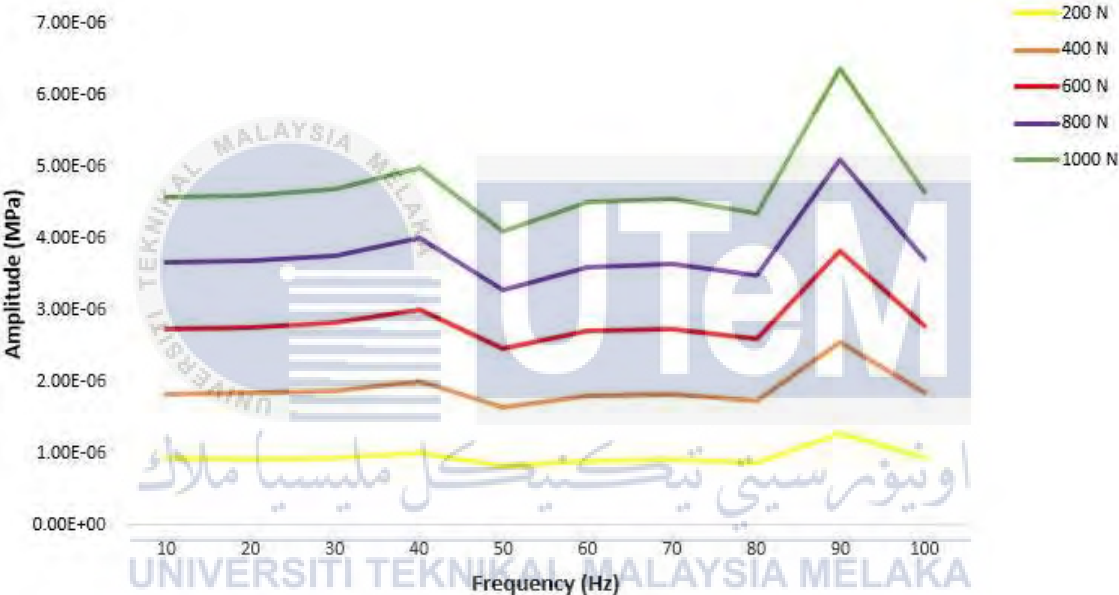


Figure 4.36: Result of Five Different Data with Different Value of Force Due to the 3 Embedded Plate Due to the Natural Rubber Rod for Stress Frequency Response

4.3.6 Deformation Frequency Response of Nature Rubber Rod with 3 Embedded Aluminium Alloy

4.3.6.1 For Force 200 N

Table 4.31 consist of the result of the force 200 N against the LR-MS model. The result of the analysis is represented in the form of graph in Figure 4.37 below.

Table 4.31: Result of the Frequency Response Due Deformation for Force 200 N

Frequency [Hz]	Amplitude (mm)
10	6.5606×10^{-4}
20	6.6990×10^{-4}
30	6.9498×10^{-4}
40	7.3982×10^{-4}
50	7.5524×10^{-4}
60	8.4191×10^{-4}
70	9.5027×10^{-4}
80	1.1118×10^{-3}
90	1.3801×10^{-3}
100	1.8752×10^{-3}

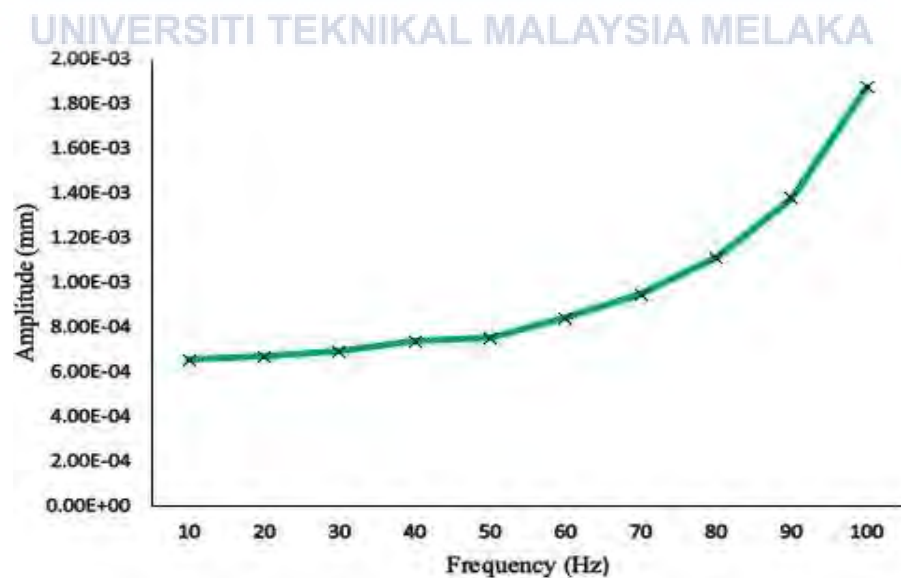


Figure 4.37: Graph Deformations Vs Frequency Response for Force 200 N

4.3.6.2 For Force 400 N

Table 4.32 consist of the result of the force 400 N against the LR-MS model. The result of the analysis is represented in the form of graph in Figure 4.38 below.

Table 4.32: Result of the Frequency Response Due Deformation for Force 400 N

Frequency [Hz]	Amplitude (mm)
10	1.3121×10^{-3}
20	1.3398×10^{-3}
30	1.3900×10^{-3}
40	1.4796×10^{-3}
50	1.5105×10^{-3}
60	1.6838×10^{-3}
70	1.9005×10^{-3}
80	2.2236×10^{-3}
90	2.7601×10^{-3}
100	3.7504×10^{-3}

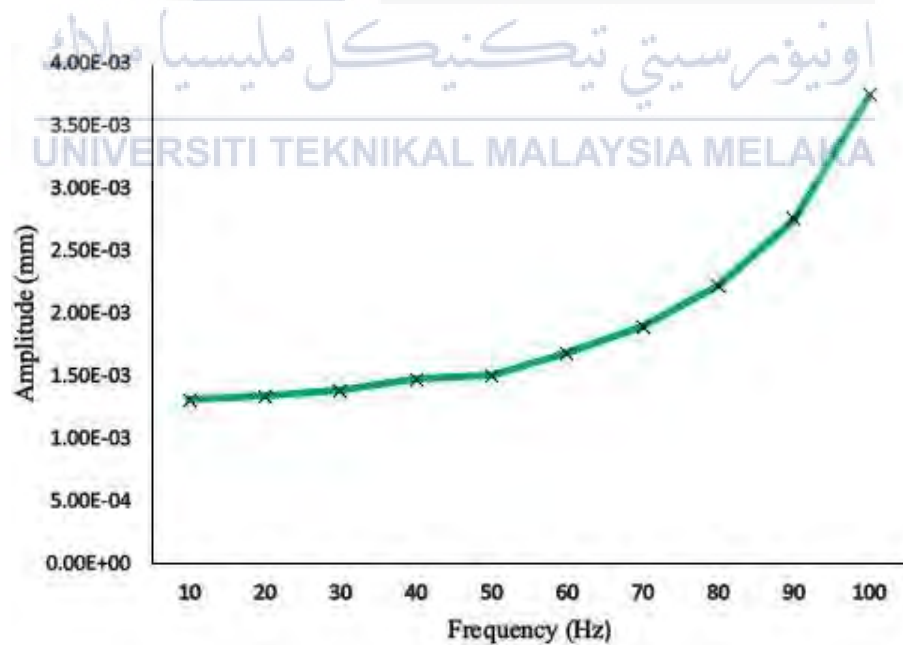


Figure 4.38: Graph Deformations Vs Frequency Response for Force 400 N

4.3.6.3 For Force 600 N

Table 4.33 consist of the result of the force 600 N against the LR-MS model. The result of the analysis is represented in the form of graph in Figure 4.39 below.

Table 4.33: Result of the Frequency Response Due Deformation for Force 600 N

Frequency [Hz]	Amplitude (mm)
10	1.9682×10^{-3}
20	2.0097×10^{-3}
30	2.0849×10^{-3}
40	2.2195×10^{-3}
50	2.2657×10^{-3}
60	2.5257×10^{-3}
70	2.8508×10^{-3}
80	3.3354×10^{-3}
90	4.1402×10^{-3}
100	5.6256×10^{-3}

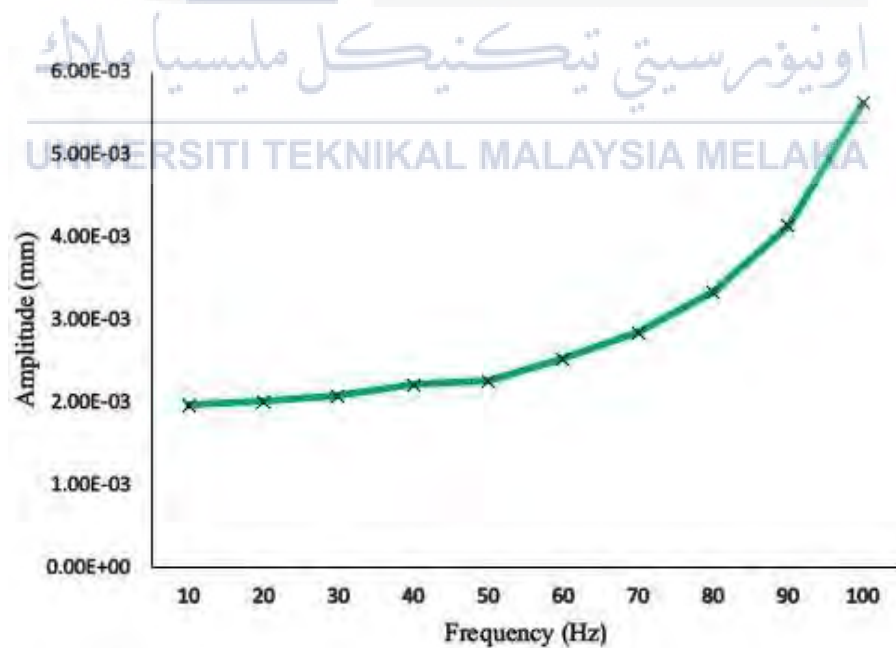


Figure 4.39: Graph Deformations Vs Frequency Response for Force 600 N

4.3.6.4 For Force 800 N

Table 4.34 below consist of the result of the force 800 N against the LR-MS model. The result of the analysis is represented in the form of graph in Figure 4.40.

Table 4.34: Result of the Frequency Response Due Deformation for Force 800 N

Frequency [Hz]	Amplitude (mm)
10	2.6242×10^{-3}
20	2.6796×10^{-3}
30	2.7799×10^{-3}
40	2.9593×10^{-3}
50	3.0210×10^{-3}
60	3.3677×10^{-3}
70	3.8011×10^{-3}
80	4.4472×10^{-3}
90	5.5202×10^{-3}
100	7.5008×10^{-3}

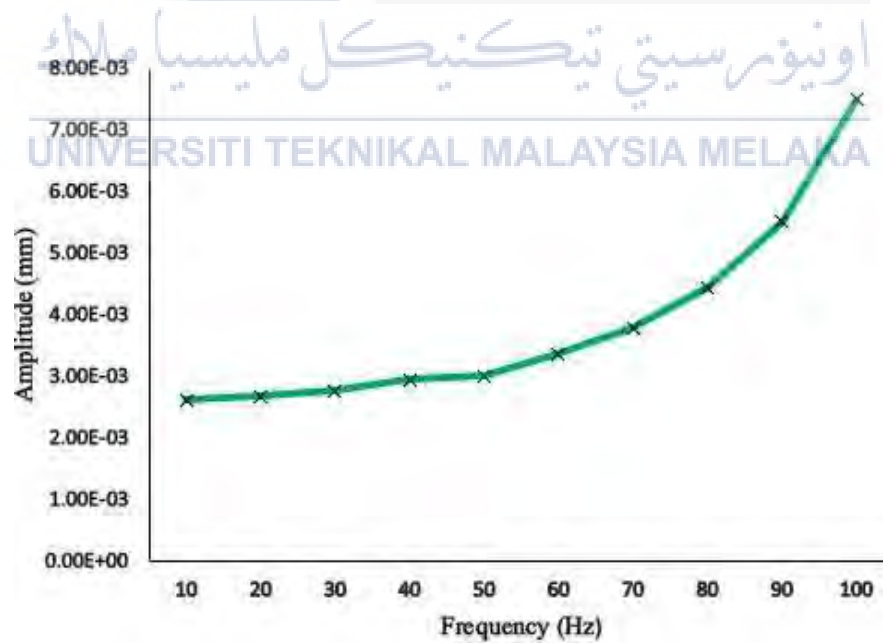


Figure 4.40: Graph Deformations Vs Frequency Response for Force 800 N

4.3.6.5 For Force 1000 N

Table 4.35 consist of the result of the force 1000 N against the LR-MS model. The result of the analysis is represented in the form of graph in Figure 4.41 above.

Table 4.35: Result of the Frequency Response Due Deformation for Force 1000 N

Frequency [Hz]	Amplitude (mm)
10	3.2803×10^{-3}
20	3.3495×10^{-3}
30	3.4749×10^{-3}
40	3.6991×10^{-3}
50	3.7762×10^{-3}
60	4.2096×10^{-3}
70	4.7513×10^{-3}
80	5.5590×10^{-3}
90	6.9003×10^{-3}
100	9.376×10^{-3}

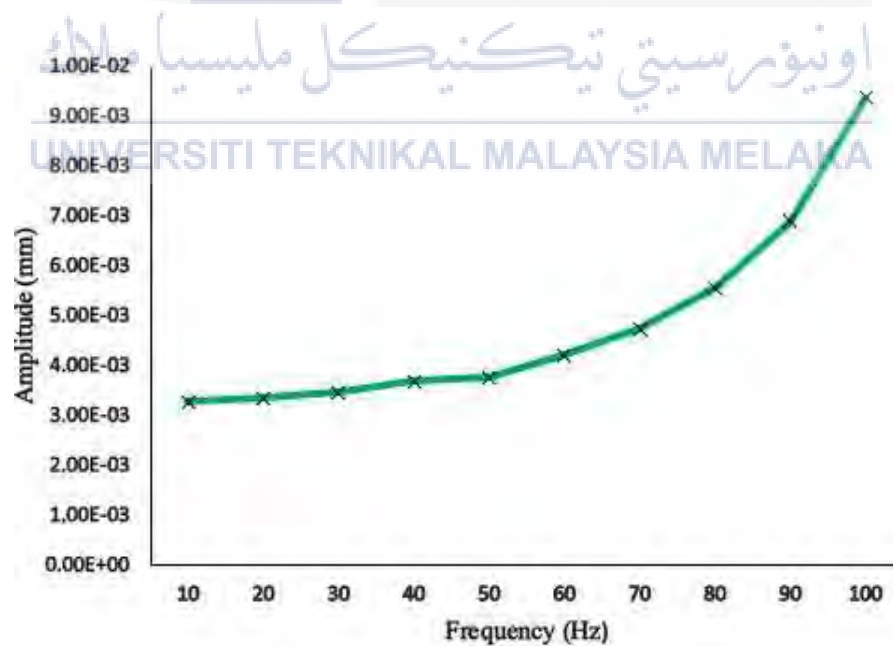


Figure 4.41: Graph Deformations Vs Frequency Response for Force 1000 N

Based on Figure 4.42 below, it shows the five-different line that represents the value of each analysis that completely done with the different value of the force due to the four-embedded plate on the natural rubber rod. The value of force is set to be 200N represent the yellow line, 400N represent the brown line, 600N represent the red line, 800N represent the purple line, and lastly, 1000N represent the green line. The data that obtain show that the graph is linearly increasing. The value of the amplitude increases with respectively to the value of the force.

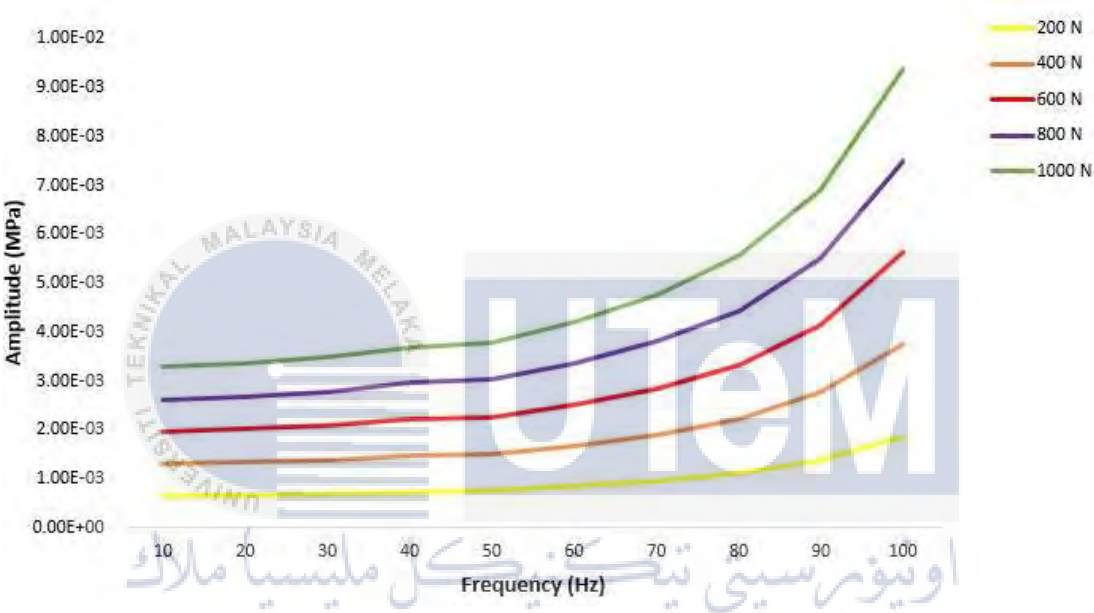


Figure 4.42: Result of Five Different Data with Different Value of Force Due to the 3 Embedded Plate Due to the Natural Rubber Rod for Deformation Frequency Response

4.3.7 Stress Frequency Response of the Nature Rubber Rod with 4 Embedded Aluminium Alloy

4.3.7.1 For Force 200 N

Table 4.36 consist of the result of the force 200 N against the LR-MS model. The result of the analysis is represented in the form of graph in Figure 4.43 below.

Table 4.36: Result of the Frequency Response Due Stress for Force 200 N

Frequency [Hz]	Amplitude (MPa)
10	1.1591×10^{-6}
20	1.1757×10^{-6}
30	1.2067×10^{-6}
40	1.2698×10^{-6}
50	1.0588×10^{-6}
60	1.2849×10^{-6}
70	1.3706×10^{-6}
80	1.4401×10^{-6}
90	1.2488×10^{-6}
100	2.5088×10^{-6}

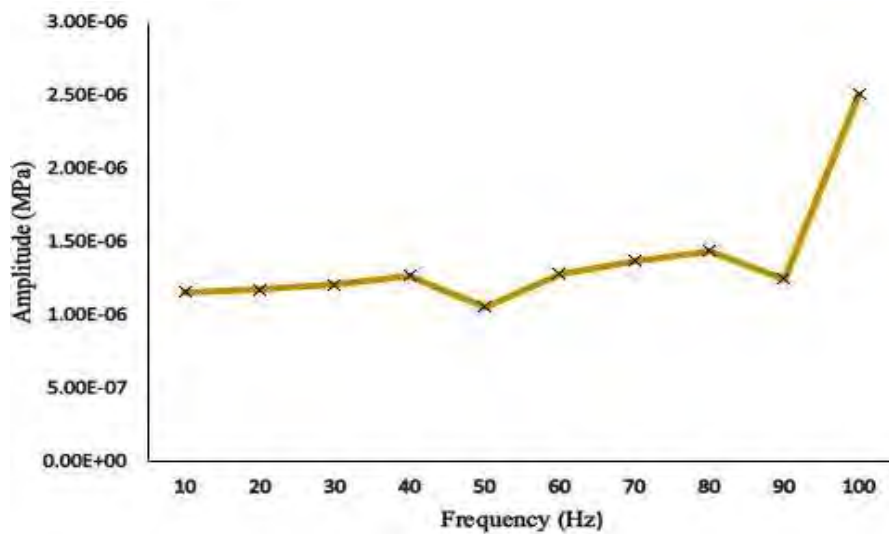


Figure 4.43: Graph Stress Vs Frequency Response for Force 200 N

4.3.7.2 For Force 400 N

Table 4.37 consist of the result of the force 400 N against the LR-MS model. The result of the analysis is represented in the form of graph in Figure 4.44 below.

Table 4.37: Result of the Frequency Response Due Stress for Force 400 N

Frequency [Hz]	Amplitude (MPa)
10	2.3183×10^{-6}
20	2.3514×10^{-6}
30	2.4133×10^{-6}
40	2.5396×10^{-6}
50	2.1176×10^{-6}
60	2.5698×10^{-6}
70	2.7412×10^{-6}
80	2.8802×10^{-6}
90	2.4977×10^{-6}
100	5.0176×10^{-6}

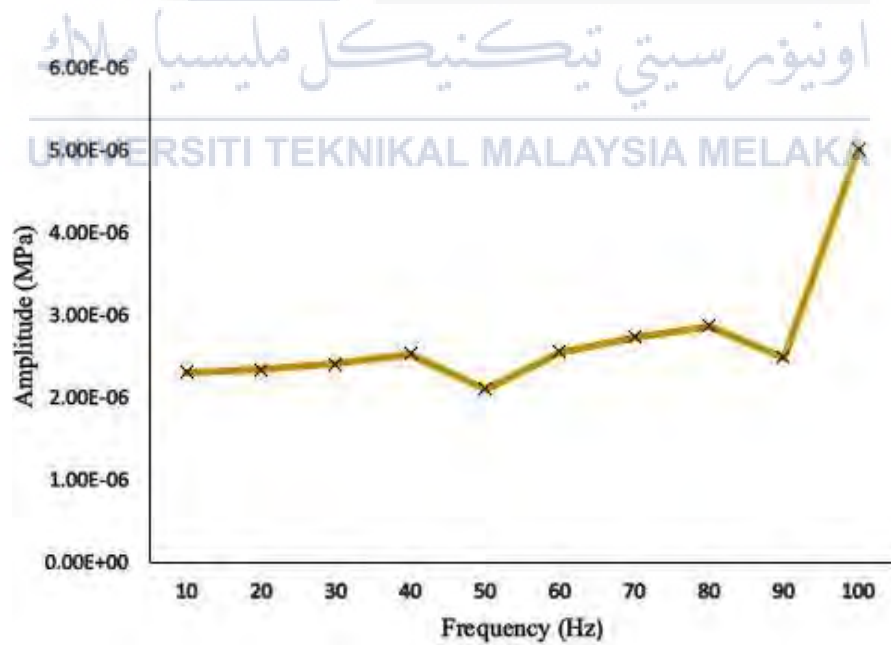


Figure 4.44: Graph Stress Vs Frequency Response for Force 400 N

4.3.7.3 For Force 600 N

Table 4.38 consist of the result of the force 600 N against the LR-MS model. The result of the analysis is represented in the form of graph in Figure 4.45 below.

Table 4.38: Result of the Frequency Response Due Stress for Force 600 N

Frequency [Hz]	Amplitude (MPa)
10	3.4774×10^{-6}
20	3.5271×10^{-6}
30	3.6200×10^{-6}
40	3.8094×10^{-6}
50	3.1764×10^{-6}
60	3.8547×10^{-6}
70	4.1118×10^{-6}
80	4.3203×10^{-6}
90	3.7465×10^{-6}
100	7.5263×10^{-6}

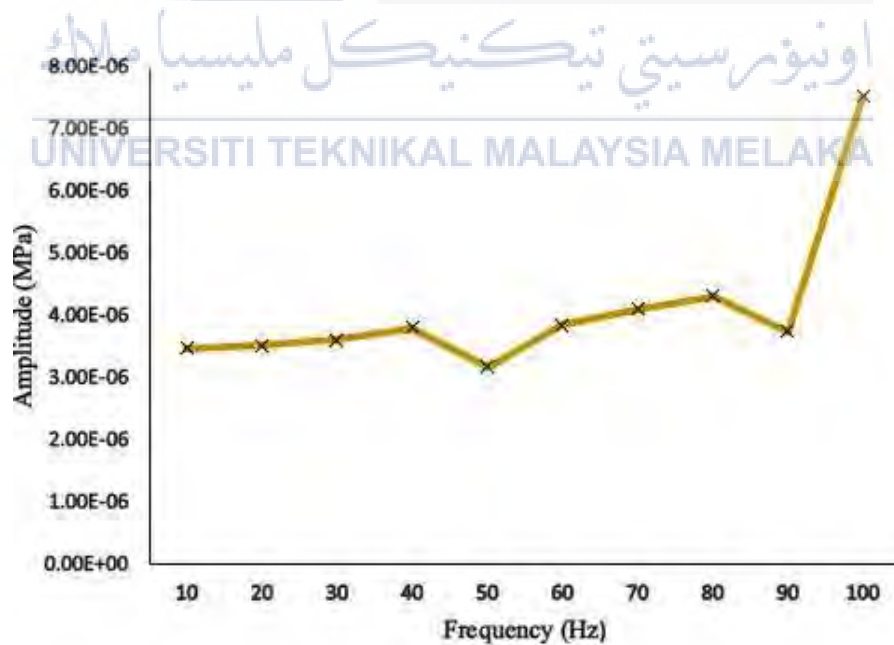


Figure 4.45: Graph Stress Vs Frequency Response for Force 600 N

4.3.7.4 For Force 800 N

Table 4.39 consist of the result of the force 800 N against the LR-MS model. The result of the analysis is represented in the form of graph in Figure 4.46 below.

Table 4.39: Result of the Frequency Response Due Stress for Force 800 N

Frequency [Hz]	Amplitude (MPa)
10	4.6365×10^{-6}
20	4.7027×10^{-6}
30	4.8267×10^{-6}
40	5.0792×10^{-6}
50	4.2351×10^{-6}
60	5.1396×10^{-6}
70	5.4824×10^{-6}
80	5.7604×10^{-6}
90	4.9954×10^{-6}
100	1.0035×10^{-5}

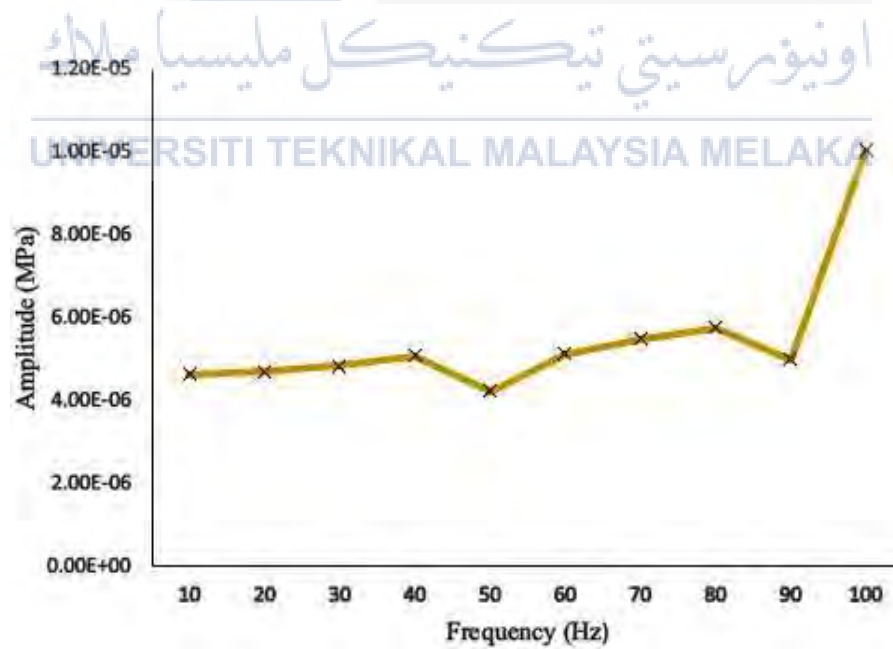


Figure 4.46: Graph Stress Vs Frequency Response for Force 600 N

4.3.7.5 For Force 1000 N

Table 4.40 consist of the result of the Force 1000 N against the LR-MS model. The result of the analysis is represented in the form of graph in Figure 4.47 below.

Table 4.40: Result of the Frequency Response Due Stress for Force 1000 N

Frequency [Hz]	Amplitude (MPa)
10	5.7957×10^{-6}
20	5.8784×10^{-6}
30	6.0334×10^{-6}
40	6.3490×10^{-6}
50	5.2939×10^{-6}
60	6.4246×10^{-6}
70	6.8530×10^{-6}
80	7.2004×10^{-6}
90	6.2442×10^{-6}
100	1.2544×10^{-5}

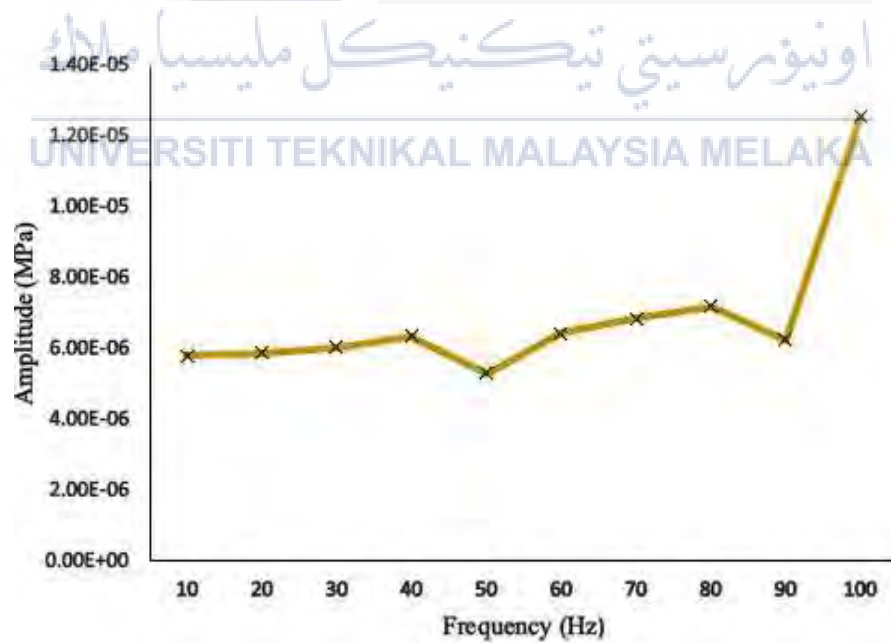


Figure 4.47: Graph Stress Vs Frequency Response for Force 1000 N

Based on figure 4.48 below, it shows the five-different line that represents the value of each analysis that completely done with the different value of the force due to the four-embedded plate on the natural rubber rod. The value of force is set to be 200N represent the yellow line, 400N represent the brown line, 600N represent the red line, 800N represent the purple line, and lastly, 1000N represent the green line. The data that obtain show that the graph is linearly increasing. The value of the amplitude increases with respectively to the value of the force.

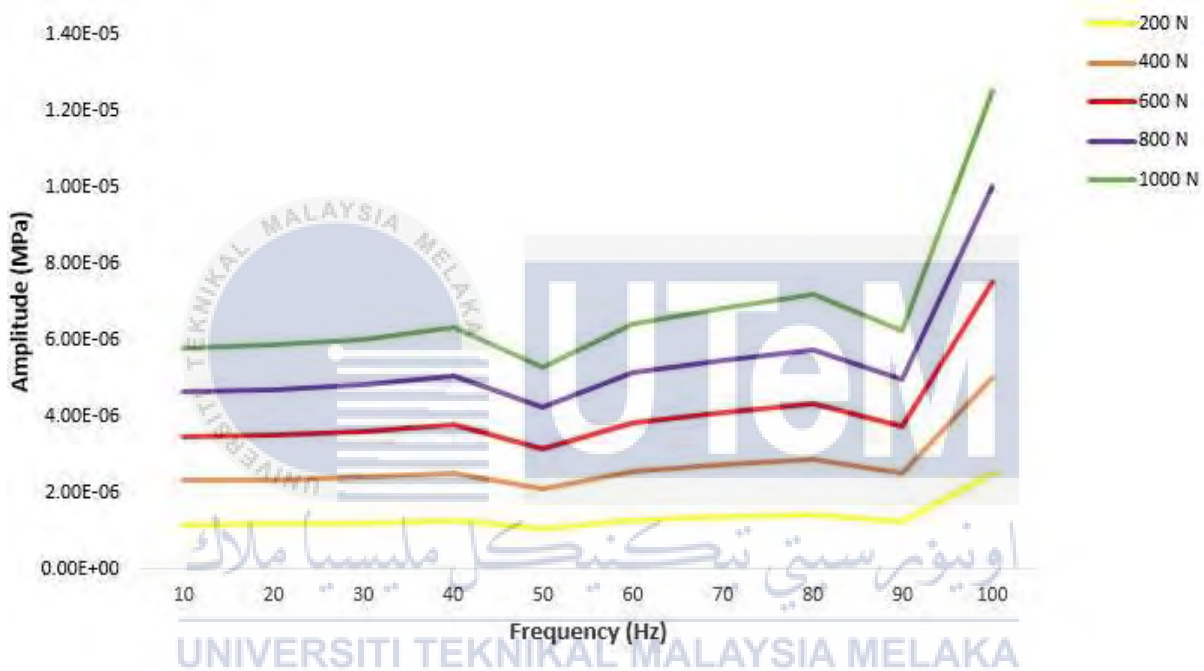


Figure 4.48: Result of Five Different Data with Different Value of Force Due to the 4 Embedded Plate Due to the Natural Rubber Rod for Stress Frequency Response

4.3.8 Deformation Frequency Response of Nature Rubber Rod with 4 Embedded Aluminium Alloy

4.3.8.1 For Force 200 N

Table 4.41 consist of the result of the force 200 N against the LR-MS model. The result of the analysis is represented in the form of graph in Figure 4.49 below.

Table 4.41: Result of the Frequency Response Due Deformation for Force 200 N

Frequency [Hz]	Amplitude (mm)
10	6.9514×10^{-4}
20	7.0495×10^{-4}
30	7.2245×10^{-4}
40	7.5228×10^{-4}
50	7.2764×10^{-4}
60	8.0863×10^{-4}
70	8.7050×10^{-4}
80	9.5050×10^{-4}
90	1.0591×10^{-3}
100	1.2158×10^{-3}

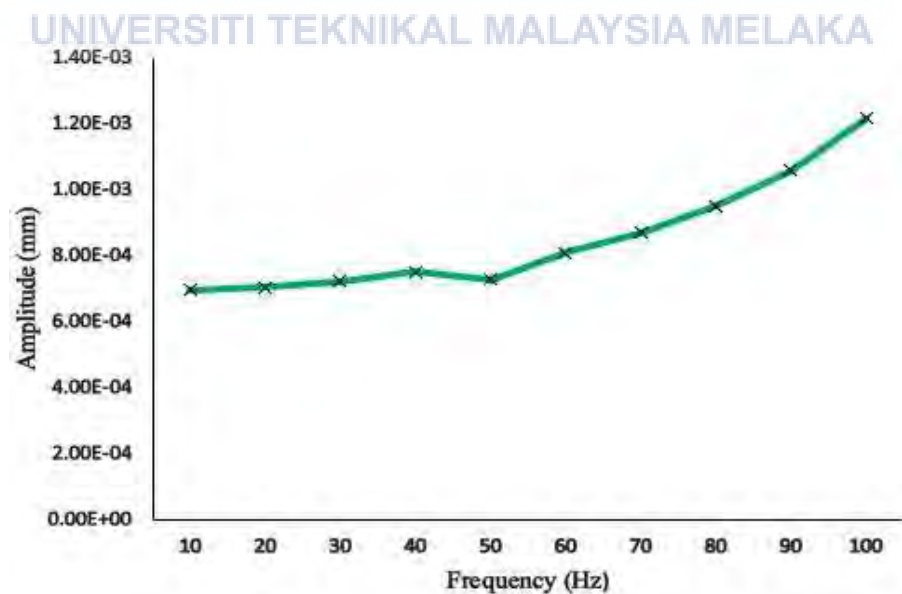


Figure 4.49: Graph Deformations Vs Frequency Response for Force 200 N

4.3.8.2 For Force 400 N

Table 4.42 consist of the result of the force 400 N against the LR-MS model. The result of the analysis is represented in the form of graph in Figure 4.50 below.

Table 4.42: Result of the Frequency Response Due Deformation for Force 400 N

Frequency [Hz]	Amplitude (mm)
10	1.3903×10^{-3}
20	1.4099×10^{-3}
30	1.4449×10^{-3}
40	1.5046×10^{-3}
50	1.4553×10^{-3}
60	1.6173×10^{-3}
70	1.7410×10^{-3}
80	1.9010×10^{-3}
90	2.1181×10^{-3}
100	2.4316×10^{-3}

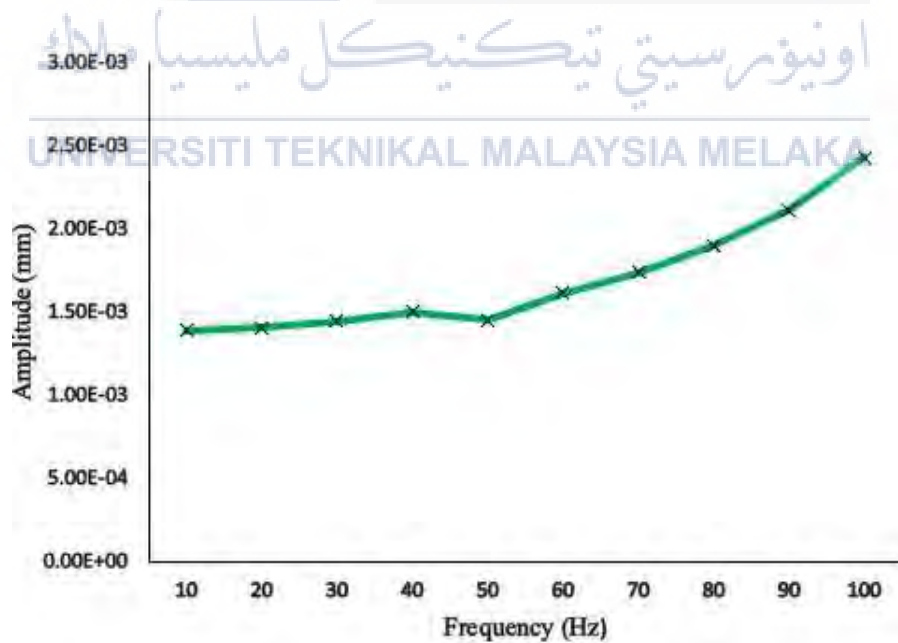


Figure 4.50: Graph Deformations Vs Frequency Response for Force 400 N

4.3.8.3 For Force 600 N

Table 4.43 consist of the result of the force 600 N against the LR-MS model. The result of the analysis is represented in the form of graph in Figure 4.51 below.

Table 4.43: Result of the Frequency Response Due Deformation for Force 600 N

Frequency [Hz]	Amplitude (mm)
10	2.0854×10^{-3}
20	2.1148×10^{-3}
30	2.1674×10^{-3}
40	2.2568×10^{-3}
50	2.1829×10^{-3}
60	2.4259×10^{-3}
70	2.6115×10^{-3}
80	2.8515×10^{-3}
90	3.1772×10^{-3}
100	3.6474×10^{-3}

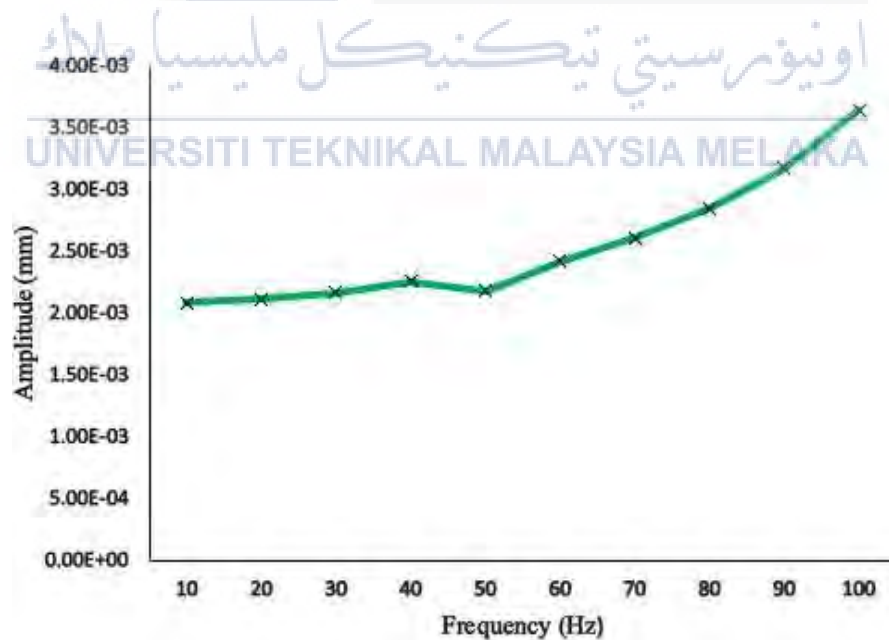


Figure 4.51: Graph Deformations Vs Frequency Response for Force 600 N

4.3.8.4 For Force 800 N

Table 4.44 below consist of the result of the force 800 N against the LR-MS model. The result of the analysis is represented in the form of graph in Figure 4.52.

Table 4.44: Result of the Frequency Response Due Deformation for Force 800 N

Frequency [Hz]	Amplitude (mm)
10	2.7806×10^{-3}
20	2.8198×10^{-3}
30	2.8898×10^{-3}
40	3.0091×10^{-3}
50	2.9106×10^{-3}
60	3.2345×10^{-3}
70	3.4820×10^{-3}
80	3.8200×10^{-3}
90	4.2362×10^{-3}
100	4.8632×10^{-3}

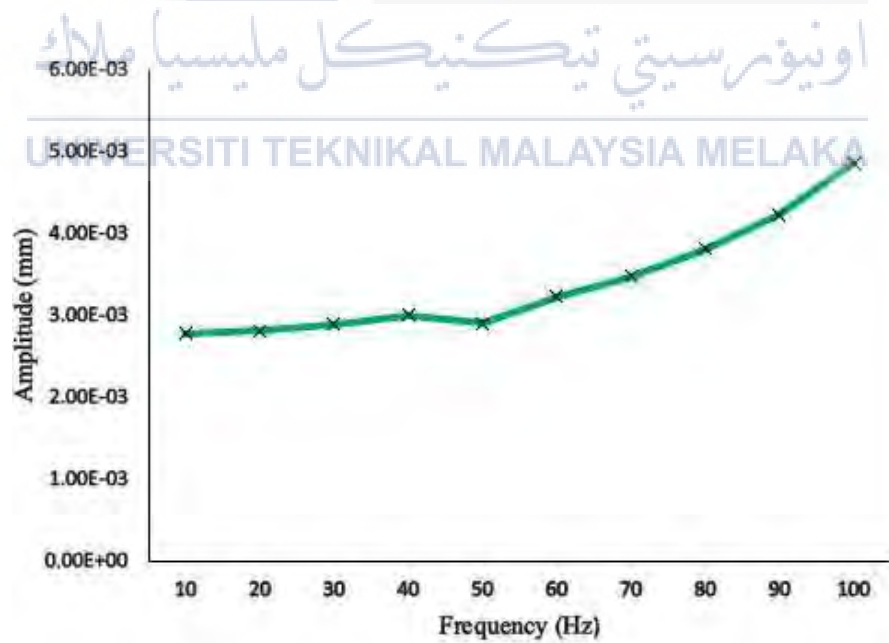


Figure 4.52: Graph Deformations Vs Frequency Response for Force 800 N

4.3.8.5 For Force 1000 N

Table 4.45 consist of the result of the force 1000 N against the LR-MS model. The result of the analysis is represented in the form of graph in Figure 4.53 above.

Table 4.45: Result of the Frequency Response Due Deformation for Force 1000 N

Frequency [Hz]	Amplitude (mm)
10	3.4757×10^{-3}
20	3.5247×10^{-3}
30	3.6123×10^{-3}
40	3.7614×10^{-3}
50	3.6382×10^{-3}
60	4.0431×10^{-3}
70	4.3525×10^{-3}
80	4.7525×10^{-3}
90	5.2953×10^{-3}
100	6.0789×10^{-3}

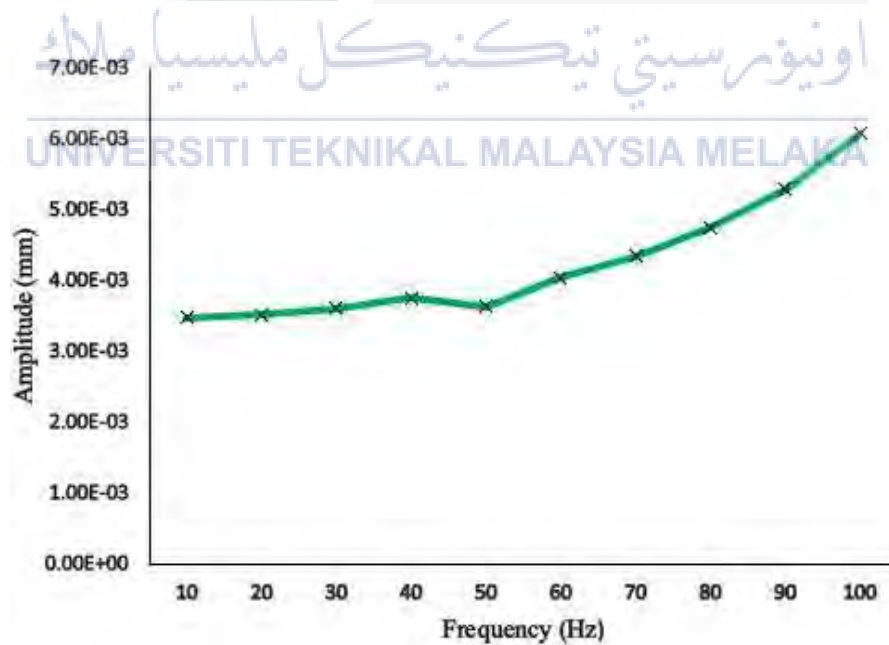


Figure 4.53: Graph Deformations Vs Frequency Response for Force 1000 N

Based on Figure 4.54 below, it shows the five-different line that represents the value of each analysis that completely done with the different value of the force due to the four-embedded plate on the natural rubber rod. The value of force is set to be 200N represent the yellow line, 400N represent the brown line, 600N represent the red line, 800N represent the purple line, and lastly, 1000N represent the green line. The data that obtain show that the graph is linearly increasing. The value of the amplitude increases with respectively to the value of the force.

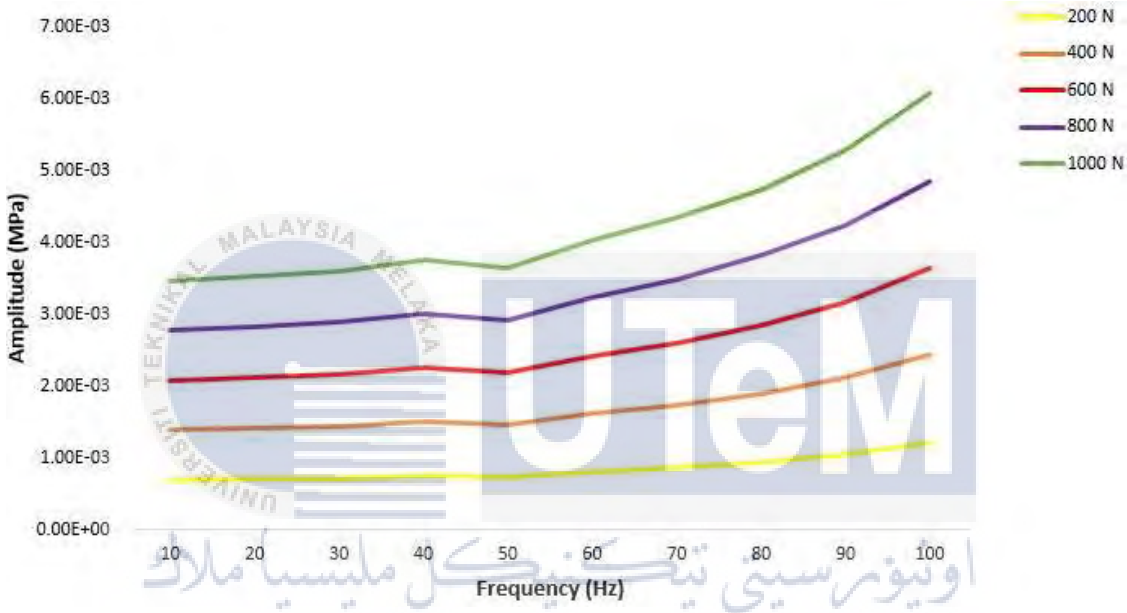


Figure 4.54: Result of Five Different Data with Different Value of Force Due to the 4 Embedded Plate Due to the Natural Rubber Rod for Deformation Frequency Response

4.4 Summary

In this section, it will show the summary of the result and discussion. The data and the result of the analysis are shown in the table and graph below.

Based on the Figure 4.55 below, it shows the result of combination of the 5 different types of lines that refer to the different types of the natural rubber rod. The red line represents the nature rubber rod without embedded plate on it, the yellow line represents for the nature rubber rod with 1 embedded plate on it, black line represents for the nature rubber rod with 2 embedded plates on it, brown line represents for the nature rubber rod with 3 embedded plates on it, and lastly, green line represents for the nature rubber rod with 4 embedded plates on it with different number of modality. Refer to the graph, the data show the value of the frequency is increase follow by the increasing the number of the modality and the value of the frequency is increased followed by the increasing number of embedded plate on the nature rubber rod.

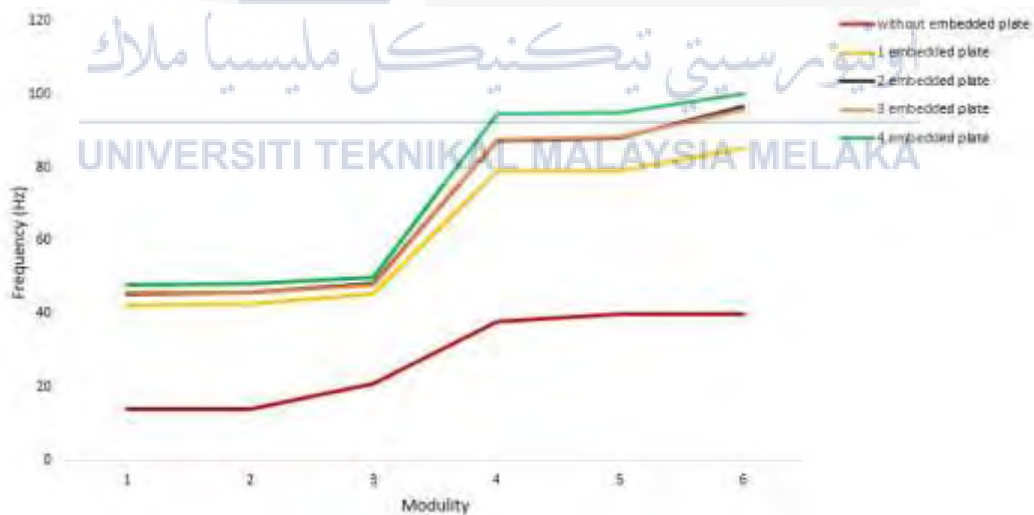


Figure 4.55: Combination of Graph of the Different Types of Modality with the Frequency

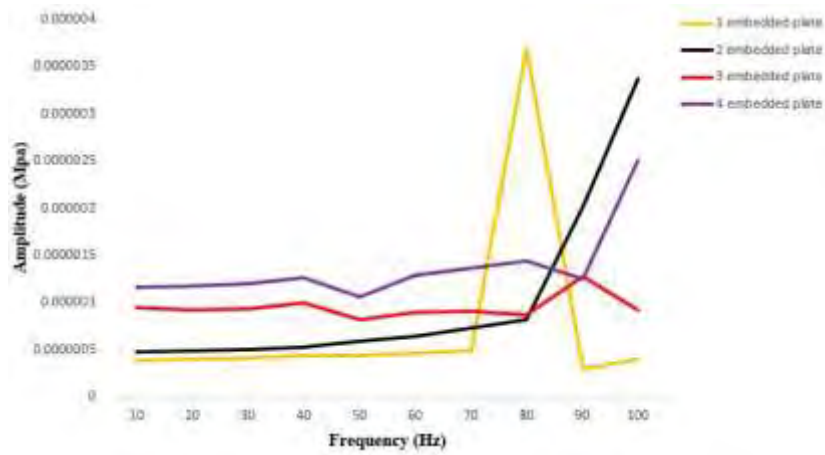
Table 4.46: Natural Frequency for Plate Model from Finite Element Method.

Vibration Mode	Natural Frequency (Hz)				
	Without Embedded Plate	1 Embedded Plate	2 Embedded Plate	3 Embedded Plate	4 Embedded Plate
1	13.951	42.490	45.585	45.644	47.927
2	14.039	42.720	45.976	45.842	48.117
3	21.009	45.385	48.274	47.839	49.977
4	37.949	79.064	87.232	87.704	94.532
5	39.925	79.072	87.845	88.136	94.923
6	39.947	85.246	96.550	95.636	99.916

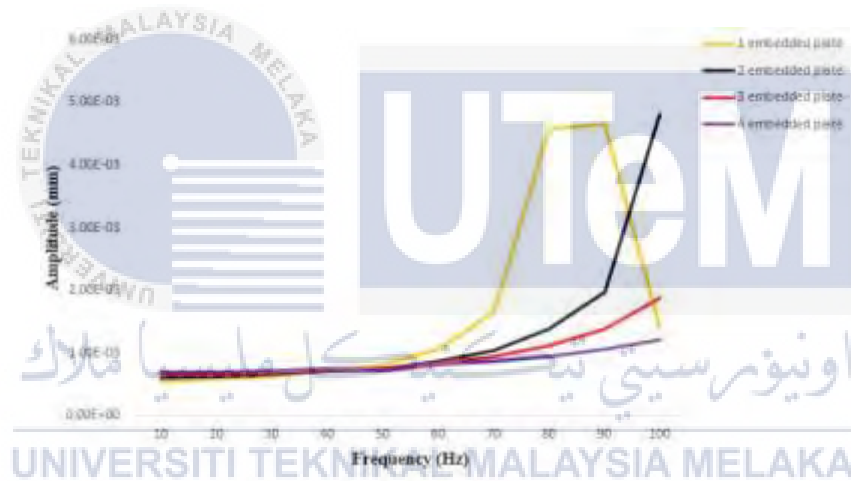
Based on the Table 4.46 above, it shows the data is intemperate from the graph in the Figure 4.55. From the table, the value of the frequency against the increasing modality for every type of the nature rubber rod can be seen. Based on that data, the lowest frequency is located on the modality 1 with the without the embedded plate on natural rubber rod. The value is increasing following the increasing of the modality in every type of rubber rod and increasing the number of the plate that embedded on the natural rubber rod.

Table 4.47: Result of Stress and Deformation Frequency Response for 200 N

Frequency (Hz)	1 Embedded plate	2 Embedded plate	3 Embedded plate	4 Embedded plate
Stress Frequency Response (MPa)				
10	3.9708×10^{-7}	4.7996×10^{-7}	9.5120×10^{-7}	1.1591×10^{-6}
20	4.0281×10^{-7}	4.9030×10^{-7}	9.2308×10^{-7}	1.1757×10^{-6}
30	4.1346×10^{-7}	5.0839×10^{-7}	9.4026×10^{-7}	1.2067×10^{-6}
40	4.4022×10^{-7}	5.3400×10^{-7}	1.0005×10^{-6}	1.2698×10^{-6}
50	4.4091×10^{-7}	5.8789×10^{-7}	8.2064×10^{-7}	1.0588×10^{-6}
60	4.7211×10^{-7}	6.4536×10^{-7}	9.0224×10^{-7}	1.2849×10^{-6}
70	4.9077×10^{-7}	7.3387×10^{-7}	9.1348×10^{-7}	1.3706×10^{-6}
80	3.6803×10^{-6}	8.2827×10^{-7}	8.7069×10^{-7}	1.4401×10^{-6}
90	3.0103×10^{-7}	2.0089×10^{-6}	1.2751×10^{-6}	1.2488×10^{-6}
100	4.0517×10^{-7}	3.3665×10^{-6}	9.2946×10^{-7}	2.5088×10^{-6}
Deformation Frequency Response (mm)				
10	5.5757×10^{-4}	6.0542×10^{-4}	6.5606×10^{-4}	6.9514×10^{-4}
20	5.8221×10^{-4}	6.2264×10^{-4}	6.6990×10^{-4}	7.0495×10^{-4}
30	6.2941×10^{-4}	6.5427×10^{-4}	6.9498×10^{-4}	7.2245×10^{-4}
40	7.2785×10^{-4}	7.1064×10^{-4}	7.3982×10^{-4}	7.5228×10^{-4}
50	8.1789×10^{-4}	7.4638×10^{-4}	7.5524×10^{-4}	7.2764×10^{-4}
60	1.0689×10^{-3}	8.6898×10^{-4}	8.4191×10^{-4}	8.0863×10^{-4}
70	1.6519×10^{-3}	1.0492×10^{-3}	9.5027×10^{-4}	8.7050×10^{-4}
80	4.5724×10^{-3}	1.3794×10^{-3}	1.1118×10^{-3}	9.5050×10^{-4}
90	4.6564×10^{-3}	1.9673×10^{-3}	1.3801×10^{-3}	1.0591×10^{-3}
100	1.4007×10^{-3}	4.8077×10^{-3}	1.8752×10^{-3}	1.2158×10^{-3}



(a)



(b)

Figure 4.56: (a) Graph of Comparison for the Stress Frequency Response for 200N (b) Graph of Comparison for the Deformation Frequency Response for 200N

All the table above show the combination all the data and the result of the analysis done by using the ANSYS Finite Element Analysis software. In Table 4.77 above, it contains the result of the natural rubber rod embedded with the different number of aluminium alloy plate against the frequency. Every type of the rubber rod will contain the 3-types of the result and for every result has been tested with 5-different of forces. Every type of natural rubber rod

is the 1- aluminium alloy plate embedded, 2-aluminium alloy plate embedded, 3-aluminium alloy plate embedded and lastly 4-aluminium alloy plate embedded, it produced the 2-different result which is the stress frequency response, and the deformation frequency response. For every type of the natural rubber rod has been tested with the 5-different type of forces which is 200N, 400N, 600N, 800N and the last one is 1000N.

Based on the Figure 4.56 below, it shows the 4-different line that represents the value of the number of the embedded plate on the natural rubber rod. The 1- aluminium alloy plate embedded represent the yellow line, 2- aluminium alloy plate embedded represent the black line, 3- aluminium alloy plate embedded represent the red line, and lastly 4- aluminium alloy plate embedded 800N represent the purple line. For Figure 4.56 (a), for the stress frequency response, the analysis was carried out by using the 200N force. From this analysis, the natural rubber rod with 1- aluminium alloy plate embedded was produced the higher value of the stress frequency response, followed by natural rubber rod with 2- aluminium alloy plate embedded, natural rubber rod with 3- aluminium alloy plate embedded, and the lastly natural rubber rod with 4- aluminium alloy plate embedded. The value of the stress frequency decrease with increase the number of embedded aluminium alloy plate on the natural rubber rod.

For Figure 4.56 (b), the deformation frequency response analysis was carried out with the same 200N value of force. From this analysis, the natural rubber rod with 1- aluminium alloy plate embedded was produced the higher value of the stress frequency response, followed by natural rubber rod with 2- aluminium alloy plate embedded, natural rubber rod with 3- aluminium alloy plate embedded, and the lastly natural rubber rod with 4- aluminium alloy plate embedded. The value of the deformation frequency decrease with increase the number of embedded aluminium alloy plate on the natural rubber rod.

And next, the analysis was carried out with the increasing value of force due to the all of the number of aluminium alloy embedded on the natural rubber rod which is 400N, 600N, 800N and 1000N, the natural rubber rod with 1- aluminium alloy plate embedded also was produce the higher value of the stress frequency response and deformation frequency response, followed by natural rubber rod with 2- aluminium alloy plate embedded, natural rubber rod with 3- aluminium alloy plate embedded, and the lastly natural rubber rod with 4-

aluminium alloy plate embedded. The value of every type of frequency decrease with increase the number of embedded aluminium alloy plate on the natural rubber rod.



CHAPTER 5

CONCLUSION AND RECOMMENDATION

5.1 Conclusion

This chapter summarised overall progress of this project is presented including all part that related to this project. The conclusion consists of the effect of each type of embedded aluminium alloy with the applied force due to the analysis.

This project has the 5 type of the natural rubber rod that was been analyse by using the 5-different value of force. The analysis involved is the modal analysis, stress frequency response and the deformation frequency response. The type of the natural rubber rod is the nature rubber rod without embedded plate, the nature rubber rod with 1 embedded aluminium alloy plate, the nature rubber rod with 2 embedded aluminium alloy plate, the nature rubber rod with 3 embedded aluminium alloy plate and the last one is the nature rubber rod with 4 embedded aluminium alloy plate. The value of force that involve in this analysis is 200N, 400N, 600N, 800N and 1000N.

From the analysis, refer to the graph and data, it showed the value of the frequency is increase followed by the increasing the number of the modality and the value of the frequency is increase followed by the increasing number of the embedded plate on the nature rubber rod. The lowest frequency is from the analysis of the vibration mode 1 for the natural rubber rod without embedded aluminium alloy plate with 13.951Hz and the highest frequency for this analysis is from the analysis of the vibration mode 6 for the nature rubber rod with 4 embedded aluminium alloy plate. As conclusion, the value of the natural frequency of the natural rubber rod will increase with increase the number of embedded aluminium alloy plate.

Next is about the stress frequency response analysis. As the conclusion, from the result obtain it show that the value of stress (MPa) against the frequency will decrease when the number of embedded plates applied to the natural rubber rod. The value of deformation (mm) against the frequency also decrease when the number of embedded plates applied to the natural rubber rod. From the analysis, the number of the stress and the deformation against the frequency is increased when the value of the force is increase, but decrease against the increasing number of the embedded plate on the natural rubber rod.

For the overall, every type of embedded that has been analysed in this analysis create the different result and outcome. The result obtained is show the effectiveness in every parameter used.

5.2 Recommendation

In the future, from the result and conclusion made, the improvement and modification for this project should be carried out for the future to make the discovery of this project to become more challenge and interesting. The modified on the natural rubber rod can be improved based on the research by carrying out the experiment by using the real equipment, tools, and models in the laboratory. Based on the result of the experiment, we also can compare the result such as the percentage of error of this experiment result with the result of analysis that obtains by using the ANSYS Finite Element Analysis software. Besides that, we should try another alternative to ensure the validity of the data that gained from the analysis by comparing the result from the analysis with the other type of the Finite Element Analysis Software such as CATIA Finite Element Analysis Software or ABAQUS Finite Element Analysis Software.

Other than that, the modification on the natural rubber rod should be carried out. For example, the modification on the diameter of the natural rubber rod, the modification on the height of the natural rubber rod, and the modification if the thickness of every plate that embedded on the natural rubber rod. With this modification, we can see the comparison and make the better conclusion whether which one from this study will produce the productive result.

REFERENCES

Salim, M. A., Putra, A., Thompson, D., Ahmad, N., & Abdullah, M. A. (2013). Transmissibility of a Laminated Rubber-Metal Spring: A Preliminary Study. *Applied Mechanics and Materials*, 393, 661-665. doi:10.4028/www.scientific.net/amm.393.661

Putra, A., Norfarizan, S., Samekto, H., & Salim, M. A. (2013). Static Analysis of a Laminated Rubber-Metal Spring Using Finite Element Method. *Advanced Materials Research*, 845, 86-90. doi:10.4028/www.scientific.net/amr.845.86

Conference Calendar. (2007). *Engineering Applications of Artificial Intelligence*, 20(5). doi:10.1016/s0952-1976(07)00065-6

Du, B., Wang, X., Feng, Y., Yu, D., & Xu, G. (2014). Intelligent Assembly Technology Based on Standard Parts Feature of CATIA. *Modern Applied Science*, 8(2). doi:10.5539/mas.v8n2p49

Salim, M. A., Putra, A., Thompson, D., Ahmad, N., & Abdullah, M. A. (2013). Transmissibility of a Laminated Rubber-Metal Spring: A Preliminary Study. *Applied Mechanics and Materials*, 393, 661-665. doi:10.4028/www.scientific.net/amm.393.661

Salim, M. A., Putra, A., & Abdullah, M. A. (2013). Analysis of Axial Vibration in the Laminated Rubber-Metal Spring. *Advanced Materials Research*, 845, 46-50. doi:10.4028/www.scientific.net/amr.845.46

Salim, M., Putra, A., Mansor, M., Musthafah, M., Akop, M., & Abdullah, M. (2016). Analysis of Parameters Assessment on Laminated Rubber-Metal Spring for Structural Vibration. *IOP Conference Series: Materials Science and Engineering*, 114, 012014. doi:10.1088/1757-899x/114/1/012014

Modeling Material Damping Properties in Ansys - Documents. (2014, November 17). Retrieved May 14, 2017, from <http://documents.mx/documents/modeling-material-damping-properties-in-ansys.html>

Lian, K., Fan, B., Miao, Y., & Zhu, X. (2016). Research on Optimal Design and Modal Analysis of the Frame. *Proceedings of the 2016 International Conference on Artificial Intelligence: Technologies and Applications*. doi:10.2991/icaita-16.2016.6

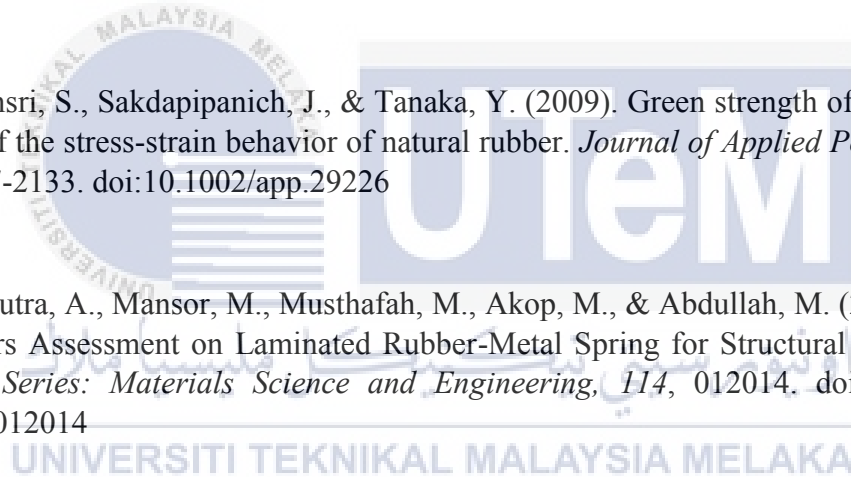
Li, Z., Zang, X. Z., Suo, L. C., Zhu, Y. H., & Zhao, J. (2014). Static Analysis and Modal Analysis of Heavy-Load Manipulator Based on ANSYS. *Applied Mechanics and Materials*, 556-562, 1059-1064. doi:10.4028/www.scientific.net/amm.556-562.1059

A. (n.d.). ANSYS Mechanical APDL Theory Reference. Retrieved May 14, 2017, from <https://www.scribd.com/document/290527666/ANSYS-Mechanical-APDL-Theory-Reference>

Meng, J., Liu, Y., & Liu, R. (2011). Finite Element Analysis of 4-Cylinder Diesel Crankshaft. *International Journal of Image, Graphics and Signal Processing*, 3(5), 22-29. doi:10.5815/ijigsp.2011.05.04

Amnuaypornsrri, S., Sakdapipanich, J., & Tanaka, Y. (2009). Green strength of natural rubber: The origin of the stress-strain behavior of natural rubber. *Journal of Applied Polymer Science*, 111(4), 2127-2133. doi:10.1002/app.29226

Salim, M., Putra, A., Mansor, M., Musthafah, M., Akop, M., & Abdullah, M. (2016). Analysis of Parameters Assessment on Laminated Rubber-Metal Spring for Structural Vibration. *IOP Conference Series: Materials Science and Engineering*, 114, 012014. doi:10.1088/1757-899x/114/1/012014



APPENDICES

Appendix A

Gantt Chart for PSM I

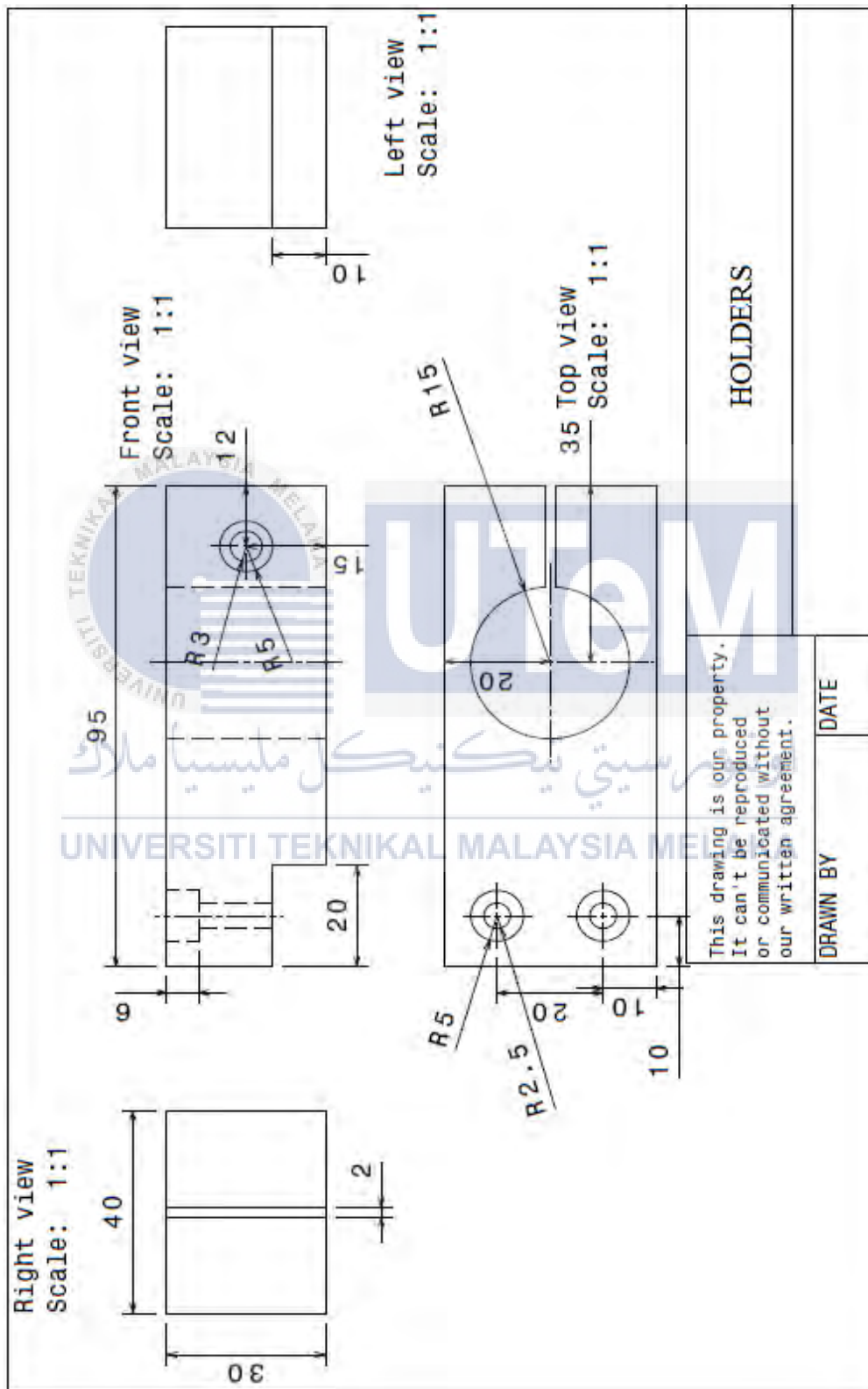
WEEK	1	2	3	4	5	6	7	8	9	10	11	12	13	14	15
Literature review															
ANSYS FEA tutorial															
Methodology															
Progress report submitted															
Setup for 3-D drawing															
Report writing															
Submission draft final report															
Seminar presentation															

Appendix B

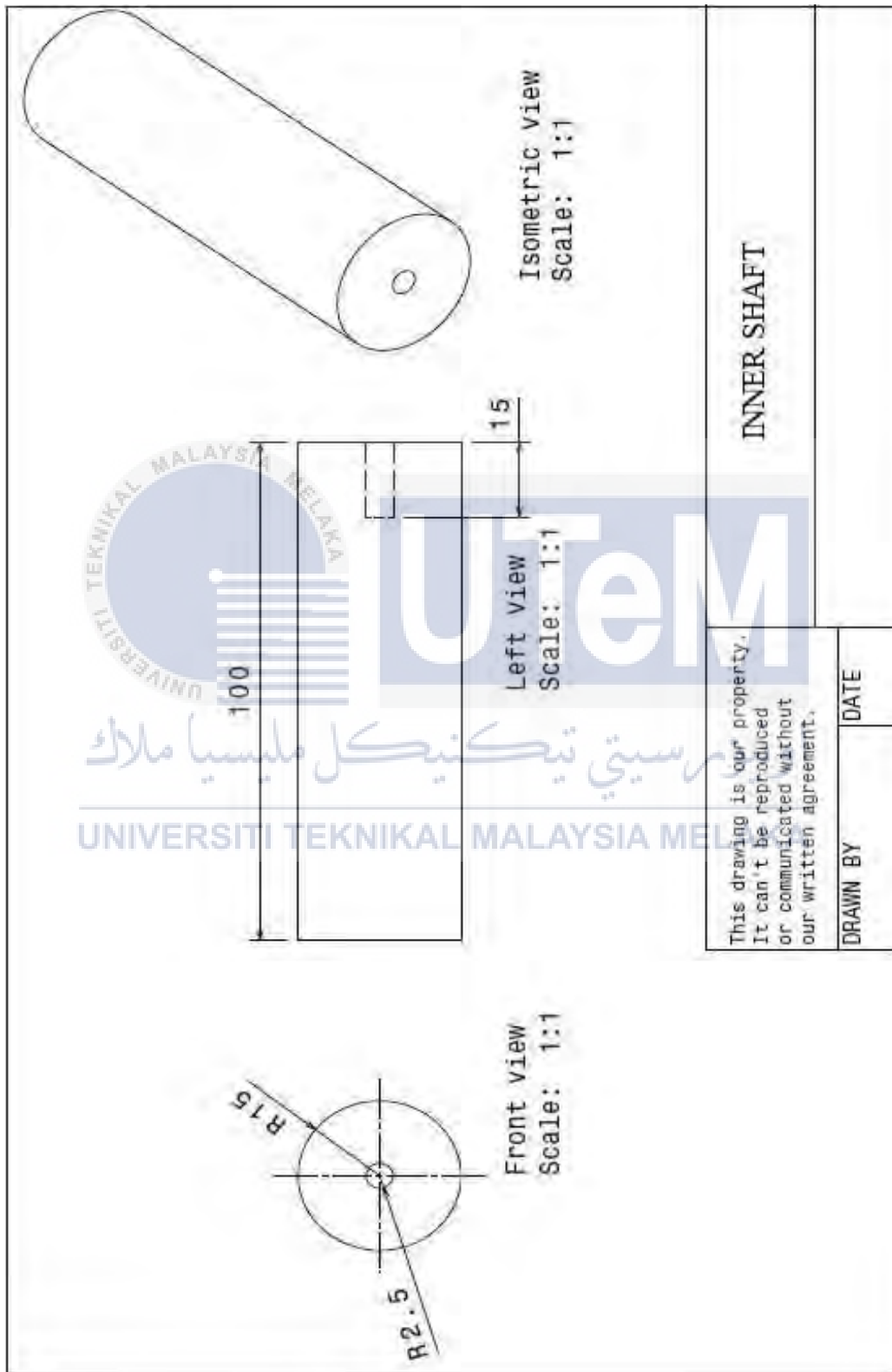
Gantt Chart for PSM II

TASK	WEEK														
	1	2	3	4	5	6	7	8	9	10	11	12	13	14	15
Continuous study of the of the model															
Draw the 5-different type of rubber rod on CATIA															
Figure out the transmissibility formula related to the types of rubber rod															
Analysis the type 2 and 3 of the rubber rod															
Analysis the type 4 and 5 of the rubber rod															
Combination result of parameters															
Report writing															
Submit the draft report															
Seminar PSM 2															
Complete report submits															

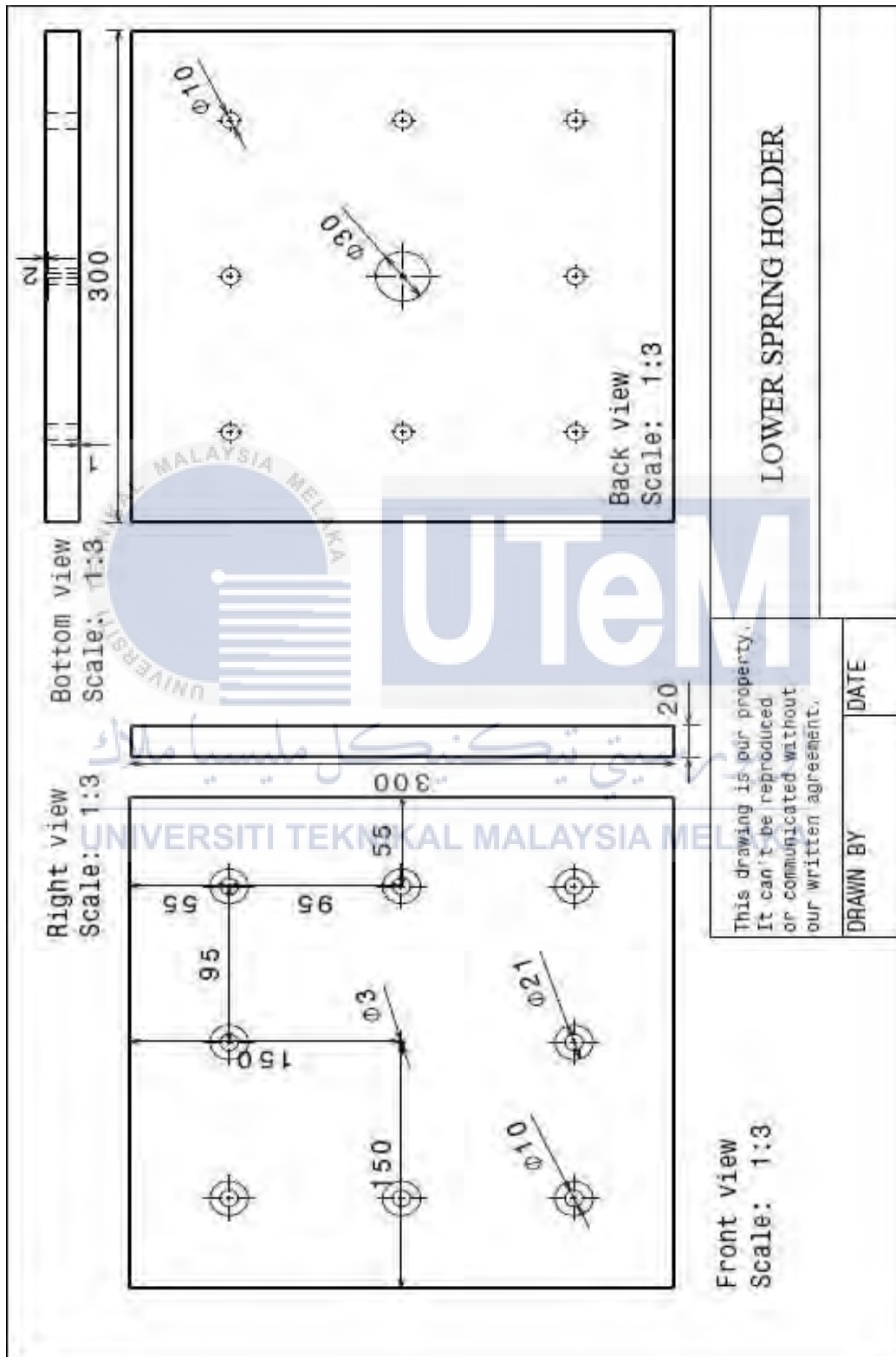
Appendix C



Appendix D



Appendix E



Front view
Scale: 1:3

Right view
Scale: 1:3

Bottom view
Scale: 1:3

Back view
Scale: 1:3

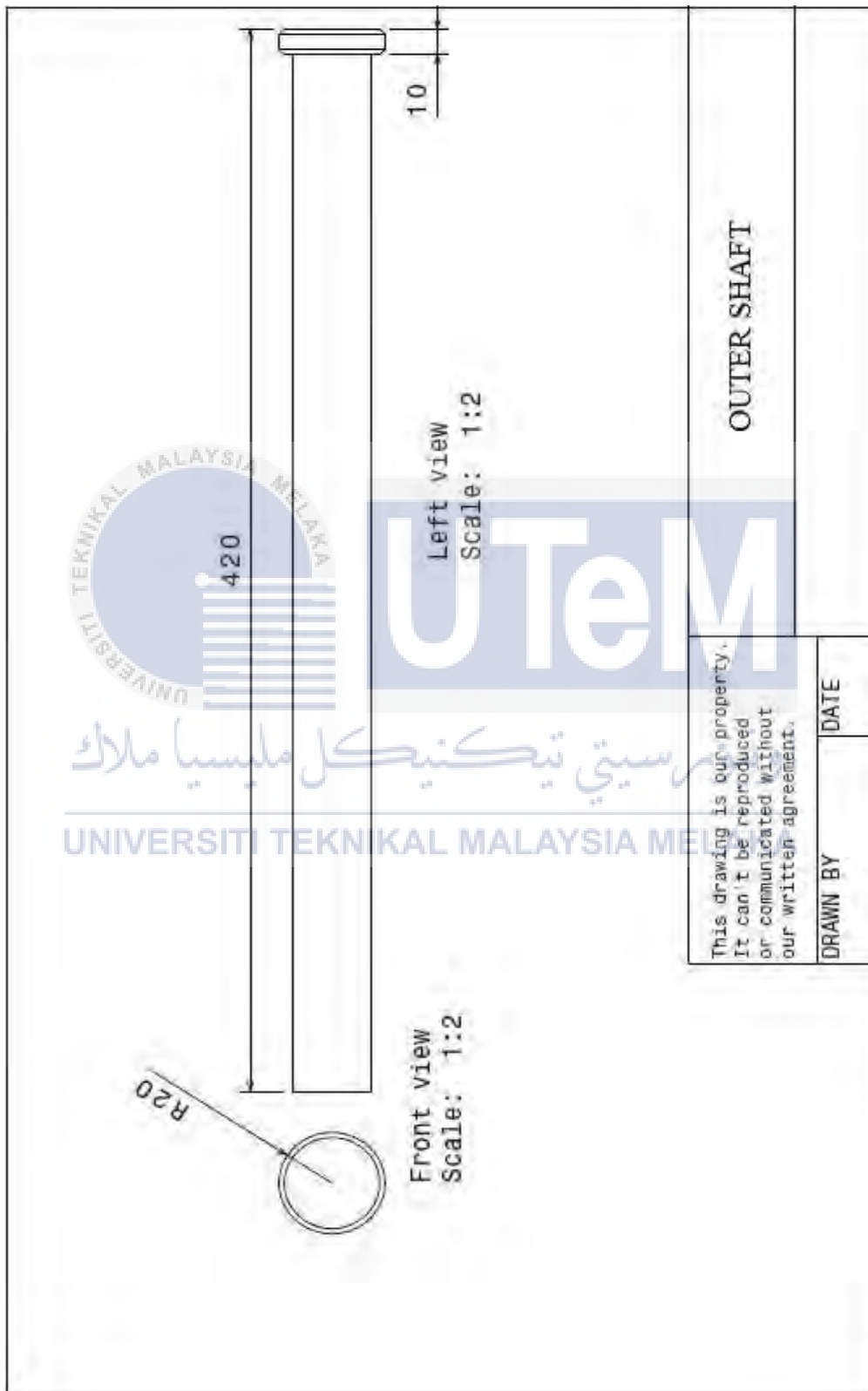
LOWER SPRING HOLDER

This drawing is our property.
It can't be reproduced
or communicated without
our written agreement.

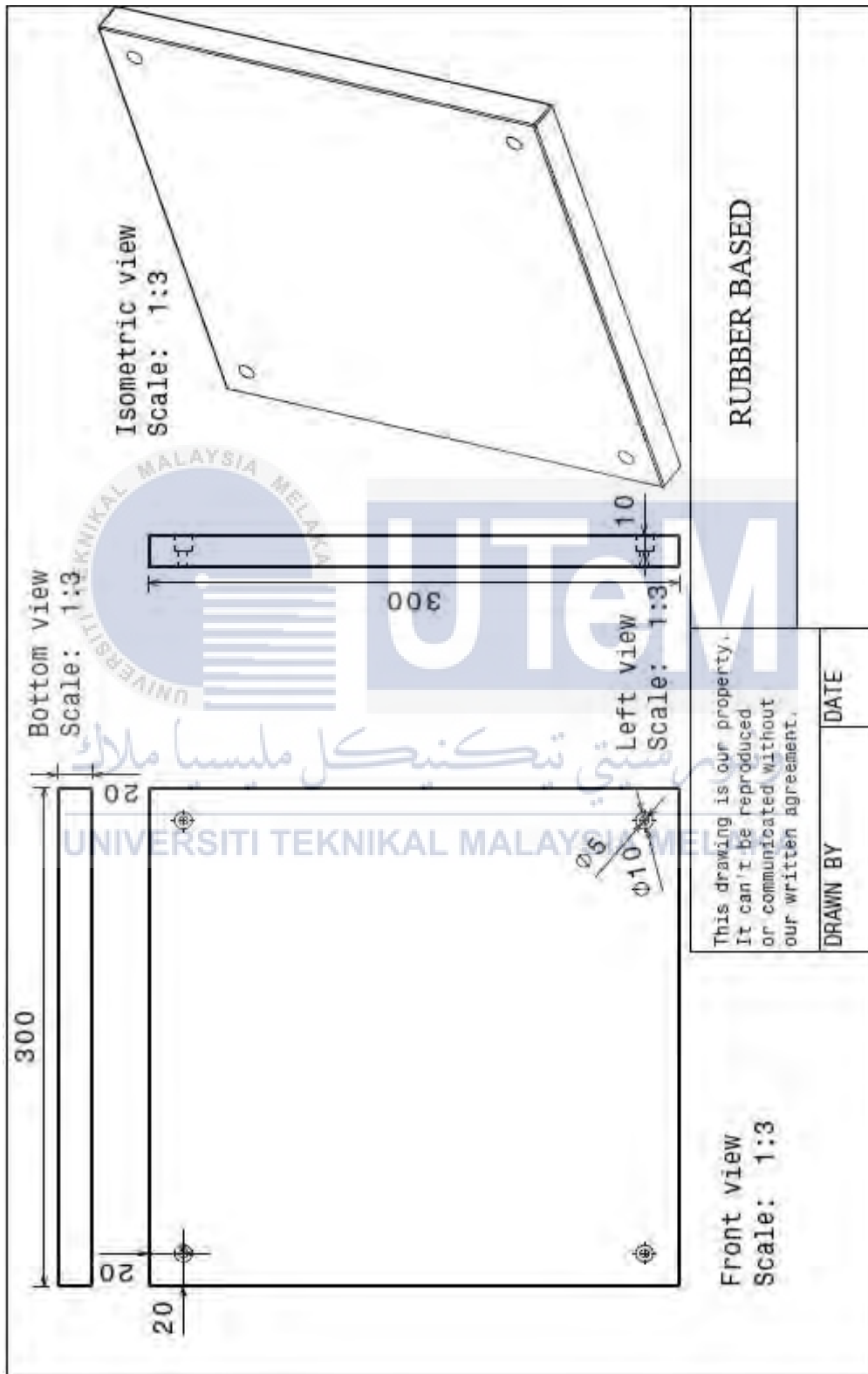
DRAWN BY

DATE

Appendix F



Appendix G



This drawing is our property.
It can't be reproduced
or communicated without
our written agreement.

RUBBER BASED

DRAWN BY _____ DATE _____

Appendix I

The drawing consists of four views of a spring:

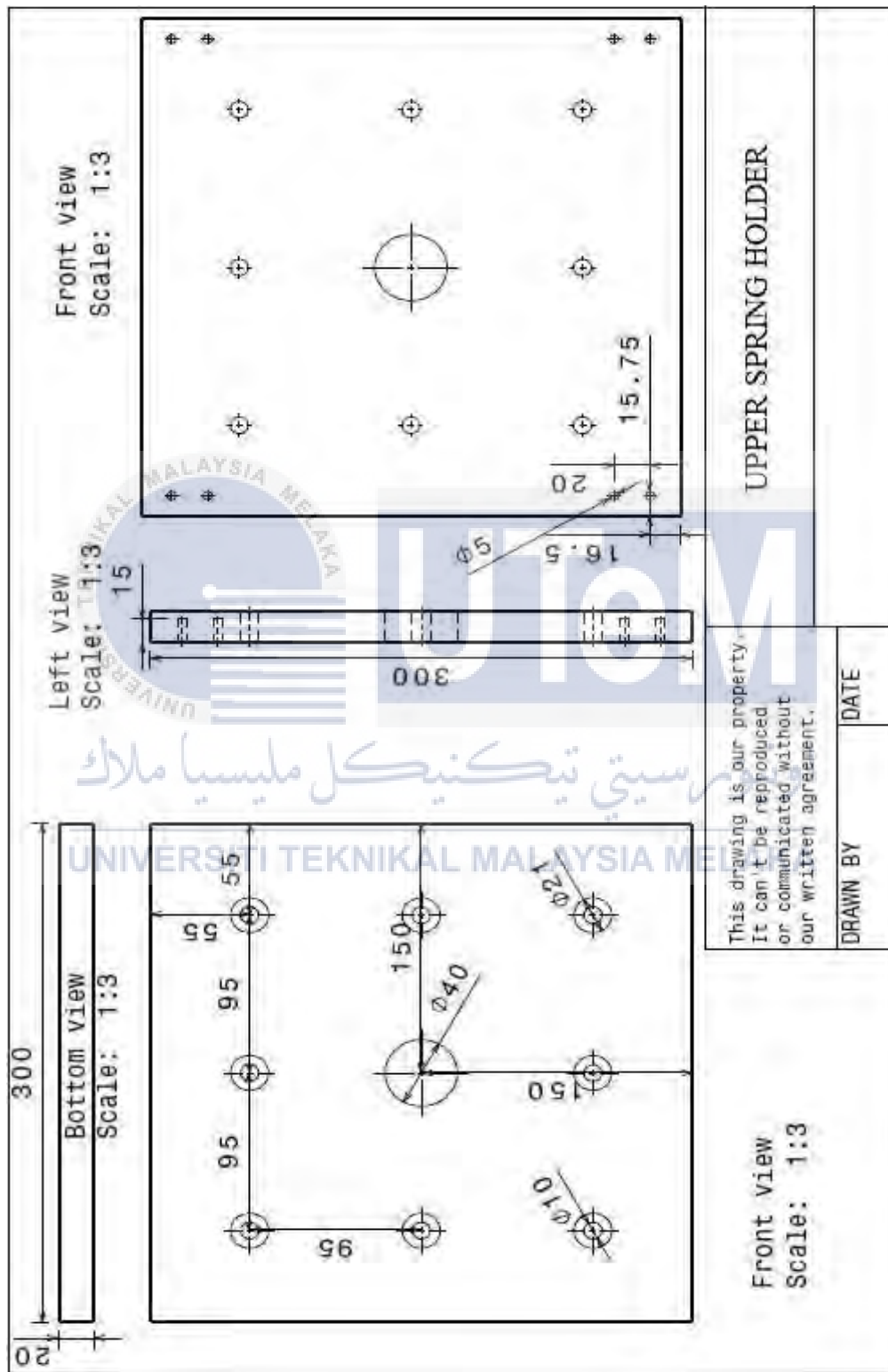
- Isometric view:** Located at the top right, showing a 3D perspective of the spring. Scale: 1:1.
- Left view:** Located in the center, showing the spring's profile with a vertical dimension line on the left indicating a height of 54. Scale: 1:1.
- Front view:** Located at the bottom right, showing the spring's profile with a horizontal dimension line at the top indicating a diameter of $\phi 3.5$. Scale: 1:1.
- Bottom view:** Located at the bottom left, showing the circular end view of the spring with a horizontal dimension line indicating a diameter of $\phi 3.4$. Scale: 1:1.

Watermarks for 'UNIVERSITI TEKNIKAL MALAYSIA MELAKA' and 'UTEM' are visible across the drawing.

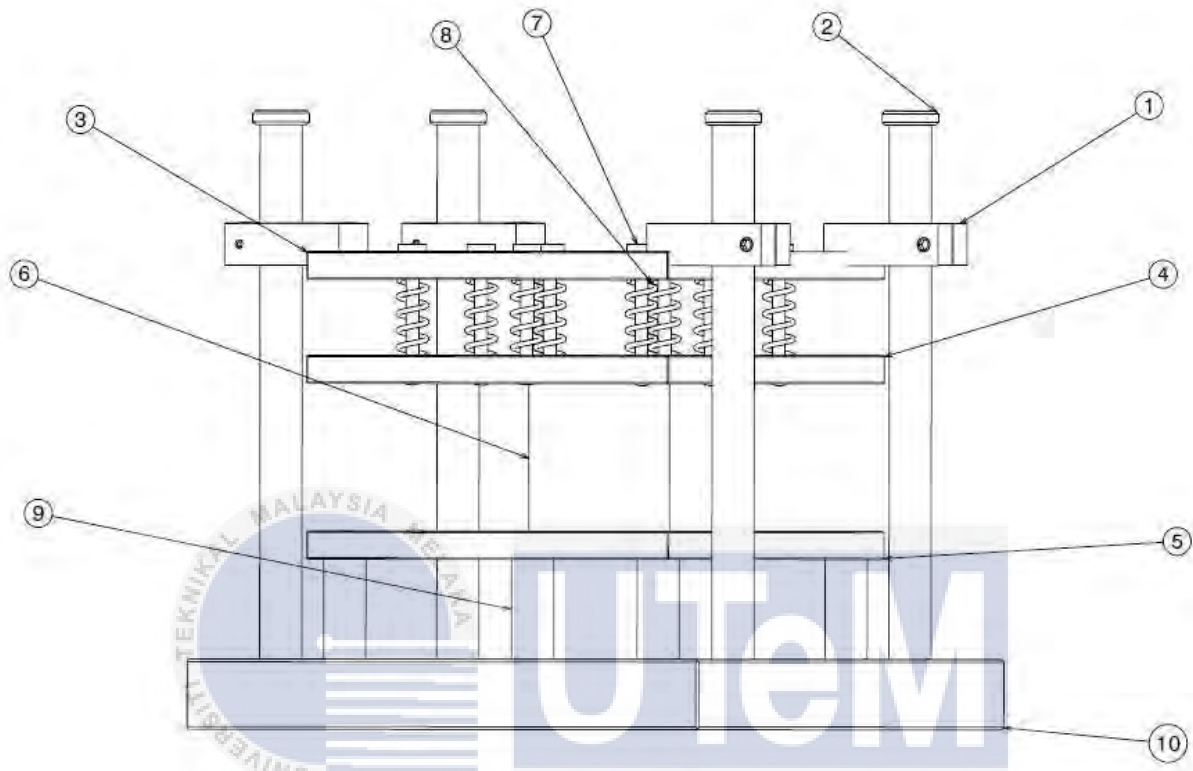
This drawing is our property. It can't be reproduced or communicated without our written agreement.		DATE	
		DRAWN BY	

SPRING

Appendix J



Appendix K



Isometric view

Scale: 1:3

اونيورسيتي تيكنيك مليسيا ملاك

UNIVERSITI TEKNIKAL MALAYSIA MELAKA

No	Part Name	Quantity
1	Holder	4
2	Outer Shaft	4
3	Upper Spring Holder	1
4	Lower Spring Holder	1
5	Rubber Base	1
6	Rubber	1
7	Spring Holder	8
8	Spring	8
9	Inner Shaft	4
10	Structure Base	1